THESIS

MONITORING GROUNDWATER-SURFACE WATER INTERACTION AND NUTRIENT MASS EXCHANGE IN THE RIPARIAN CORRIDOR OF THE LOWER ARKANSAS RIVER VALLEY, COLORADO

Submitted by

Alexander Paul Huizenga

Department of Civil and Environmental Engineering

In partial fulfillment of the requirements

For the Degree of Master of Science

Colorado State University

Fort Collins, Colorado

Spring 2015

Master's Committee:

Advisor: Ryan Bailey
Co-Advisor: Timothy Gates

Timothy Covino

ABSTRACT

MONITORING GROUNDWATER-SURFACE WATER INTERACTION AND NUTRIENT MASS EXCHANGE IN THE RIPARIAN CORRIDOR OF THE LOWER ARKANSAS RIVER VALLEY, COLORADO

The Lower Arkansas River Valley in southeastern Colorado is an irrigated, agricultural valley suffering from high concentrations of nutrients (Nitrogen N; phosphorus P) and salts in the coupled groundwater-surface water system. The majority of data collection efforts and associated spatial analysis of concentrations and mass loadings from the aquifer to the stream network have been performed at the regional scale (> 500 km^2). These regional scale assessments have indicated that river riparian areas play a major role in controlling nutrient mass flux to the Arkansas River and its tributaries. However, the water and nutrient mass exchange within the riparian-stream system have not yet been investigated in detail. The objective of this thesis is to enhance understanding of hydro-chemical stream-aquifer processes at the reach scale (< 5 km) along the main stem of the Arkansas River and along a major tributary. Using a suite of in-stream instruments and observation wells, a 4.7 km reach of the Arkansas River and a 2 km reach of Timpas Creek were monitored to quantify spatio-temporal groundwater-surface water interaction and mass inputs and outputs of nutrients. The total volume of water flowing into and out of each study reach was quantified using existing stream gages for upstream flow measurements and developing new stream gages for downstream flow measurements. Stage-discharge relationships were developed at the downstream locations using in-stream water level loggers and periodic flow measurements using Acoustic Doppler Velocimeters (ADVs).

Monitoring included growing season length and 24-hour monitoring of flow and water quality. Using these monitoring data, mass balance calculations were used to quantify groundwater-surface water interactions and nutrient mass exchanges and loadings. For growing season length analysis, surface water samples were collected and in-situ measurements were made at the stream gaging sites every two weeks during the study period to provide a data set on fluxes into and out of each reach during the irrigation season. The two 24-hour sampling events were performed in June and October of 2014 to compare groundwater-surface water exchange and mass loadings at the beginning and end of the growing season. Composite water quality samples for total N, nitrate as nitrogen (NO_3^- as N), nitrite as nitrogen (NO_2^- as N), ammonium as nitrogen (NH_4^+ as N), total P, and dissolved salts were collected at the gage locations every 2 hours using ISCO automatic samplers along with in-situ measurements of water level, temperature, and specific conductance. Water quality samples, along with in-situ measurements, were also collected from transects of shallow monitoring wells installed in the riparian corridor and on the banks of each reach during sampling events. These water quality data, as well as estimated gradients of groundwater hydraulic head between monitoring wells, were used to inform mass loading calculations.

Growing season length monitoring results from the Arkansas River show decreases in NO_3^- and total N concentrations ranging from 35% to 66% from upstream to downstream along the study reach. A growing season NO_3^- mass balance performed on the Arkansas River indicated that 73% of the total NO_3^- lost from the system can be attributed to in-channel and hyporheic processes. In addition, analysis of the water table elevations along the river suggest that there is an oscillation of the groundwater gradients during high flow periods. 24-hour monitoring suggests minimal upstream to downstream changes in total phosphorus loadings in the Arkansas River early in the growing season; however, there was a 29% increase in loadings in October. NO_3^- loadings decreased 14% in June between the upstream and downstream monitoring stations, and an average of 41% in October. Groundwater and pore water sample results suggested extensive mixing of surface and groundwater in the Arkansas River, but indicated little exchange in Timpas Creek. These samples also suggest that denitrification occurs in both the riparian floodplain and hyporheic zones of the Arkansas River and Timpas Creek, while phosphorus immobilization and mobilization in groundwater is highly variable in these systems.

These results provide a better understanding of hydro-chemical groundwater-surface interactions within the region and indicate the role of riparian and hyporheic zones in controlling and mitigating groundwater and surface water nutrient loadings to the stream network. The information derived from this study provides knowledge of hydro-chemical processes on small to medium spatial and temporal scales and provides a valuable contrast in controlling processes between main-stem and tributary riparian areas. This project also provides a database for future small to medium scale groundwater-surface water modeling efforts in the Lower Arkansas River Valley to further elucidate processes that govern nutrient mass transport in the riparian-stream system, with implications for regional-scale processes.

TABLE OF CONTENTS

LIST OF TABLES

LIST OF FIGURES

CHAPTER 1: INTRODUCTION AND LITERATURE REVIEW

1.0 Nitrogen and Phosphorus in Diffuse Pollution

Nitrogen (N) and phosphorus (P) are the primary limiting nutrients in marine and aquatic environments and a requirement in plant and animal nutrition (Novotny 2002, Mueller et al. 1992). Plants, algae, fungi, and bacteria take up P primarily in its phosphate form (PO_4^-) and N as ammonium (NH_4^+) and nitrate (NO_3^-) (Lewandowski and Nützmann 2010). Excess amounts of these nutrients from agricultural and urban diffuse pollution cause eutrophication in rivers, lakes, estuaries, and coastal ocean waters leading to toxic algal blooms, oxygen depletion, and loss of aquatic life (Mueller et al. 1992). The primary diffuse agricultural sources of N and P are from the over-application of industrial fertilizers and manure (Novotny 2002).

Nutrients are of particular concern in irrigated agriculture because as the demand for food increases, irrigated agriculture and fertilizer use will continue to increase. This will drive further eutrophication of the world's waterways (Monteagudo et al. 2012). Irrigated agriculture and food production doubled between 1964 and 1999 with a sevenfold increase in the use of N based fertilizer and a threefold increase in P based fertilizer (Tilman 1999). Irrigated agriculture is often associated with environmental degradation such as salinization, waterlogging of soils, increased erosion, polluted runoff, and changes to river flow regimes (Strange et al. 1999, Fernandez-Cirelli et al. 2009, Gates et al. 2012). According to the Spanish National Statistics Institute, irrigated agriculture is more intensive than non-irrigated due to the artificial supply of water and fertilizers to crop lands. Excess nutrients are then transported by overland and groundwater flow to receiving water bodies (Carpenter et al. 1998).

A well-documented example of the effect of excessive nutrient loading is the hypoxic zone in the Gulf of Mexico (Burkart and James 1999, Swaney et al. 2012, Alexander et al. 2008). These studies suggest that hypoxia, or oxygen depletion, is the result of excessive growth of nuisance blooms composed of bacteria, cyanobacteria, and algae. The death and decomposition of these blooms causes a drop in dissolved oxygen in the water column and sediment interface. Due to anthropogenic sources of nutrients in the Mississippi-Atchafalaya River Basin the largest hypoxic zone in the United States forms every year, covering an average area of 16,500 km^2 (EPA 2007).

Natural levels of P originate from the weathering of the mineral apatite (Novotny 2002). However, anthropogenic sources such as fertilizers (industrial and organic), sewage, and phosphate detergents have caused a net accumulation of P in soils and sediments across the globe (Sharpley et al. 1994). When excessive P is applied in fertilizers, not all of it is taken up by plants and the excess P readily sorbs to soil and sediment (Novotny 2002). For this reason, the majority of P loading to waterways is through eroded soil in drainage water in the form of particulate P (Carpenter et al. 1998, Novotny 2002). Particulate P may be the dominant source of waterway loading, but P can also travel in dissolved forms such as orthophosphate, particularly in areas with nonerosive soils (Sharpley et al. 2000). Dissolved P in surface water is often the result of rainfall or runoff interacting with surface soil and vegetative material (Sharpley et al. 1994).

There is also extensive evidence of P transport through subsurface flow (Heathwaite and Dils 2000, Simard et al. 2000, Holman et al. 2008). Heathwaite et al. suggested that preferential flow through shallow groundwater zones were significant contributors to overall P loadings, particularly during storm flow (Heathwaite et al. 2000). This is supported by research conducted by Mellander et al. which determined that well drained soils and moderately drained soils with quick-flow pathways in the shallow subsurface, such as tile drains and ditches, were a significant source of P to surface water bodies (Mellander et al. 2012). This subsurface loading can also be the result of phosphate mobilization through the mineralization of organic matter, the reductive dissolution of iron or calcium bound P, or by desorption processes (Reddy et al. 1999). While there are no direct human health issues related to excess P loading to water bodies or national standards, very small concentrations can cause eutrophication and the resulting negative effects (Sharpley et al. 2000). The EPA 1986 Quality criteria for water recommends that total phosphates should not exceed 0.05 mg/L in a stream where it enters a lake or reservoir and total P should not exceed 0.1 mg/L in flowing waters that do not discharge directly into lakes or reservoirs.

Instead of accumulating in soils like P, N is readily transported to ground and surface water in its dissolved forms (Novotny 2002, Mellander et al. 2012). The primary anthropogenic sources of N are atmospheric deposition of N oxides from burning fossil fuels and organic and industrial fertilizers (Jordan and Weller 1996). With the advent of industrial fertilizer use, following the discovery of the Haber-Bosch process, the production of N based fertilizer significantly altered the N budget of the planet (Erisman et al. 2008). While terrestrial and marine biological N_2 fixation dominated prior to this discovery, the current production of N fertilizer accounts for nearly 40% of the total amount of reactive N inputs (Gijzen and Mulder 2001). NO_3^- (NO_3^-) is often the most prevalent N species in surface and groundwater and can persist in groundwater for decades, accumulating to high levels as more N fertilizer is applied each year (Nolan et al. 1998).

The dominant transfer pathway for N is for NO_3^- to leach from a surface source into groundwater (Mellander et al. 2012). However, significant losses of N can occur through surface runoff as well (Jiao et al. 2012). N can be taken up by plants, immobilized in soil, denitrified, volatilized, and leached during its journey from a source to delivery into a receiving water body. Denitrification in the subsurface (Jarvis and Hatch 1994), as well as in-stream transformations (Birgand et al. 2007), are important processes in determining the existence of N in receiving waters. High NO_3^- concentrations in groundwater have been linked to toxic effects on livestock and to "blue baby disease" (methemoglobinemia) in infants (Carpenter et al. 1998). For this reason the EPA has set a national drinking water standard of 10 mg/L NO_3^- as N.

1.1 Nitrogen and Phosphorus Dynamics in the Riparian and Hyporheic Zones

Many studies have shown the importance of the riparian zone (Cooper 1990, Peterjohn and Correll 1984, Jacobs and Gilliam 1985) and groundwater-surface water interactions in the removal of contaminants from surface water, groundwater, and overland flow (McMahon and Böhlke 1996, Lewandowski and Nützmann 2010, Puckett et al. 2008, Stelzer et al. 2011). The floodplain is considered the reactive interface between the upland zones and the river on a landscape scale, while the hyporheic zone is the reactive interface between the aquifer and the surface water on the floodplain scale (Lewandowski and Nützmann 2010). Riparian zones may be considered nutrient sinks but only N can be removed permanently through denitrification. P, on the other hand, can only be trapped in the riparian zone and will accumulate in sediments and organic matter, leading to possible remobilization (Burt et al. 2002a, Vanek 1991).

Peterjohn and Correll (1984) sampled N and P species in shallow groundwater and surface runoff, over the course of one year, in an agricultural watershed consisting of riparian forest and cropland. Their research showed that the major pathway of N removal in the riparian forest was through subsurface flow, which accounted for 75% of the retained N and was attributed to vegetative uptake and denitrification. On the other hand, the primary pathway of N removal from cropland was through harvest. P retention in the riparian forest was calculated to be 80%, with export from the forest fairly evenly distributed between subsurface and surface flow (Peterjohn and Correll 1984).

Jacobs and Gilliam (1985) used a similar approach; sampling shallow groundwater wells and surface runoff to determine the fate of NO_3^- as it moved with groundwater and surface runoff from cultivated fields through the riparian zone. Very little NO_3^- (<0.1 mg/L) was measured at the wells near the stream and there was a clear decrease from the upper elevation wells to the lower elevation wells. The researchers determined that most of this depletion was from denitrification because their vegetation samples could only account for <20% of the losses and there was no evidence of deep seepage. Further research indicated that the riparian areas contained poorly drained soils and a high water table, conditions which often create a denitrifying environment (Jacobs and Gilliam 1985).

Denitrification as groundwater moves from upper gradients to lower gradients is not the only source of NO_3^- depletion in some stream environments. McMahon and Böhlke (1996) showed that only 15-30% of the NO_3^- depletion in the South Platte River could be accounted for by denitrification as groundwater moved through the floodplain and riverbed sediments. The rest was made up of complex mixing patterns between the river water and groundwater, as evidenced by hydraulic head data showing both upward and downward movement of water beneath the channel. This exchange between the river water and the aquifer allowed for further contact with denitrifying floodplain and riverbed sediments, decreasing the NO_3^- load as the river water moved downstream (McMahon and Böhlke 1996).

Similarly, Puckett et al. (2008) showed the importance of residence time in the bed sediments for denitrification and the influence of hydrogeological controls. In zones of high surface water infiltration to the hyporheic zone due to coarse grains and strong gradients, NO_3^- concentrations decreased. In zones where hydrogeological controls prevented infiltration of surface water, groundwater discharge to the stream contributed to surface water NO_3^- loads. However, both of these situations depend on the amount of potential electron donors available, such as organic matter. If the residence time is low and there is an abundance of electron donors, only minimal denitrification will occur. On the other hand, if residence time is high and there are only a small amount of electron donors the slow reactions will remove more NO_3^- (Puckett et al. 2008).

Lewandowski and Nützmann (2010) also found high NO_3^- depletion through denitrification in the floodplain, but in addition, they found spatially variable phosphate concentrations throughout the study. This spatial heterogeneity was likely caused by long lasting sources of P mobilization and immobilization. They found that mobilization was the result of mineralization of organic matter and dissolution of iron hydroxide-phosphate complexes leading to high dissolved P concentrations. They also determined that P immobilization was caused by sorption to aquifer material and coprecipitation of P and dissolved iron when water levels dropped, resulting in constant low dissolved P concentrations (Lewandowski and Nützmann 2010).

Similarly, Lewandowski and Nützmann (2010) showed that the river bed sediments were an important source of P mobilization due to reduction of iron hydroxide and phosphate complexes causing the release of phosphate into the hyporheic zone. P concentrations measured in the riverbed below the sediment-water interface were two times larger than P concentrations in the groundwater close to the river, and much higher than P concentrations in the river water (Lewandowski and Nützmann 2010). McDowell and Sharpley (2003) found that bed sediment can serve as a source of P as well as a sink. They used fluvarium tests (an analysis using an artificial channel to assess field collected sediments) to show a net uptake of P (dissolved and particulate) when P-enriched water flowed over sediments from forested and agricultural settings and a net release of P when "clean water" flowed over the P-enriched sediment solution. This sediment uptake and release of P has been found in other soil and stream studies (Khalid et al. 1977, Logan 1982). McDowell and Sharpley (2003) determined that although abiotic sediment processes, such as sorption and deposition, played the dominant role in P uptake, biotic processes also played an important role (McDowell and Sharpley 2003).

1.2 Investigating Fate and Transport of Nutrients Through Mass Balance Methods

Loading of solute mass from the aquifer to the stream is often estimated by applying the conservation of mass principle to a river reach during a defined time period (Jain 1996, Jaworski et al. 1992, Tessier et al. 2008). Measurements of solute concentrations and water flow are taken at the upstream and downstream ends of the reach to provide an estimate of solute mass flux into and out of the reach, with differences accounted for by fluxes that leave or enter the reach along its length or, changes in dissolved mass stored within the reach (Tessier et al. 2008, Martin and Gates 2014). For many studies this process involves extensive data collection on all aspects of the reach including groundwater and surface water contributions, chemical reaction rates in bed sediments and soil media, hyporheic exchange, soil properties, and vegetative cover (Duff et al. 2008, House and Warwick 1998, Tessier et al. 2008).

Duff et al. (2008) performed a study on three geographically distinct agricultural stream reaches in Washington, Maryland, and Nebraska varying in length from 400 to 1000 m to determine NO_3^- dynamics. They determined that groundwater contributed to both flow and potential NO_3^- concentration to the streams but that streambed processes such as areas of high denitrification rate and assimilation by benthic diatoms potentially retained 45% to 75% of NO_3^- contributions. However, once in the main stream flow, NO_3^- loads increased along the reaches and were transported long distances due to limited bed contact (Duff et al. 2008).

Stelzer et al. (2011) focused their efforts on one 700 m reach of Emmons Creek in Wisconsin and intensively monitored NO_3^- concentrations in surface water at up- and downstream points and groundwater in longitudinal wells installed in the middle of the thalweg over approximately one year. They determined there was net NO_3^- retention in the spring and fall and that there were higher rates of NO_3^- retention during periods of higher groundwater discharge and moderate temperatures. Net NO_3^- retention made up 2% to 4% of all inputs to the reach during the spring and autumn, while it only accounted for 1% during the summer and winter. Their mass balance approach calculated that 57% of the variation in areal net NO_3^- retention was explained by the amount of groundwater discharge during the warmer season. They concluded that most of the NO_3^- retention occurred in the organic rich bed sediments at the wetted channel margins, through biological assimilation and denitrification by bacteria, and that it was limited by the upwelling flux of NO_3^- rich groundwater (Stelzer et al. 2011).

Cooper (1990) performed a mass balance on a small stream in New Zealand to determine the NO_3^- retention in the riparian zones and stream channel. NO_3^- samples were collected from wells in the riparian zone, the stream source, and the stream outlet. Denitrification rates were also determined through lab analysis of riparian soils and channel sediments. Through the mass balance calculations it was determined that riparian zones with organic soils retained a disproportionate amount of the NO_3^- flux when considering their aerial extent around the stream.

While these zones only made up 12% of the soils surrounding the stream, they accounted for 56% to 100% of the NO_3^- depletion. This was partly due to the majority of the groundwater flowing through these zones, but they were also more suitable for denitrification. However, an increase in NO_3^- flux in the stream was still measured due to flow through the mineral riparian soils with less ability to deplete NO_3^-. In-stream NO_3^- depletion was shown to be dominantly due to uptake by in-stream biological uptake since the denitrifying capacity of the channel sediments could only account for 15% of the in-stream depletion (Cooper 1990).

The mass balance approach has also been used for nutrient dynamics analysis in larger rivers, as evidenced by Tessier et al. (2008) and House et al. (1998). Tessier et al. (2008) sampled inorganic N species at upstream, midstream, and downstream points along two 30 km reaches of the Garonne River in France to compare variable residence time versus constant residence time loading calculations. They determined that in large rivers with highly variable flow rates, it is necessary to account for varying residence times with varying flows. On the other hand, when discharges are constant over the entire study period an evaluation of residence time is unnecessary. While no real analyses on in-stream nutrient dynamics were performed, their inorganic N sampling showed NO_3^- concentrations increasing from upstream to downstream and ammonium concentrations decreasing from upstream to downstream (Tessier et al. 2008).

House et al. (1998) put more focus on P and N species dynamics in a large river environment. Three, 100 hour monitoring campaigns during the autumn, spring, and winter yielded water quality data from the main stem and all the contributing tributaries. Large decreases in soluble P were found, which they attributed to uptake by bed sediments and riverine flora during low flow conditions and uptake by suspended sediments during a storm event. They argued that the loss in concentration could not be due to loss to groundwater and showed that the equilibrium phosphate concentration (EPC_o) of the surface sediment was less than the concentrations in the overlying water, suggesting a net uptake of SRP. This argument was supported by fluvarium experiments with collected sediment. Smaller changes in NO_3^- were shown with losses in the autumn, gains in the spring, and little evidence of riverine processes in the winter. The losses in autumn were consistent with the denitrification rate of the bed sediment and the increase in the spring was consistent with diffuse inputs of NO_3^- during rain events. Bacterial activity decreases during the winter months, which may explain the lack of riverine processing (House et al. 1998).

1.3 Nutrient Impacts in the Lower Arkansas River Valley

This study will focus on a region in southeastern Colorado known as the Lower Arkansas River Valley (LARV). The region is an agricultural valley which, relying heavily on irrigation to sustain crops, suffers from high concentrations of nutrients and salts in the coupled groundwater-surface water system (Gates et al. 2009). The extensive use of N based fertilizers has led to high NO_3^- concentrations in groundwater and surface water in the valley. In addition to its effect on marine and aquatic eutrophication, high N concentrations in groundwater are a particular problem for this region because the trace element selenium (Se) is present in the underlying marine shale. Se is an essential nutrient for humans and animals but at high concentrations can prove detrimental to health (Bailey et al. 2012). NO_3^- can influence Se species in irrigated soil and groundwater systems by inhibiting selenite reduction and oxidizing reduced Se from the marine shale (Bailey et al. 2012). Few studies have focused on P concentrations or loadings in groundwater or surface water in the LARV but the influence of P on algae and bacteria growth in aquatic environments has been well documented as mentioned in sections 1.0 and 1.1.

The majority of data collection efforts and associated spatial analysis of concentrations and mass loadings from the aquifer to the stream network have been performed at the regional scale (Gates et al. 2009, Bailey 2012, Morway et al. 2013). Samples for NO_3^- and to a lesser extent orthophosphate have been collected from surface water points and monitoring wells spread throughout the LARV since 2006. These regional scale assessments have indicated that river riparian areas play a major role in controlling nutrient mass flux to the Arkansas River and its tributaries, however, the water and nutrient mass exchange within the riparian-stream system have not yet been investigated in detail. This lack of information on reach scale, short term water and nutrient mass exchange in the riparian zone limits modeling capabilities in the region. Without improved knowledge of these processes, future modeling efforts would be an incomplete representation and restricted to regional scale observations.

1.4 Study Objectives

As stated previously, the majority of the data collection and associated spatial analysis of concentrations and mass loadings from the aquifer and the stream network has been performed at the regional scale for the LARV. This study seeks to monitor and quantify the nutrient loadings in the Arkansas River network and the loadings from groundwater to the network on a small scale in the LARV. It also seeks to develop a working knowledge of the influence that the riparian floodplain, hyporheic zone, and in-stream environment have on these loadings. Specific methods to accomplish these objectives include: establishing growing season and 24-hour monitoring schemes within the LARV stream network; focusing on a reach of the main stem and a reach of a major tributary, Timpas Creek, to compare and contrast different stream orders; and collecting data for water quality, water quantity, and physical characteristics of each study reach.

The remaining chapters of the thesis are organized as follows:

- Chapter 2 presents the study area and monitoring network design. Historic information on the ranges of discharge and nutrient concentrations are included as well as maps displaying the monitoring setups along each study reach.
- Chapter 3 presents the methods and results of field work and data analysis associated with growing season monitoring. For this analysis, upstream and downstream surface water samples were collected from the river and the creek approximately every 2 weeks from June to October 2014. Continuous water level readings at 15 minute intervals at these locations allowed for stage-discharge rating curves to be developed. Specific conductivity readings were also logged at 15 minute intervals. Groundwater levels within monitoring wells along each study reach also were logged at 15 minute intervals. A methodology for developing and using a specific conductivity-NO_3^- concentration rating curve to calculate a NO_3^- mass balance on the Arkansas River is also presented in this chapter.
- Chapter 4 presents the methods and results of field work and data analysis associated with 24-hour monitoring. 24 hour sampling events in June and October were performed at each study reach. Auto-samplers collected two hour composite samples of surface water and groundwater quality samples were collected from monitoring wells along each study reach. Pore water quality samples were also collected from the bed sediments of the two study reaches.

A summary of the findings and major conclusions as well as avenues for future research is presented in Chapter 5. Appendices are included to provide supplemental support to the findings from this study and to present additional data.

- Appendix A contains soil type maps from the USDA Web Soil Survey online tool.
- Appendix B contains a description of the slug testing field procedure used and the USGS hydraulic conductivity calculation tool used to determine hydraulic conductivities at monitoring well locations.
- Appendix C contains cross sectional surveys of each study reach and associated stage-top width relationships used in surface storage calculations.
- Appendix D contains growing season water quality results for dissolved solids and major cations and anions.
- Appendix E contains a procedure for channel bed and bank sediment collection as well as the sediment sample lab analysis results.
- Appendix F contains maps locating longitudinal sampling points for the June and October sampling events.
- Appendix G contains the procedures for installation and sampling of two multi-level groundwater samplers installed in the floodplain on the Arkansas River. It also contains the water quality results from those samplers.
- Appendix H contains aerial images, ground level photographs, and descriptions of the riparian floodplain of the Arkansas River and Timpas Creek.
- Appendix I contains information on the W-1 analysis for dissolved constituents from Ward Laboratories, Inc.

- Appendix J contains the 24-hour total P and NO_3^- concentrations from Timpas Creek and the Arkansas River during the June and October sample events.

CHAPTER 2: STUDY AREA AND STUDY DESIGN

2.0 Introduction

The study area and a description of the monitoring network system are explained in this chapter. The study area description outlines past research that was performed in the area, provides a general overview of the physical and climatic characteristics of the region, and presents a spatial context for the location of this study. The monitoring network descriptions provide a schematic of the sampling locations at each study reach and their relevance to either the growing season or 24-hour monitoring aspects of this research.

2.1 Description of Study Area

The Lower Arkansas River Valley (LARV) in southeast Colorado, which spans from the Pueblo Reservoir in Pueblo, CO and into Kansas, is shown in Figure 1. The LARV is an alluvial valley known for its valuable agricultural production and has been extensively irrigated for over 100 years (Gates et al. 2009). This region suffers from many of the issues stated earlier such as rising groundwater tables and salinization. Most of the research in this area has focused on salinization and contamination of ground and surface water by selenium species released from bedrock formations, often initiated by excessive NO_3^- loadings from irrigation and fertilization (Gates et al. 2009, Bailey et al. 2012) as well as regional scale modeling of these processes (Bailey 2012, Morway et al. 2013). The alluvial valley relies heavily on irrigation water diverted from surface water sources or pumped from groundwater aquifers to maintain its agricultural practices. The growing season begins in mid to late-March and ends in early November, corresponding with the irrigation season which runs from March 15th to November 15th. The climate is semi-arid and average monthly temperatures and precipitation in the region range from

-1^{o}C and 0.7 cm during the winter months to 25^{o}C and 5 cm during the summer months. In particular, this study focused on a reach of the main stem of the Arkansas River and a contributing tributary, Timpas Creek, in what has been referred to in past studies as the Upstream Study Region (USR). An aerial image of the two study reaches, highlighted in red, within the USR is shown in Figure 2.

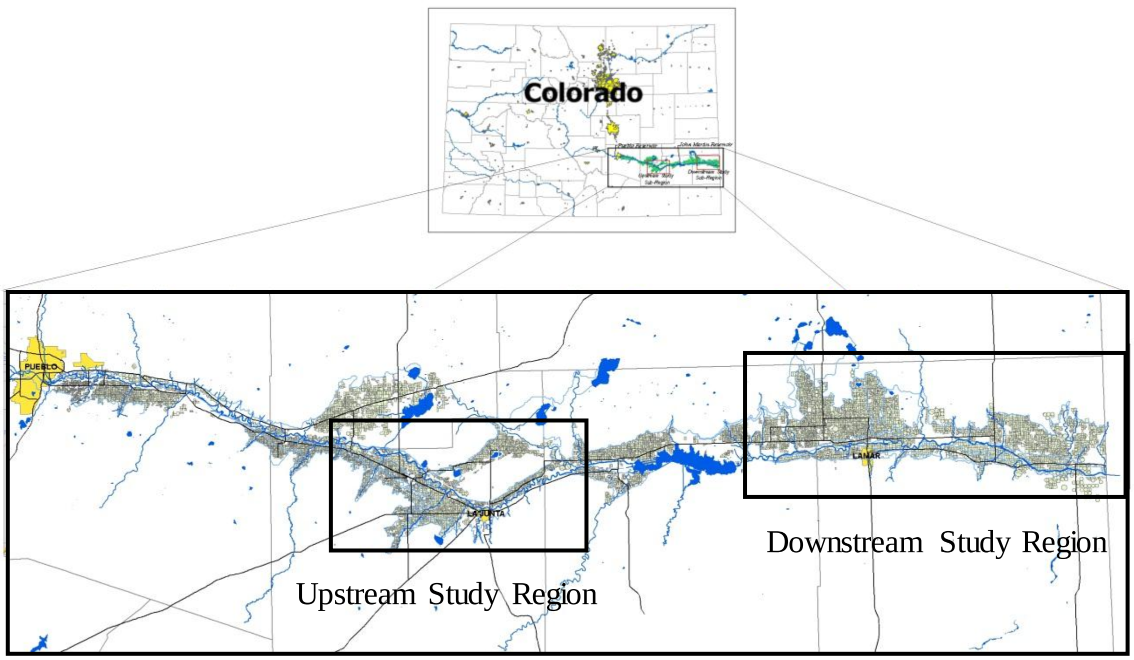

Figure 1. LARV in Colorado highlighting the upstream and downstream study regions.

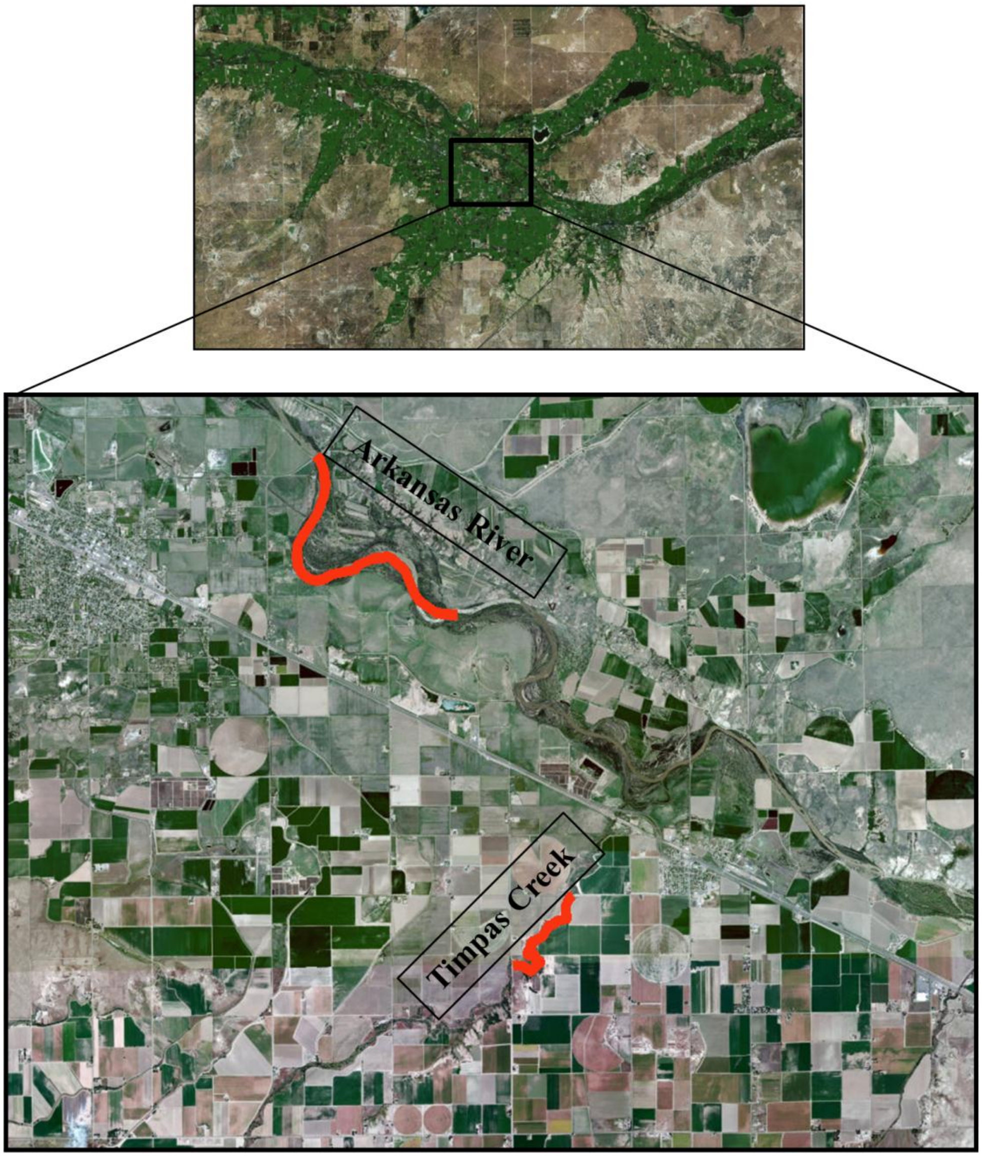

Figure 2. Study reaches on the Arkansas River and Timpas Creek in the Upstream Study Region.

2.2 Arkansas River Study Reach

The Arkansas River study reach is approximately 4.7 km in length and is located due east of the city of Rocky Ford, CO. The southwest side of the river is a mixture of irrigated fields, fallowed fields, and pasture with minimal riparian vegetation. The northeast side of the river is under the jurisdiction of the Colorado Parks and Wildlife and has been left relatively undisturbed. The area is used for outdoor recreation such as fishing and hunting and only state approved vehicles are allowed access. A few small fields are irrigated in this area for habitat and restoration purposes. Soils along the study reach are composed primarily of sand, loamy sand, and silty clay loam. Full soil maps can be seen in Appendix A and map unit descriptions are available upon request. The river reach has a sand bed channel with a typical cross sectional width of 75 meters.

At the upstream end of the reach the Colorado Division of Water Resources maintains a streamflow gage, labeled ARKROCCO (Arkansas River at Rocky Ford CO), which has collected 23 years of discharge data from 1992 through 2014. Peak flow for the river during this period at ARKROCCO was approximately 233 m^3/s (May 11 1999), the minimum was 0.00 m^3/s, and the average flow is 12.3 m^3/s. Historic nutrient data has been collected from this location since 2006 by Colorado State University (CSU) researchers. Of the 20 NO_3^- sample collected, the maximum NO_3^- concentration recorded was 2.6 mg/L, the minimum was 0.5 mg/L, and the average value was 1.4 mg/L. Only four orthophosphate samples have been collected at this location but the maximum concentration was 0.2 mg/L, the minimum was 0.03, and the average value was 0.11 mg/L. Historic nutrient data collected from existing observation wells by Colorado State University researchers within 5 km of the study reach has produced a wide range of concentrations. Since 2006, 70 samples have been collected for NO_3^-. The maximum concentration recorded near the Arkansas River study reach was 14.5 mg/L, the minimum was 0.1 mg/L, and an average of 2.5 mg/L. The maximum orthophosphate concentration of the 10 samples recorded near this study reach was 0.3 mg/L, the minimum was 0.09 mg/L, and the average was 0.19 mg/L.

The general study setup for the Arkansas River is displayed in Figure 3. The red triangles are river gages labeled ARKU (Arkansas River Upstream) and ARKD (Arkansas River Downstream). Each yellow circle represents a monitoring well and is labeled with a letter corresponding with its cross section and a reference number within the cross section (i.e. A1, B1, C1, etc…). Detailed descriptions, close up aerial images, and ground level photographs of the riparian vegetation at each cross section are contained in Appendix H. Blue arrows on the map highlight surface drains that contribute flow to the river. River water level meters (not shown on plot) were installed in the river close to the bank adjacent to wells A3, B2, and C3 to determine water level elevations of the river at each cross section. This monitoring network was used for both the growing season and 24-hour aspects of this research as described in Chapters 3 and 4, respectively.

The general soil type, map unit, range of values for saturated hydraulic conductivity (K_{sat}), and actual measurements of hydraulic conductivity (K) for each well are presented in Table 1. The soil type and expected values for hydraulic conductivity were taken from the NRCS Web Soil Survey online tool. The K_{sat} values are expected values of saturated hydraulic conductivity of the most limiting layer in the soil unit. This may explain the measured K values that fall outside of the range. The measured K values were determined by slug tests performed in November and are described in more detail in Appendix B.

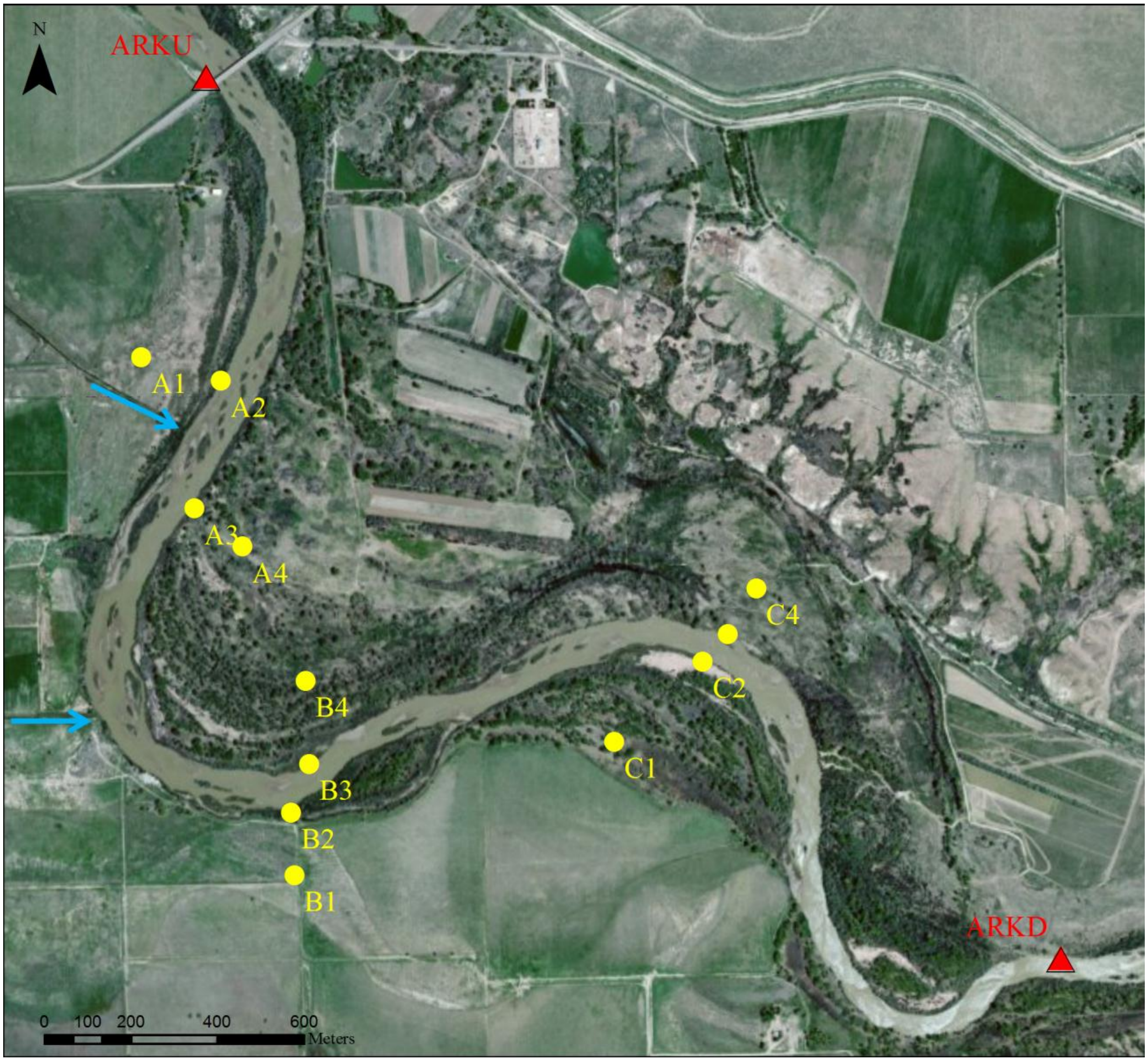

Figure 3. Arkansas River well and river gage stations. Red triangles represent river gaging stations, yellow circles represent monitoring wells, and blue arrows represent contributing surface drains.

Table 1. Descriptions of soils and hydraulic conductivity for Arkansas River study reach wells.

Well Name	Measured K (m/d)	Map Unit	Soil Type	Low Ksat (m/d)	High Ksat (m/d)
ARKA1	5.1	Bm	silty clay loam	0.12	1.2
ARKA2	2.9	Bk	sand/loamy sand	1.2	12.2
ARKA3	3.2	Bk	sand/loamy sand	1.2	12.2
ARKA4	20.5	Bk	sand/loamy sand	1.2	12.2
ARKB1	14.5	RfA	silty clay loam	0.12	0.37
ARKB2	4.1	Bk	sand/loamy sand	1.2	12.2
ARKB3	9.1	Bk	sand/loamy sand	1.2	12.2
ARKB4	2.1	Bk	sand/loamy sand	1.2	12.2
ARKC1	10.9	Bk	sand/loamy sand	1.2	12.2
ARKC2	21.7	Bk	sand/loamy sand	1.2	12.2
ARKC3	24.1	Bk	sand/loamy sand	1.2	12.2
ARKC4	29.7	GbA	fine sandy loam	1.2	3.7

2.3 Timpas Creek Study Reach

The Timpas Creek study reach is approximately 2 km in length and is located southwest of the town of Swink, CO. The land directly west of the creek is a mixture of fallowed fields and pasture, however, heavily irrigated fields exist within 0.5 km of the reach. Riparian vegetation is minimal along this side of the creek, particularly near the middle and northern end of the reach. The land east and south of the creek is a mixture of residential land and irrigated fields. Riparian vegetation is present at the southern end of the reach but is absent at the middle and northern end of the study reach. A more detailed description of the riparian vegetation along Timpas Creek and aerial and ground level images are presented in Appendix H. Soils along the creek are composed primarily of fine sandy loam and silty clay. Full soil maps can be seen in Appendix A and map unit descriptions are available upon request. The reach has a gravel bed channel underlain by hard clay. In some cases the channel has been scoured down to bedrock but maintains a thin layer of gravel. During periods of medium and low discharge sections of the channel bed are choked with fine silts, clays, and organic matter. The channel sediments vary in thickness depending on the location in the creek. The typical cross sectional width of the creek is 7.0 meters.

At the upstream end of the reach the US Geological Survey maintains a streamflow gage, labeled TIMSWICO, which has collected data consistently since 1965. The maximum flow for the creek was approximately 606 m^3/s (June 17 1965 and noted as an Historic Peak by the USGS), the minimum was 0.00 m^3/s, and the average value is 1.7 m^3/s. Historic nutrient data is not available for this location but samples have been collected from Timpas Creek at a location 2.5 km downstream since 2006 by CSU researchers. Of the 22 samples collected from this location, the maximum NO_3^- concentration recorded was 4.4 mg/L, the minimum was 1.3 mg/L, and the average value was 2.8 mg/L. Only four samples have been collected for orthophosphate but the maximum concentration was 0.21 mg/L, the minimum was 0.09, and the average value was 0.14 mg/L. Historic groundwater nutrient data collected from existing monitoring wells by CSU researchers within 3 km of the study reach has produced a wide range of concentrations. There have been 51 NO_3^- concentrations recorded near the Timpas Creek study reach. The maximum was 45.6 mg/L, the minimum was 0.4 mg/L, and an average of 9.7 mg/L. Only eight samples for orthophosphate have been collected since 2006 but the maximum concentration recorded near this study reach was 0.33 mg/L, the minimum was 0.11 mg/L, and the average was 0.2 mg/L.

The general study setup for Timpas Creek is shown in Figure 4 and is labeled in the same manner as Figure 3. The general soil type, map unit, range of values for *Ksat*, and actual measurements of *K* for each monitoring well location are presented in Table 2. River water level meters (not shown on plot) were installed in the river close to the bank adjacent to wells A3 and

B2 to determine water level elevations of the creek at each cross section. This monitoring network was also used for both the growing season and 24-hour monitoring aspects of this research as described in Chapters 3 and 4, respectively.

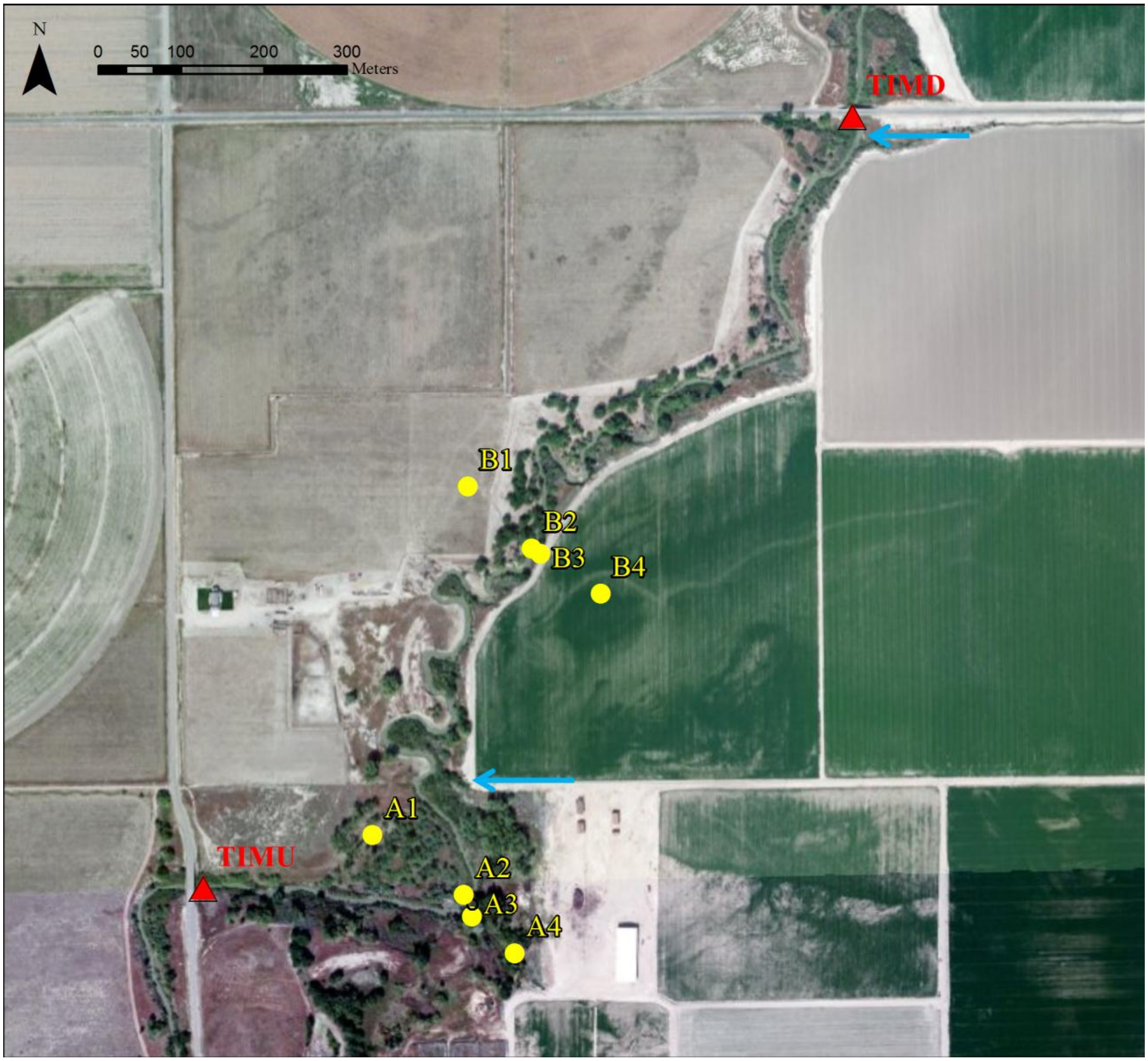

Figure 4. Timpas Creek wells and stream gage stations. Red triangles represent river gaging stations, yellow circles represent monitoring wells, and blue arrows represent contributing surface drains.

Table 2. Descriptions of soils and hydraulic conductivity for Timpas Creek study reach wells.

Well Name	Measured K (m/d)	Map Unit	Soil Type	Low Ksat (m/d)	High Ksat (m/d)
TIMA1	0.02	GbA	fine sandy loam	1.2	3.7
TIMA2	1.1	GbA	fine sandy loam	1.2	3.7
TIMA3	0.16	GbA	fine sandy loam	1.2	3.7
TIMA4	1.3	RfB	silty clay loam	0.12	0.37
TIMB1	4.1	HdB	silty clay	0.04	0.12
TIMB2	0.09	HdB	silty clay	0.04	0.12
TIMB3	0.56	GbA	fine sandy loam	1.2	3.7
TIMB4	9.0	HdB	silty clay	0.04	0.12

CHAPTER 3: GROWING SEASON MONITORING

3.0 Introduction: Overview of Data Collection Procedure

Growing season monitoring in the study region occurred from early June to mid-November to collect data during the approximate growing season. This involved a combination of in-situ hydrology and water quality monitoring instruments as well as bi-weekly trips to download data and collect water quality grab samples. The overall objective of the growing season monitoring was to investigate how the surface and groundwater hydrology as well as the surface water quality varied throughout a typical growing season.

Growing season in-situ monitoring efforts included:

- Aqua Troll installations at the up and downstream site of each study reach collecting specific conductivity measurements as well as water level measurements to be used in stream discharge calculations;
- Monitoring well installed within the riparian areas equipped with water level loggers to track water table elevations throughout the study period; and
- Water level logger installations in the river at each cross section to compare to monitoring well levels.

Bi-weekly sampling trips involved collecting water quality grab samples at the upstream and downstream site of each study reach to track water quality trends in the Arkansas River and Timpas Creek.

3.1 Methods

3.1.1 Aqua Troll Installation and Rating Curve Development

At the upstream and downstream location of each study reach an In-Situ Aqua TROLL 200 Data Logger was installed to measure and log specific conductivity, temperature, and water level. Each Aqua TROLL (AT) was housed in a piece of perforated 6.35 cm (2.5 inch) PVC pipe that was anchored by O-rings to an eight foot T-post with one half to three quarters of its length driven into the channel bed, shown in Figure 5. The pipes were positioned vertically as close to the main flow of the channel as possible and the AT was hung from the top of the PVC pipe by a communication cable that ran from the end of the AT back to the channel bank. The communication end of the cable was housed in a small shelter on the bank and accessed for periodic data downloads.

Continuous water level monitoring at the upstream and downstream sites allowed for continuous monitoring of flow at these locations. At both upstream locations of the study reaches there are existing USGS (Timpas Creek) or Colorado Division of Water Resources (Arkansas River) flow gages as mentioned in Chapter 2. AT installation still occurred at the upstream locations to check the level and conductivity readings given by these agencies but rating curves were not developed. At the downstream locations of the study reaches stage-discharge rating curves were developed by measuring discharge at various stages.

Figure 5. Aqua Troll housed in PVC pipe at ARKD monitoring station.

Discharge measurements at TIMD (Timpas Downstream cross section) were taken using a FlowTracker Handheld-Acoustic Doppler Velocimeter (ADV). This involved stringing a measuring tape across the channel perpendicular to flow and dividing the channel into at least 25 sections. In each section a velocity measurement was taken at 60% of the depth if flow was less than 0.3 m (1 ft) or at 20%, 60%, and 80% if flow was greater than 0.3 m. After taking velocity measurements for each section, the FlowTracker software calculated a total discharge for the cross section. The rating curve in Figure 6 shows a linear relationship between stage and discharge at the TIMD station.

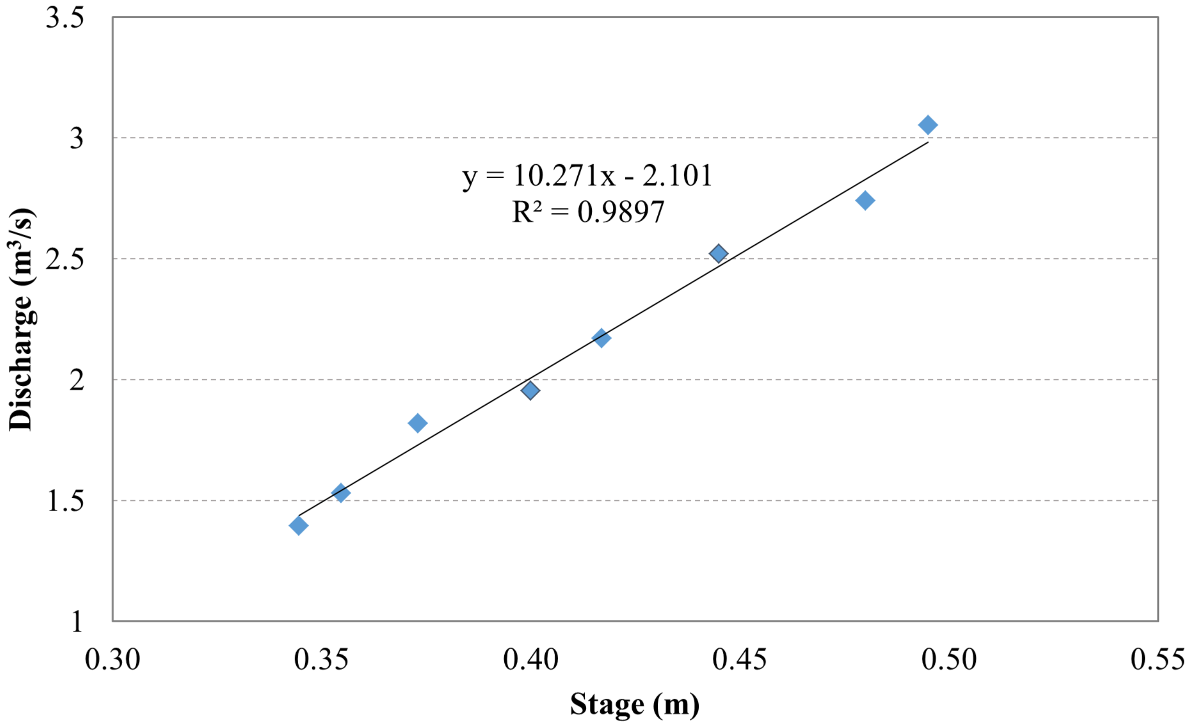

Figure 6. Stage-discharge rating curve for the downstream cross section of the Timpas Creek study reach.

A rating curve was also developed for a contributing surface drain on Timpas Creek, shown in Figure 7, which will be referred to as TIM Drain. This surface drain is a primary outlet for surface runoff and interflow from irrigated fields. Discharge was measured at a concrete structure approximately 150 m above the confluence with Timpas Creek which provided a constant cross section. A HOBO Onset Water Level Logger was used to collect the necessary stage measurements beginning in May and flow measurements were collected throughout the study period.

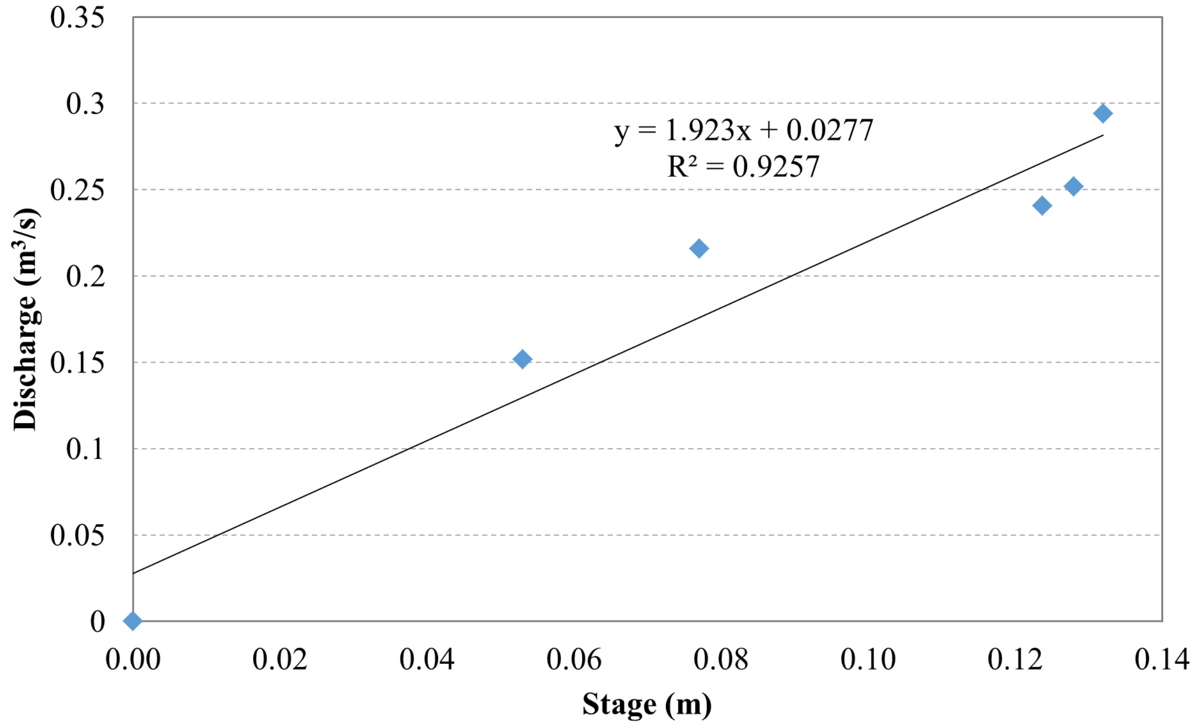

Figure 7. Stage-discharge rating curve for TIM Drain.

Discharge measurements at ARKD were also taken with an ADV. However, flows could only be measured safely up to approximately 12.7 m^3/s (450 ft^3/s), thus preventing an accurate measurement of discharge at higher stages. To overcome this issue the assumption was made that discharges above 9.9 m^3/s (350 ft^3/s) do not differ significantly from upstream to downstream. This assumption was confirmed when two measurements above 9.9 m^3/s at the downstream station were compared to flows upstream and there was less than a 10% difference between the two. Equating upstream and downstream discharge for high flows allowed an approximate rating curve to be developed for the downstream Arkansas River station. During times of constant discharge greater than two hours in duration, to minimize the effect of transit time and possible in-reach storage changes, the discharge measurement from the upstream station was assigned to the stage measured at the downstream AT. Two rating curves were developed for the Arkansas River, one for low flows below 9.9 m^3/s through a direct relationship with stage and measured discharge (Figure 8) and one for high flows using the upstream-downstream equating method mentioned above (Figure 9).

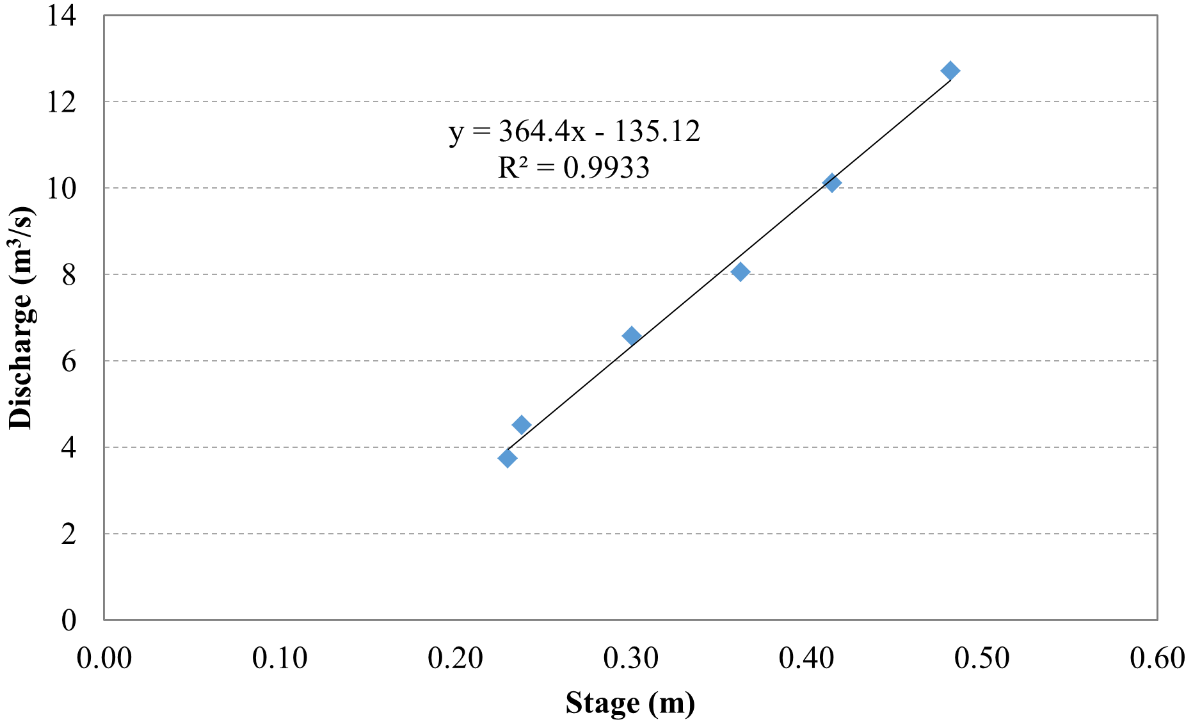

Figure 8. Arkansas River, downstream monitoring station stage-discharge rating curve used for low flows. Constructed using direct measurements of discharge and stage.

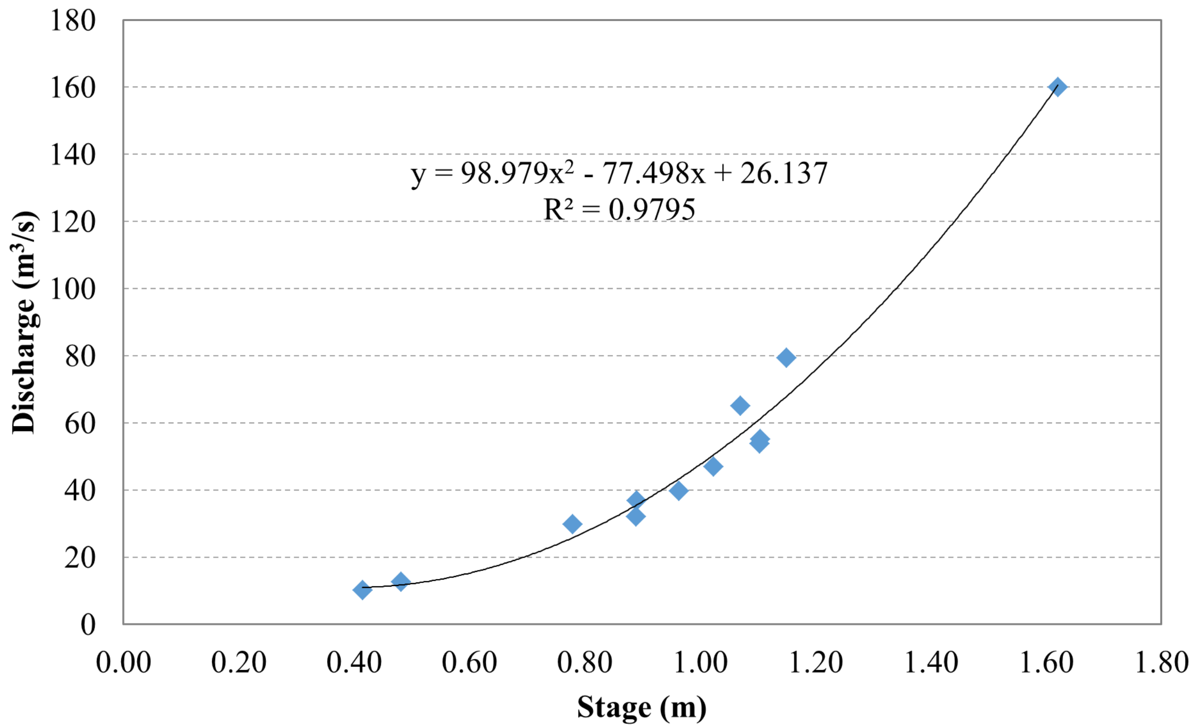

Figure 9. Arkansas River, downstream monitoring station stage-discharge rating curve used for high flows. Constructed using upstream-downstream equating method.

3.1.2 Monitoring Well Installation

Cross sections of shallow groundwater wells were installed using a Giddings drill rig with a rotating auger head where accessible or a hand auger for the shallower, less accessible locations. The wells are 6.35 cm (2.5 inch) PVC with perforations along the entire length and were installed to depths ranging from two to eight meters below ground surface. Depth varied depending on location but the typical protocol was to drill or hand auger until reaching the water table and then to continue another two to three meters to allow for any water table variation. A cap was inserted into the bottom of the perforated PVC pipe and then the pipe was lowered into the auger hole. A solid piece of 6.35 cm (2.5 inch) PVC was then joined with the perforated section and capped. A small hole was drilled in the side of the solid PVC to allow atmospheric pressure to match inside the well casing. In many locations the soil media was either loose sand (near Arkansas River) or loose silty clay (near Timpas Creek) which would collapse as soon as the auger was removed. In these situations the well casing was hammered with a hand sledge until refusal.

Each cross section includes four wells, two on each side of the channel. One of the wells was placed farther from the channel (exterior) and one closer to the channel (interior). The wells were placed from 150 to 300 meters apart on the Arkansas River and 60 to 125 meters apart on Timpas Creek. The interior wells tended to be shallower (1.5-3 meters) and installed with a hand auger whereas the exterior wells were typically greater than three meters in depth and installed with the drill rig. Monitoring well locations were chosen based on varying riparian vegetation thicknesses, ease of access, and assumed groundwater flowpaths based on modeling results from regional groundwater studies (Morway et al. 2013).

In each well a HOBO Onset Water Level Logger was installed to continually monitor the water table and temperature at 15 minute intervals. The logger was hung from a piece of static string attached to an I-bolt that was screwed into the well cap and hung approximately 15 cm from the bottom of the well. The I-bolt was fitted so that the end of the string approximately matched the top of the well casing. For each logger the string length was measured and recorded to determine its elevation compared to the elevation of the ground surface. The loggers measure absolute pressure, which requires a measurement of atmospheric pressure to convert to height of water. For this reason, an additional logger was placed in the open air in a central location to the two study sites.

3.1.3 River Level Monitoring

In addition to water level loggers in the wells, one was placed in the channel at each cross section on either the right or left bank. The choice of right or left bank was determined by ease of access and if the logger would be submerged throughout the growing season. The loggers were hung from the top of a 6.35 cm (2.5 inch) perforated PVC pipe that was anchored in place by an eight foot T-post with half its length driven into the channel bed. Monitoring the river level at these locations allowed for comparison between the interior well water levels and the river water level as well as a method for calculating water storage within the reach.

To calculate surface water storage in the reach, stage-top width relationships were developed for each cross section and a simple prism and wedge geometry was assumed between cross sections. A surveyed cross section and example relationship for cross section ARKU is shown in Figure 10. To develop the stage-top width relationships, surveyed cross sections were organized in spreadsheet form and the distance from left bank to right bank was calculated at 0.1 m intervals of stage. The rest of the cross section relationships for the Arkansas River and all cross sections for Timpas Creek are presented in Appendix C. Daily values for surface water storage were calculated using the following steps:

1) Measuring the change in wetted area of each cross section over the 24 hours using the top widths calculated through the stage-top width relationship at the beginning and end of the time step and calculating a trapezoidal area.

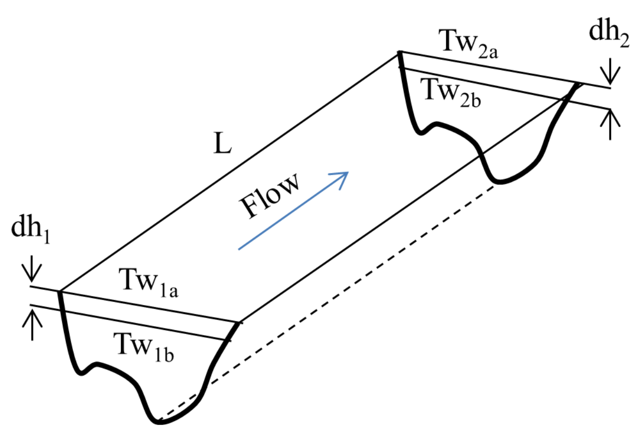

$$dA_1 = \frac{1}{2}(Tw_{1a} + Tw_{1b})dh_1 \quad [1]$$

$$dA_2 = \frac{1}{2}(Tw_{2a} + Tw_{2b})dh_2 \quad [2]$$

2) Assuming the channel between the cross sections was a prism and multiplying the average change in area by the distance between the cross sections (L).

$$\frac{dV}{dt} = \frac{1}{2}\left[\left(\frac{dA_1}{dt}\right) + \left(\frac{dA_2}{dt}\right)\right] L \quad [3]$$

3) Assuming the volume of the wedge between the upstream and downstream cross sections equaled the stored volume within that section of the channel over the time step.

4) Summing the stored volumes from each section of the reach.

Performing this calculation and including surface water storage in the water balance allows for a more accurate calculation of groundwater contribution or surface water removal in each study reach. The cross section plots also provide insight into the variation in the channel dimensions moving from up to downstream.

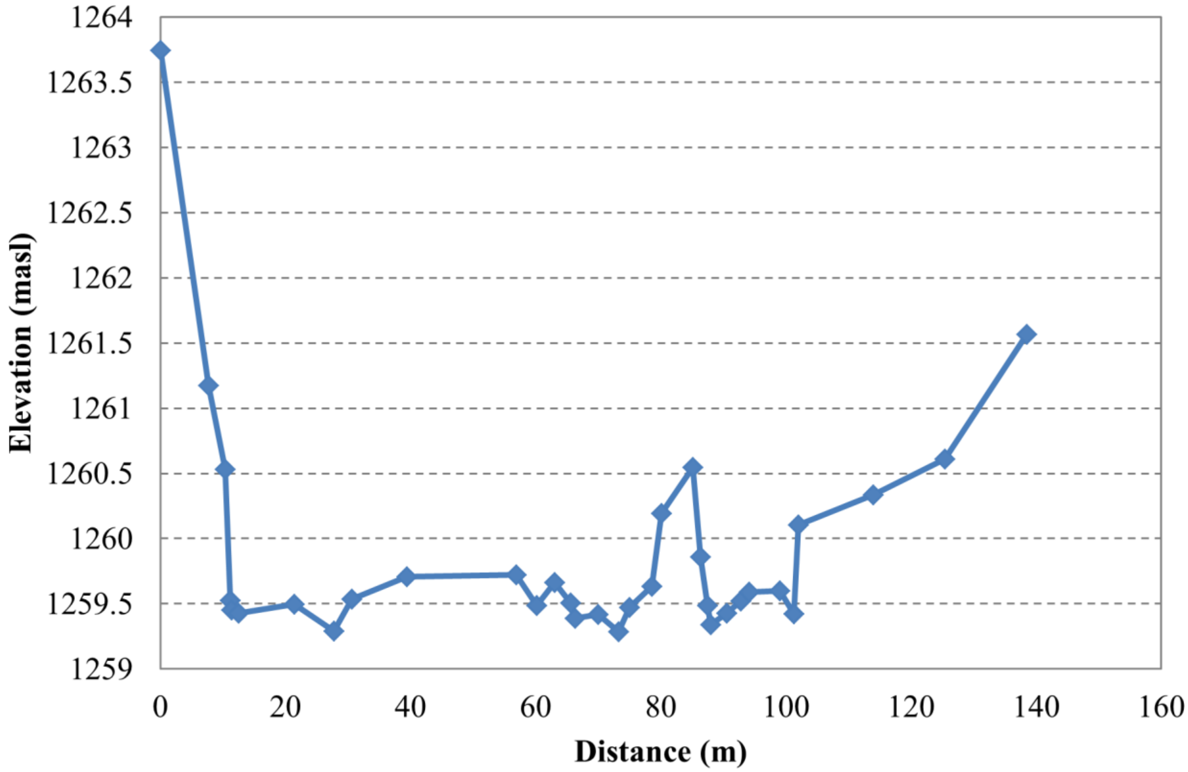

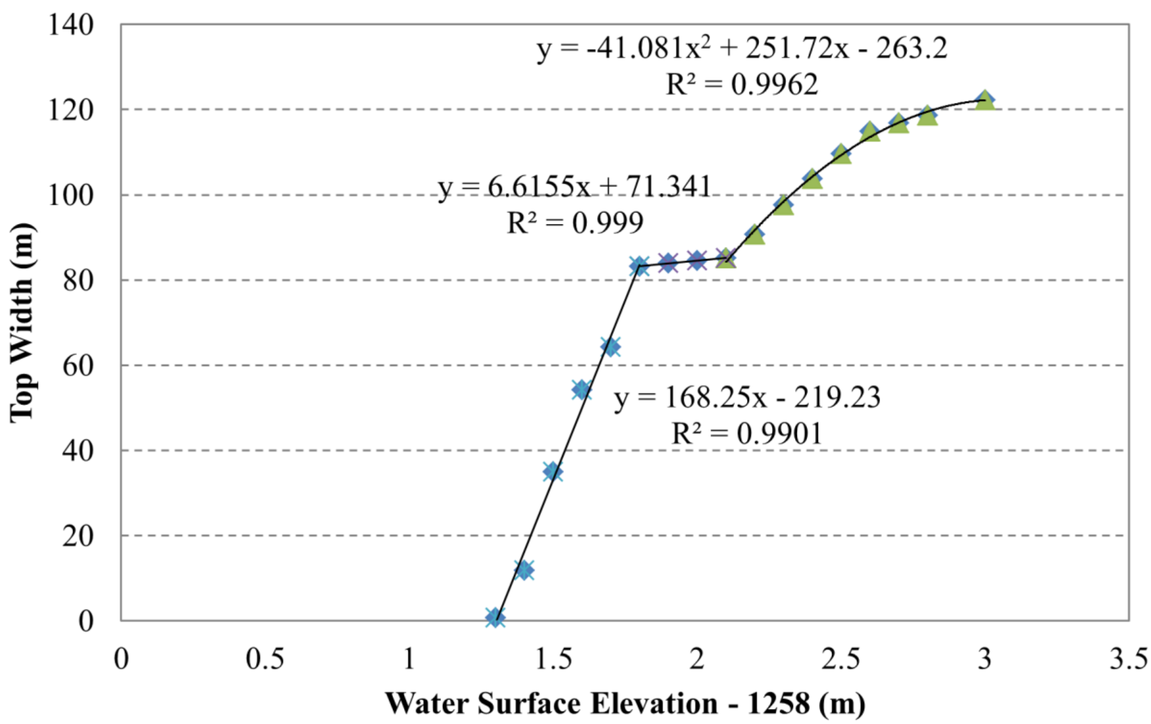

Figure 10. ARKU cross section survey and stage-top width relationship.

3.1.4 Water Quality Sampling

Throughout the study period water quality samples were collected at the upstream and downstream locations of each study reach at approximately two week intervals. Samples were also collected from a major contributing surface drain on Timpas Creek approximately every two weeks. Water samples were collected in 1.0 L plastic bottles as close to the main flow as possible. Total samples for total P and total N were taken by shaking the 1.0 L collection bottle to suspend all sediment and then decanting into a 0.25 L sample bottle. Dissolved samples for NO_2^- as N, NH_4^+ as N, NO_3^- as N, and dissolved salts were filtered through a 0.45 µm filter and into another 0.25 L sample bottle. Filters were changed for each sample and the peristaltic pump tubing was cleaned with acid, phosphate free detergent, and two rinses with distilled water. All water samples were stored on ice in coolers or refrigerated with a maximum hold time of three days before being overnighted to Ward Laboratories, Inc. in Kearney, Nebraska for analysis.

3.1.5 Arkansas River Nitrate Mass Balance

A mass balance approach was used for calculating NO_3^- loads in an attempt to further quantify nutrient loadings in the Arkansas River. To begin, a general mass balance equation is presented (Equation 4a). By rearranging and inputting NO_3^- specific variables, Equation 4b for unaccounted for NO_3^- mass is created.

$$(\text{Mass In} - \text{Mass Out}) \pm (\text{Sources and Sinks}) = \text{Change in Mass Storage} \quad [4a]$$

$$M_{NO_3^-} = \left(\frac{dV}{dt} \text{ x } C_{sw}\right) - (Q_{I_{US}} \text{x } C_{US}) + (Q_{O_{DS}} \text{ x } C_{DS}) \quad [4b]$$

$M_{NO_3^-}$ = daily unaccounted for NO_3^- mass

$\left(\frac{dV}{dt} \text{ x } C_{sw}\right)$ = NO_3^- mass stored in the channel

$(Q_{I_{US}} \text{x } C_{US})$ = NO_3^- load at upstream monitoring station

$(Q_{O_{DS}} \times C_{DS}) = NO_3^-$ load at downstream monitoring station

The C variables stand for NO_3^- concentration in respective sources. For example, C_{sw} represents the concentration of NO_3^- in the surface water which was assumed to be the average of the upstream and downstream concentrations. To determine this surface water average NO_3^- concentration and concentrations at the upstream and downstream monitoring stations (C_{US} and C_{DS} respectively), specific conductivity-NO_3^- relationships were developed. Specific conductivity and NO_3^- relationships were developed for the ARKU and ARKD monitoring stations using data collected throughout the study period and historic data where available. Similar relationships have been developed between conductivity and NO_3^- in other water quality studies to determine seasonal trends and storm event concentrations of nutrients (Gali et al. 2012, Iwanyshyn et al. 2009). This analysis was not performed on the Timpas Creek study reach because a continuous record of specific conductivity was not available due to flooding (discussed further in Section 3.2.1.2). Total P was not included because no relationship with specific conductivity was found.

After removing one outlier value from each dataset, the specific conductivity-NO_3^- rating curves for the Arkansas River showed a strong positive relationship at ARKU and a moderate positive relationship at ARKD with R^2 values of approximately 0.91 and 0.65 respectively. The rating curves are shown in Figure 11.

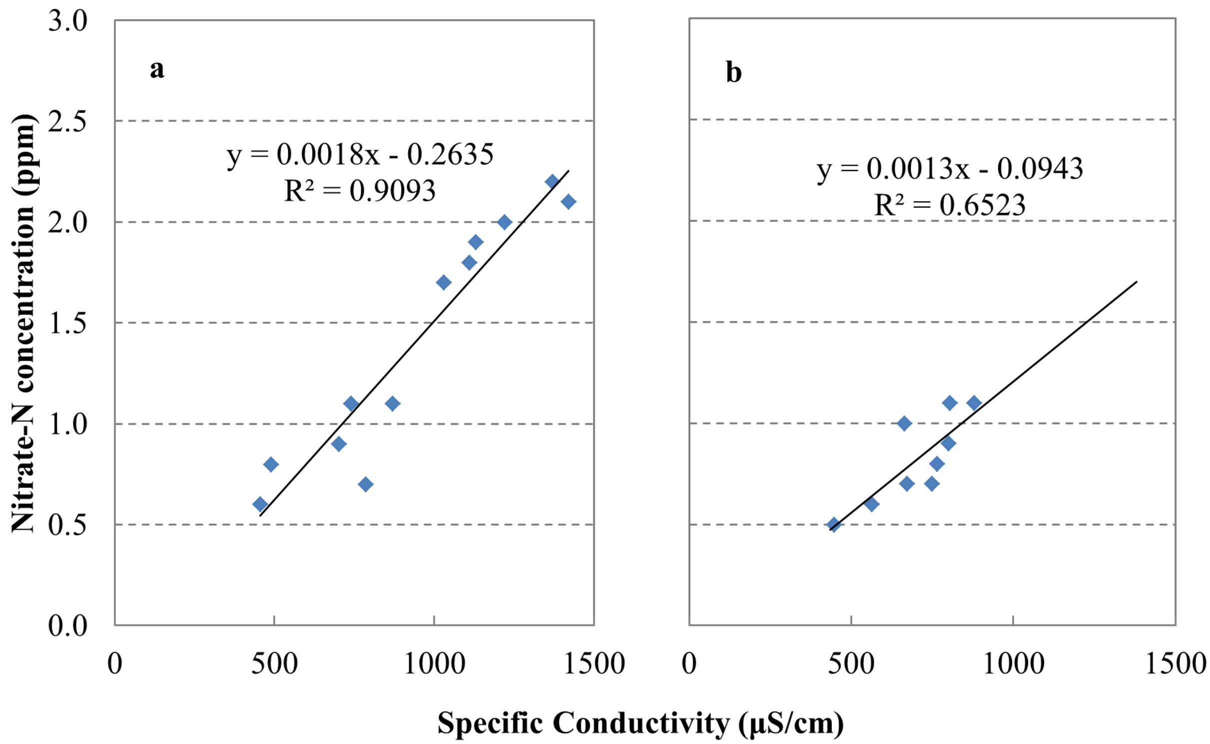

Figure 11. The relationship between specific conductivity and NO_3^- at a) ARKU and b) ARKD.

Using these rating curves and the continuous measurement of specific conductivity at ARKU and ARKD a concentration for NO_3^- could be determined at 15 minute intervals for both monitoring stations. This in turn allowed for a NO_3^- loading to be calculated for the Arkansas River study reach for every day during the study period.

Daily unaccounted for NO_3^- mass includes all other sources and sinks of NO_3^- along the length of the reach. This includes groundwater contributions and in-stream processes such as denitrification or biological uptake. To separate groundwater and in-stream processes, unaccounted for flow values from the growing season water balance presented in Section 3.2.1.2 were coupled with NO_3^- concentrations to calculate daily averaged loadings into and out of the reach. The NO_3^- concentrations for the unaccounted for flows depended on whether the reach was losing or gaining on that day. For losing periods the same average of up and downstream concentrations, C_{sw}, was used as in Equation 4. For gaining periods, the median value (0.1

mg/L) of the interior wells and pore water concentrations, presented in Chapter 4, was used. This is a slight overestimation since many of the concentrations were actually reported as <0.1 mg/L.

3.2 Results and Discussion

3.2.1 Flow Estimation

3.2.1.1 Arkansas River

Using the stage-discharge rating curves described above, daily averaged flows were calculated during the study period at ARKU and ARKD. Due to flooding and readjustment of the AT, flows for ARKD were only calculated after June 9. A comparison of ARKU and ARKD with average daily flows in cubic meters per second is shown in Figure 12. The flow increase after May 16 was associated with the spring snowmelt while the remaining peaks were the result of intense rain events.

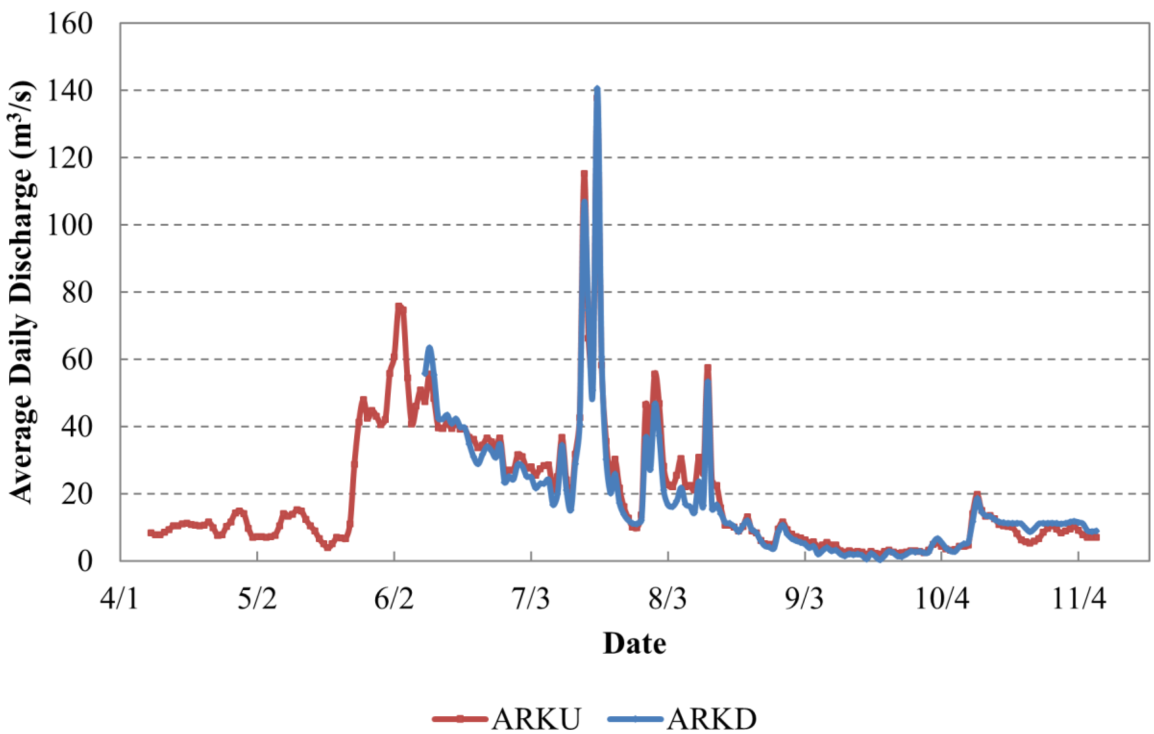

Figure 12. A flow comparison of ARKU and ARKD during the growing season.

The precipitation received by the region during the study period is presented in Figure 13. The monthly averages show a drier than average year except for the months of July and October, each of which received more than twice its average rainfall. Half of the rainfall in July came during a single event, beginning just after July 12. The 5.7 cm of local precipitation as well as other contributing regions in the watershed receiving similar rainfall amounts caused the two peaks in mid-July. The provisional peak flow measured during this time period was over 208 m^3/s before the ARKU gage was compromised. The two peaks beginning on July 30 resulted from two separate rain events each amounting to approximately 1.25 cm. The final peak occurred on October 13 and was caused by a rain event of approximately 2 cm over two days.

Figure 14 depicts the water surface elevation at cross section ARKA at peak flow during the study period (red line) as well as the water elevation during average flow conditions (green line). As shown, the high flows overtopped the riverbanks and inundated much of the low lying floodplain, flooding monitoring wells, during this time period. A normalized flow plot for the ARKU monitoring station is presented in Figure 15 to determine how the average daily flows compare to historic records. The thick black line at the 1.0 horizontal represents equilibrium between 2014 data and historic values. The analysis uses individual historic daily averages since 1992 to normalize the 2014 data. Based on this plot, nearly the entire high flow period beginning in mid-May during snowmelt and mid-August after the flooding occurred was approximately two to four times greater than the daily historic averages. The flows in June normalized approximately to unity and the flow peak in mid-October suggests flows were three times higher than average.

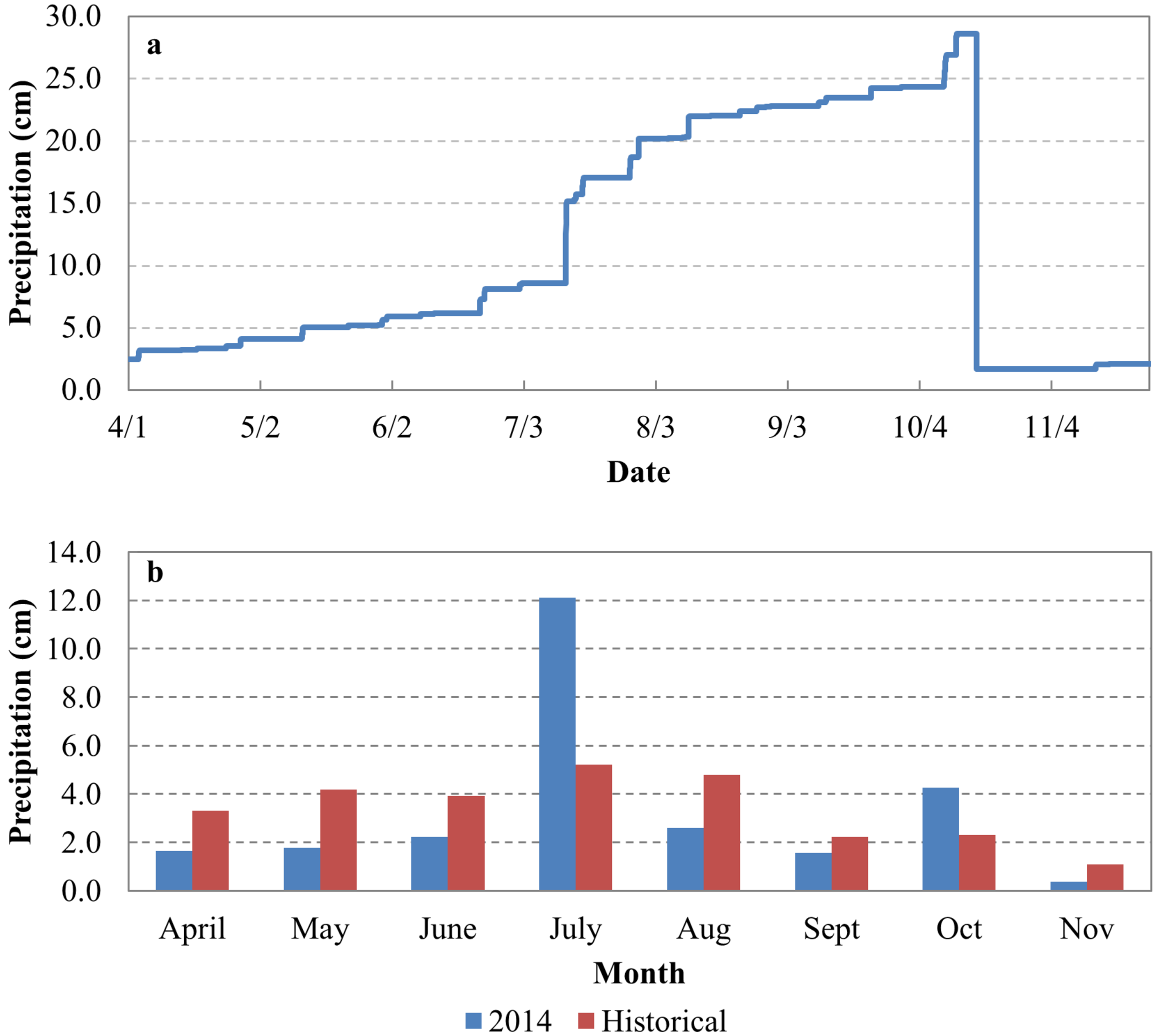

Figure 13. a) Cumulative daily and b) monthly precipitation measured over the study period.

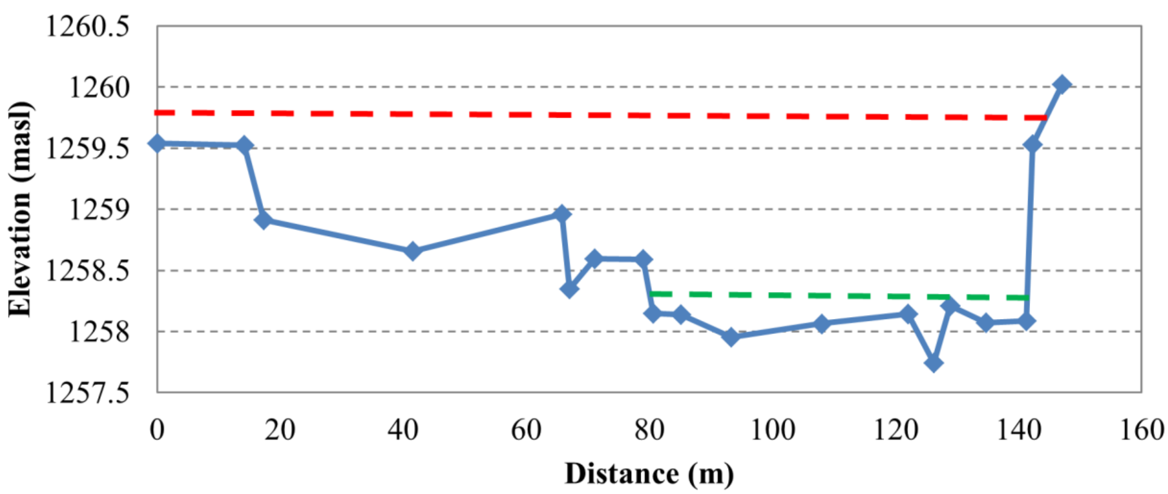

Figure 14. ARKA cross section during average flow and 2014 peak flow.

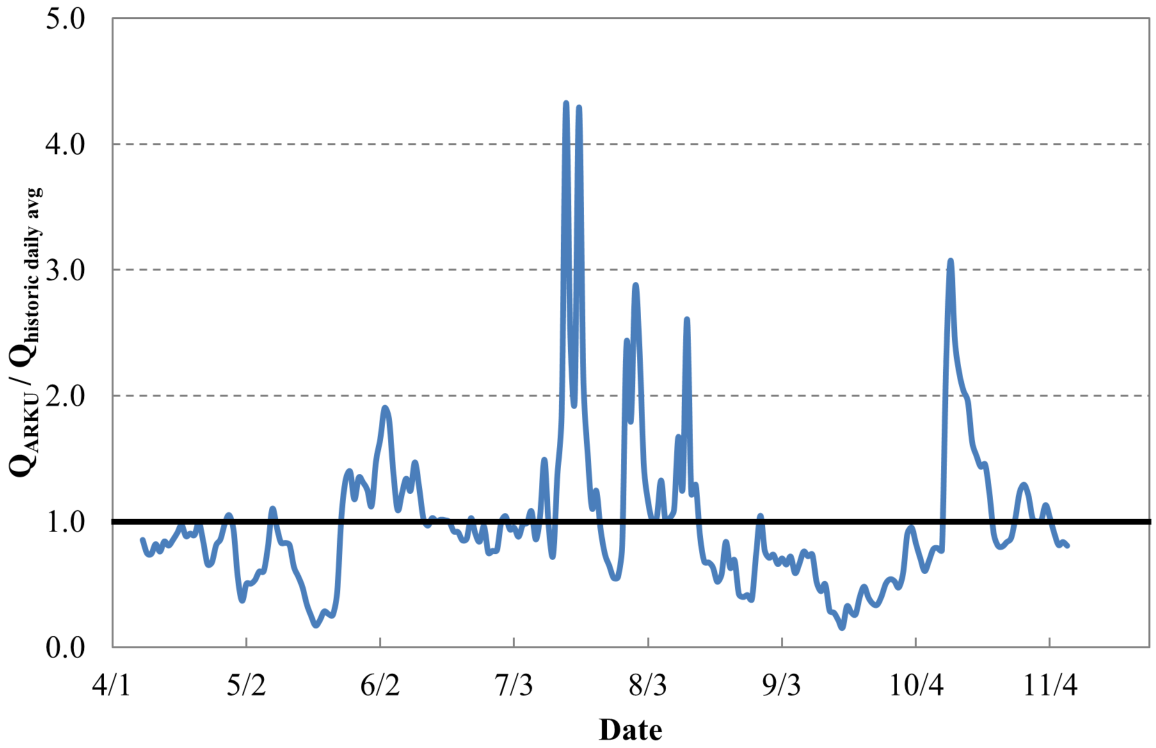

Figure 15. Normalized plot of discharge at ARKU using the historic daily averages for each day in the study period.

As stated in Section 3.1.1 the stage-discharge rating curve at the ARKD monitoring station is only supported by physical discharge measurements up to 12.7 m³/s. Any discharges greater than 12.7 m³/s rely on values from the upstream station. Therefore, most of the period during the high flooding in mid-July has been removed from subsequent groundwater quantification calculations. An approximation of the daily unaccounted for flow is presented in Figure 16. Unaccounted for flow can either be positive if the study reach is gaining water volume or negative if it is losing volume. These values were calculated using Equation 5 and account for the change in surface storage over the 24 hours.

$$Q_{net_{GW}} = \frac{dV}{dt} - Q_{I_{US}} + Q_{O_{DS}} \quad [5]$$

$Q_{net_{GW}}$ = unaccounted for flow

$\frac{dV}{dt}$ = change in storage in the channel

$Q_{I_{US}}$ = discharge at upstream monitoring station

$Q_{O_{DS}}$ = discharge at downstream monitoring station

The procedure for surface storage calculation presented in section 3.1.3 produced values that accounted for between 0.0% and over 100% of the difference between the ARKU and ARKD discharges with an average of 19%. Surface storage values were generally between 0.0% and 10% of the ARKU and ARKD discharges. Based on these values, in channel surface storage was considered to have a significant effect on the overall water balance and was therefore included in the water balance calculations.

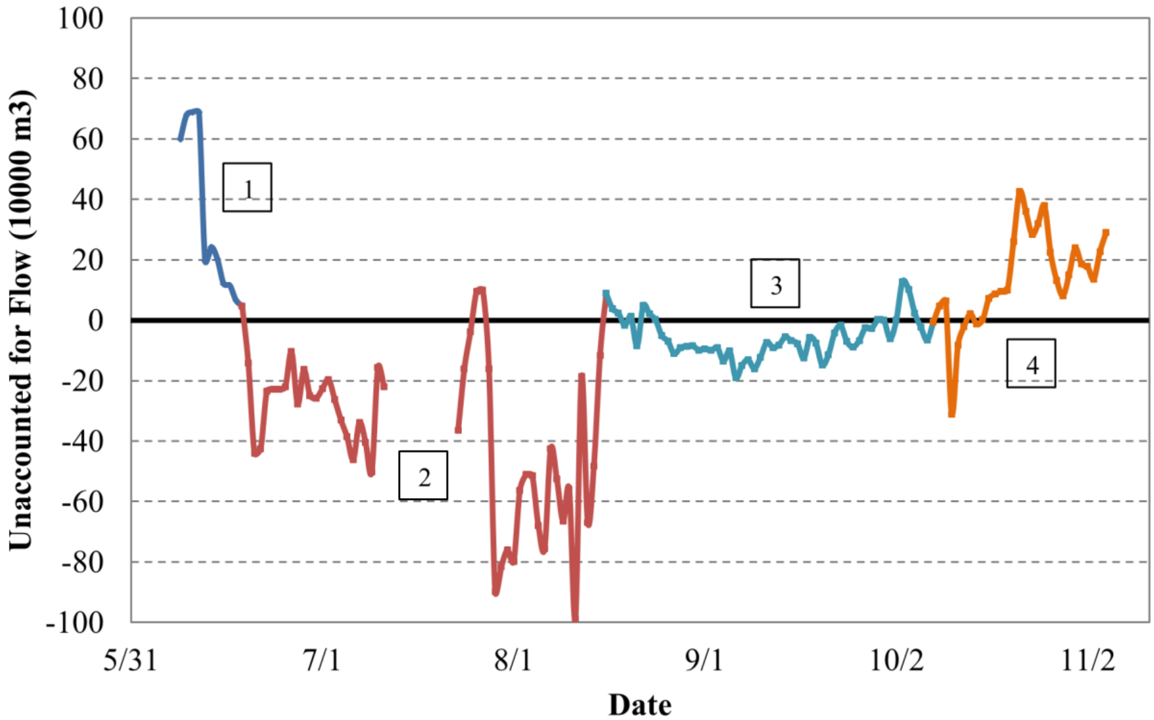

Figure 16. Summed daily values of unaccounted for flow in the Arkansas River during the study period. Section 1 corresponds to the Snowmelt Period, section 2 to Flooding Period, section 3 to End of Summer Period, and section 4 to End of Season Period.

In general, this section of the river appears to lose flow from the river to the aquifer since the unaccounted for flow is primarily negative. This is particularly noticeable during sustained flooding events, for example, after the spring snowmelt in early June or during the multiple large floods in July and August. The large variations between June and mid-August could also be the result of errors in the ARKD rating curve due to the assumption made for higher flows described in section 3.1.1. An unpublished stochastic modeling study performed by CSU researchers provided estimates of average unaccounted for flow along the entire length of the Arkansas River in the USR. This information is presented in Table 3. Positive values in the table indicate a gain of water volume to the river. The values highlighted in red in the table are of particular interest to this study because they suggest a range of potential values for water volume gained or water volume lost from the river. The Stochastic 2.5% and Stochastic 97.5% percentile models provide estimates of the high and low extremes. One caveat for these values is that they are based on the entire ~50 km reach of the Arkansas River in the USR and over a much longer time period (3-5 years). This large spatial and temporal scale includes many diverse and variable parameters such as riparian vegetation cover, hydraulic conductivity, soils, depth to bedrock, rainfall, high or low flow years, etc… This immense amount of variation which has been reduced to a set of six numbers is representative of the entire study region on average, but not necessarily of a 5 km reach within it.

Table 3. Upstream Study Region groundwater flows. All values are in m^3/s per km.

Model	**2.5%**	**Mean**	**97.5%**
Stochastic 2.5%	-0.1122	-0.0088	0.09072
Stochastic Mean	-0.0405	0.05	0.1794
Stochastic 97.5%	0.02927	0.109	0.272

If the entire study period in Figure 16 is considered, the total volume of unaccounted for flow sums to approximately -1.32×10^7 cubic meters. This translates to -0.22 m^3/s per km of the study reach. This value is nearly twice the amount of the negative extreme in Table 3 but within an order of magnitude. If the study period is split into four distinct periods (see Figure 16);

1) Snowmelt Period from July 8-July 18

2) Flooding Period from July 19-August 15

3) End of Summer Period from August 16-October 8

4) End of Season Period from October 9-November 5

all of the values for unaccounted for flow are still within an order of magnitude of the two extremes as shown in Table 4. As expected, the End of Season Period shows that the aquifer is contributing flow to the river when irrigation water has moved through the aquifer and been able to affect the groundwater gradients.

Table 4. Periods of unaccounted for flow and their associated length averaged values.

Period	Total Unaccounted for Flow (m^3)	Length Averaged Flow ($m^3/s/km$)
Snowmelt	3,649,922	0.83
Flooding	-17,884,967	0.95
End of Summer	-2,934,482	-0.14
End of Season	3,938,268	0.35

3.2.1.2 Timpas Creek

Similar to the Arkansas River, daily averaged flows were calculated during the study period at TIMU and TIMD. A flow comparison between the two stations, shown in Figure 17a and b, is comparable to that of the Arkansas River. Two graphs were required to present the variation in the data with more clarity. Peaks in the flow hydrographs correspond with the same rain events described in section 2.2.1.1 and shown in Figure 13. Timpas Creek is not directly affected by the spring snowmelt and therefore, exhibits no peak in the hydrograph in May. Flow contributed by the surface drain mentioned in section 2.1.4 is also shown in Figure 17. Contributions from the drain were typically below 0.5 m^3/s. The rain events in June and July caused excessive flooding in Timpas Creek. Flows overtopped the banks along much of the reach carrying debris and displacing equipment. The daily flow average on July 13 reached a value of 68 m^3/s but the peak flow during that day was 195.1 m^3/s which amounts to approximately a 14 year flow. This was calculated using the yearly peak flow data provided by the USGS and a Weibull plotting position method. The flood displaced the downstream AT installation, causing a significant gap in the TIMD data while equipment was repaired and replaced. Two photographs in Figure 18, taken directly after the flooding, show scoured banks and the extent of the flooding.

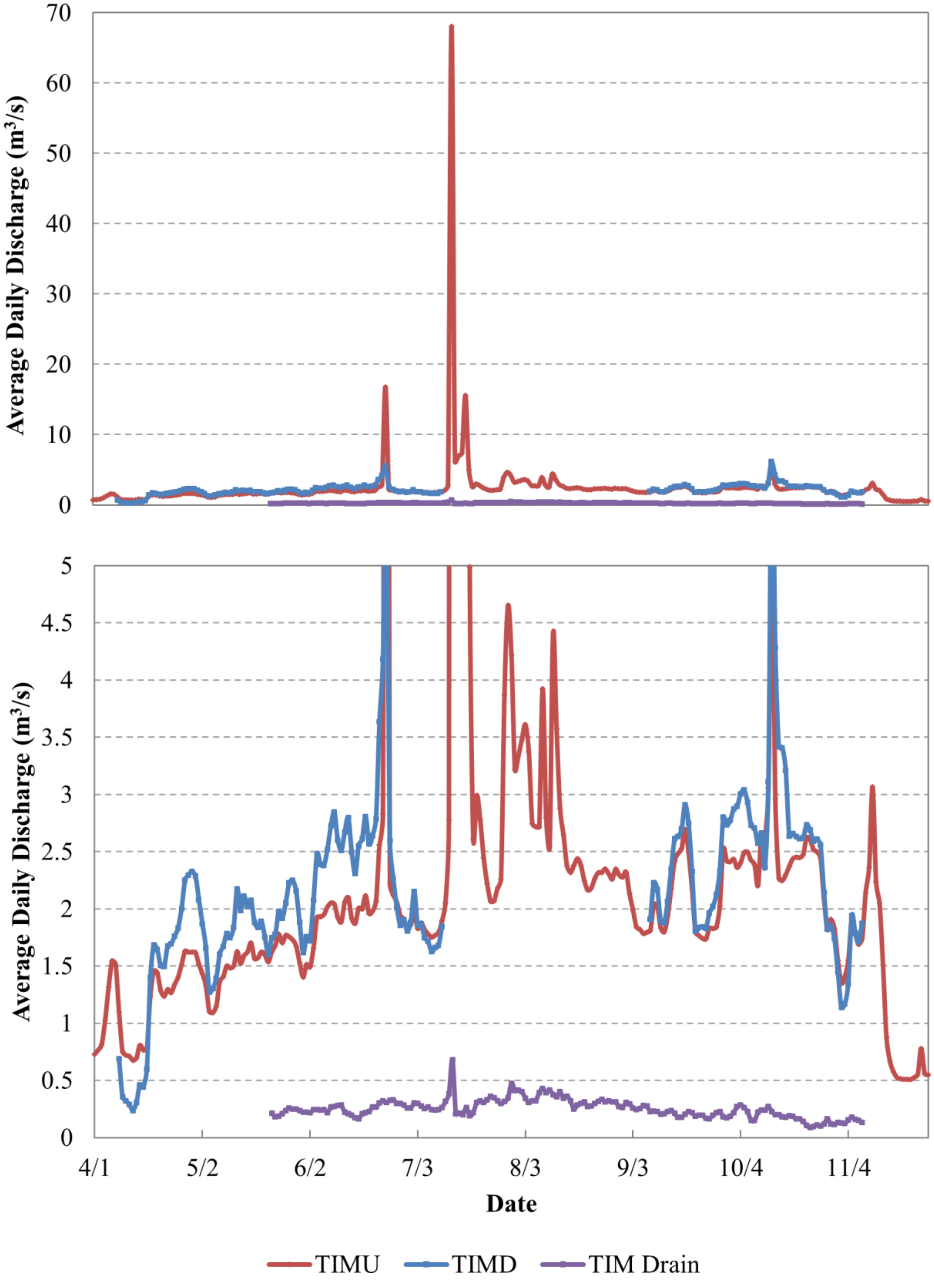

Figure 17. a) Full scale b) Zoomed in growing season flow comparison of TIMU, TIMD, and TIM Drain during the study period.

Figure 18. Photographs taken after the flooding on Timpas Creek

A normalized flow plot for the TIMU monitoring station is presented in Figure 19 to show the magnitude of the average daily flows based on historic records. Similar to the ARKU plot, the thick black line at the 1.0 horizontal represents equilibrium between 2014 data and historic values normalized by the historic average of each day. As expected, the flooding events show up clearly in this plot ranging from two times the average magnitude during the flows in October to nearly 20 times greater during the flows in July. The rest of the study period varies around unity, which suggests that flows were average for that time of year.

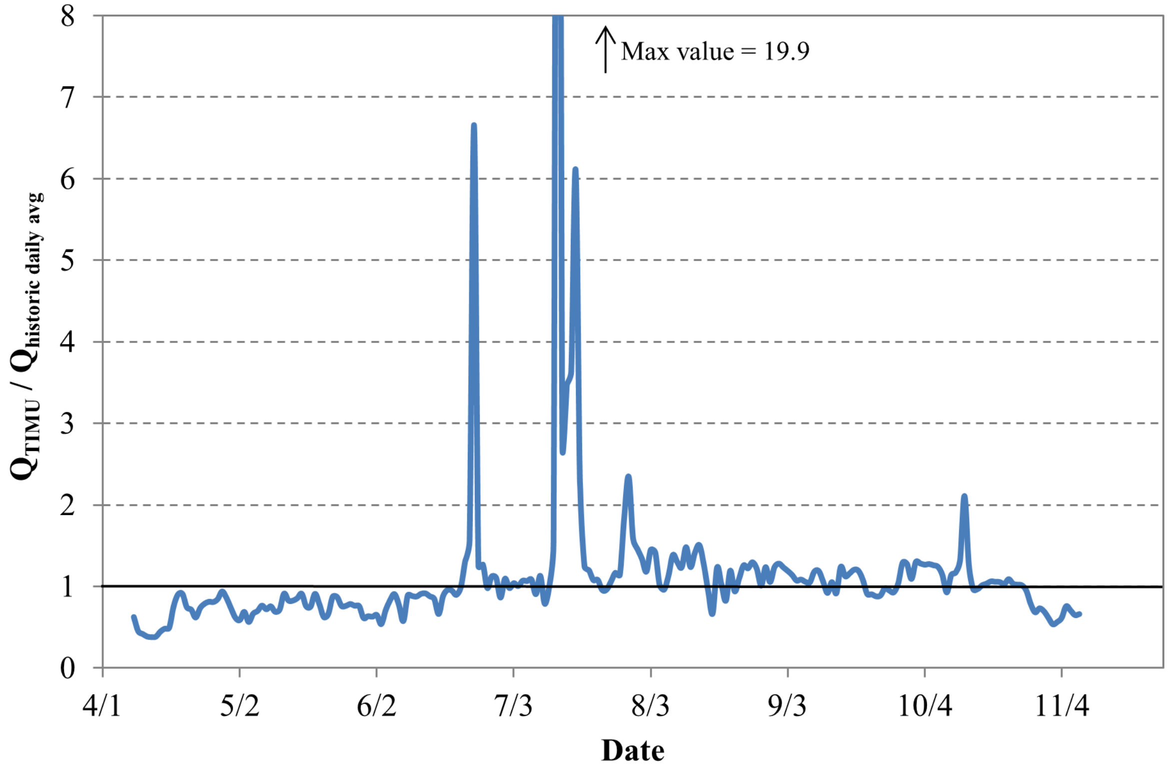

Figure 19. Normalized plot of discharge at TIMU using the historical average of the entire study period.

The discrepancies between the TIMU and TIMD flow hydrographs during the flooding are likely due to the low range of flow measurements used to construct the TIMD rating curve. Average daily flow values for Timpas Creek based on the USGS's 50 years of records indicated a range between 0.7 m^3/s (25 ft^3/s) and 4.25 m^3/s (150 ft^3/s). The TIMD flow measurements would have been sufficient for a typical year of flows on Timpas Creek, however, they are not effective in estimating flow in extreme flooding events. For this reason, the data with high discrepancies for flows above 6.0 m^3/s were removed from the calculation of unaccounted for flow in Timpas Creek. An approximation of the daily unaccounted for flow is presented in Figure 20. These values were calculated using Equation 6.

$$Q_{net_{GW}} = Q_{O_{DS}} - Q_{I_{US}} - Q_{I_{DR}} \quad [6]$$

$Q_{net_{GW}}$ = unaccounted for flow

$Q_{I_{US}}$ = discharge at upstream monitoring station

$Q_{I_{DR}}$ = discharge at TIM Drain.

$Q_{O_{DS}}$ = discharge at downstream monitoring station

The procedure for surface storage calculation presented in section 3.1.3 produced values that accounted for between 0.0% and 3.0% of the difference between the ARKU and ARKD discharges with an average of approximately 0.75%. Surface storage values were generally between 0.0% and 2.0% of the TIMU and TIMD discharges. Therefore, the effect of in channel surface storage was considered insignificant on the overall water balance and was not included in the calculations above.

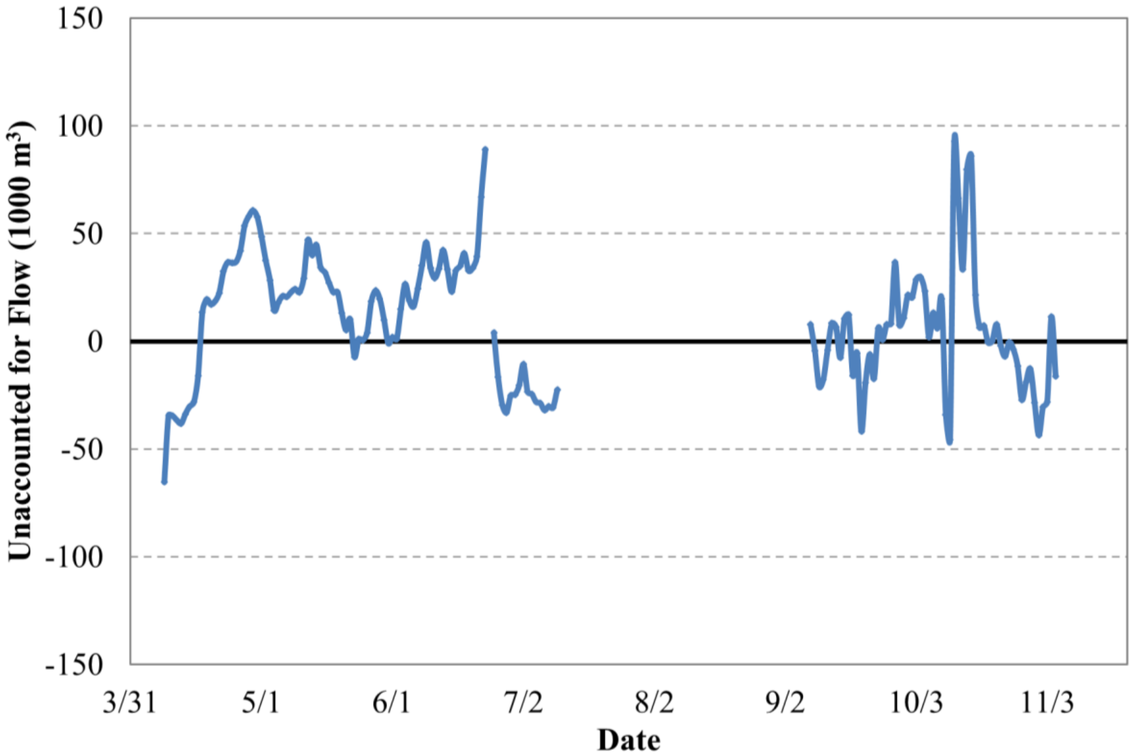

Figure 20. Summed daily values of unaccounted for flow in Timpas Creek during the study period.

The plot above shows unaccounted for flow fluctuating between -60,000 m^3/day and almost 100,000 m^3/day during the study period. Of the days where a water balance was successful the total unaccounted for flow was approximately $1.3x10^6$ m^3, which translates to 0.048 m^3/s per km of the study reach. At the beginning of the irrigation season, the creek appears to be losing flow to groundwater. In mid-April unaccounted for flow switches from negative to positive suggesting that groundwater has begun to contribute to flow in Timpas Creek. After flooding at the end of June, unaccounted for flow becomes negative again. No data is presented after the July flooding due to loss of equipment. Unaccounted for flow fluctuates around zero from early September to the end of the study period with a spike in mid-October. The October spike was likely due to the precipitation event causing unmeasured overland flow and groundwater recharge.

In comparison to the Arkansas River, Timpas Creek displays similar reactions to flood events. The reach appears to lose flow to the aquifer during sustained floods. However, the creek shows the opposite result in changes between growing and non-growing (irrigation and non-irrigation) seasons. Groundwater contributions are lower or less than zero at the beginning and end of the irrigation season. This suggests that the creek reacts more quickly to irrigation contributions to the aquifer, which is supported by the fact that there are irrigated fields directly adjacent to the creek. This also suggests that the groundwater table along this reach may in fact be lower than the creek bed during low or non-irrigation time periods and that any surface flow during these periods is the result of baseflow from upstream sources.

3.2.2 Groundwater Monitoring

3.2.2.1 Arkansas River

The well installation described in section 2.1.2 allowed for continuous monitoring of water level elevation at each cross section. The data allowed for an estimation of groundwater gradients at each cross section as well as seasonal variation in the water table. In the plots below the exterior well water elevations are represented by dark red and dark green lines, the interior wells are represented by light red and light green lines and the elevation of the water in the channel is represented by the blue lines. Each well cross section is shown in Figure 21.

The ARKA cross section is not a straight line perpendicular to the river. Wells A1 and A2 are approximately 300 meters upstream of wells A3 and A4. This explains the marked difference in water elevations between A2 and the river water level, as well as A3. Theoretically, these levels should be close to one another assuming a relatively flat water surface in the channel and high connectivity between the surface water and groundwater at the interior wells. Despite this longitudinal variation ARKA exhibited a clear gradient towards the river from A1 to A2 and away from the river from A3 to A4 during the entire study period. It was only during peak flows in the river that A2 water elevations were higher than A1. These relationships suggest that the river was consistently gaining water from the direction of wells A1 and A2 while it was consistently losing water to the aquifer in the direction of A3 and A4.

Gradients between wells in cross section ARKB were also evident. There was a gradient from B1 to B2 as well as from B4 to B3 towards the river for the majority of the study period. The exception was during the rise in water elevations in May and the flooding periods in July. This may have been due to a dampened reaction to rising water levels in the exterior wells.

Finally, the water level elevations in ARKC show a much smaller gradient between the wells than ARKA or ARKB. However, it shows a similar trend in gradients from the exterior wells to the interior wells and a quick response of the interior wells during high flow events. These growing season plots suggest that water volume was lost to the aquifer during flooding events. Once the floods subsided, the gradients switched indicating that water volume was flowing back into the river channel. This is supported by the Arkansas River unaccounted for flow in Figure 16, which shows a contribution of water volume back to surface water after the high flows from snowmelt and after the smaller flow event in October. However, this post-high flow contribution is noticeably lacking from the frequent, flashy floods in July and August despite the well water elevations showing the same switch in gradients. This may be due to the fact that these high flows were shorter in duration and therefore had less time to influence the aquifer, despite their high magnitude.

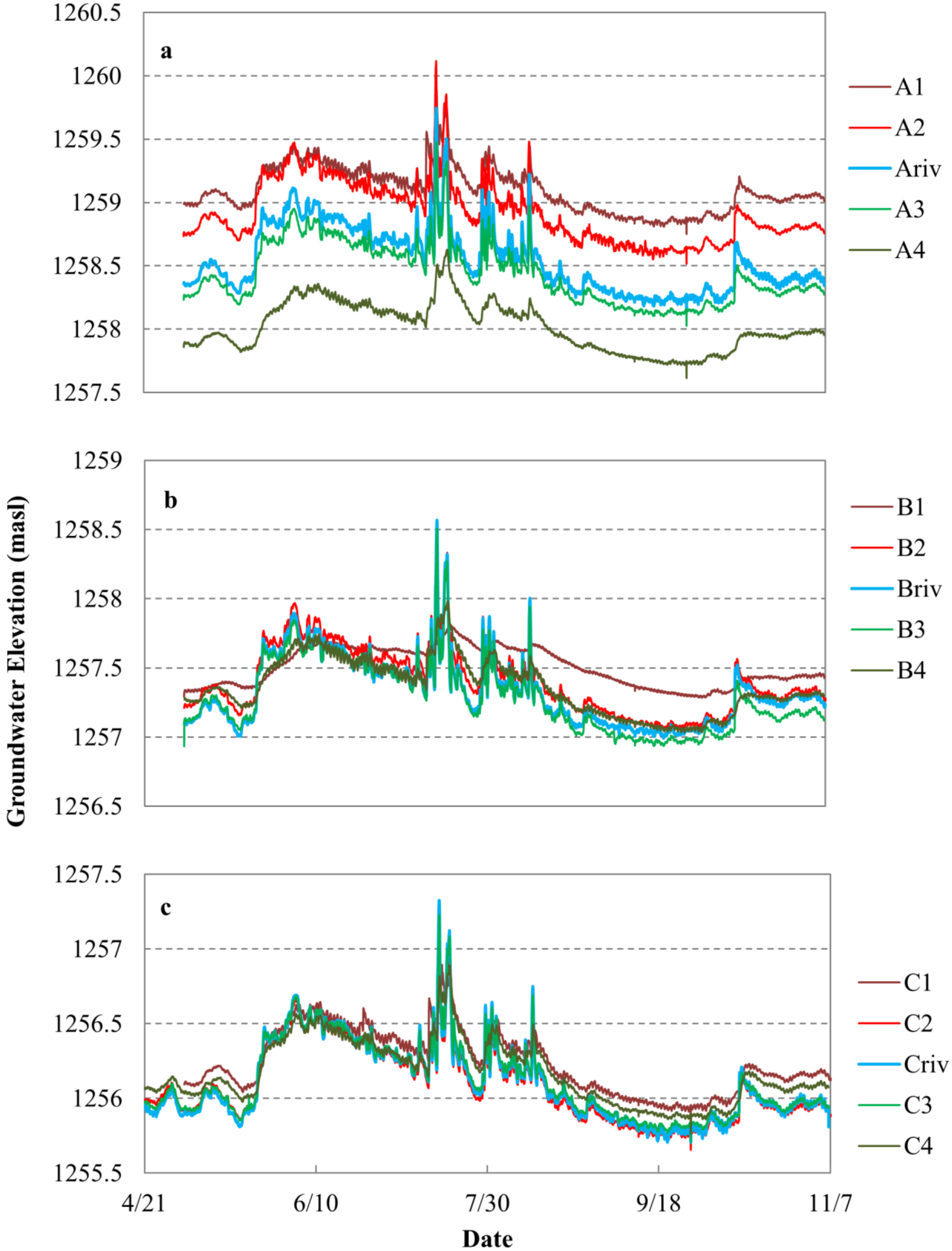

Figure 21. Growing season groundwater elevation in wells at cross section a) ARKA b) ARKB c) ARKC.

3.2.2.2 Timpas Creek

Well water level elevations for both cross sections on Timpas Creek are presented in Figure 22. Wells A4 and A3 exhibited a substantial gradient towards the creek throughout the study period, an elevation difference of nearly 5 meters. This data was confirmed by landowner reports on the southeast side of the creek who stated evidence of high groundwater tables in the area and frequent yard flooding during rain events. A smaller gradient existed from A2 to A1, suggesting a general motion of groundwater away from the creek. Floods in this area primarily affected wells A1 and A2 because of their low ground elevation in the creek floodplain. Both wells were inundated by flood water in July which is supported by the matching peak water elevations at Ariv, A1, and A2. The reported water levels were higher than the ground elevations.

Gradients in cross section TIMB were much smaller than in TIMA. Both sets of wells exhibited a gradient away from the stream, suggesting a loss of water from the creek. A larger gradient existed from B2 to B1. The head difference between these two wells averaged 36 cm throughout the study period, while the head difference between B3 and B4 averaged 7 cm. Any substantial flow contributed to the creek from the aquifer appears to occur in the vicinity of wells A3 and A4. However, the hydraulic conductivity values for this area were some of the lowest recorded values as seen in Table 2. This suggests that the low conductivity of the soils may be causing a higher groundwater table rather than high volumes of water moving through this area. Unlike the Arkansas River, the creek groundwater elevations exhibited no evidence of a gradient switch during or after large flow events. With the exception of wells A3 and A4, the gradients away from the creek simply became larger.

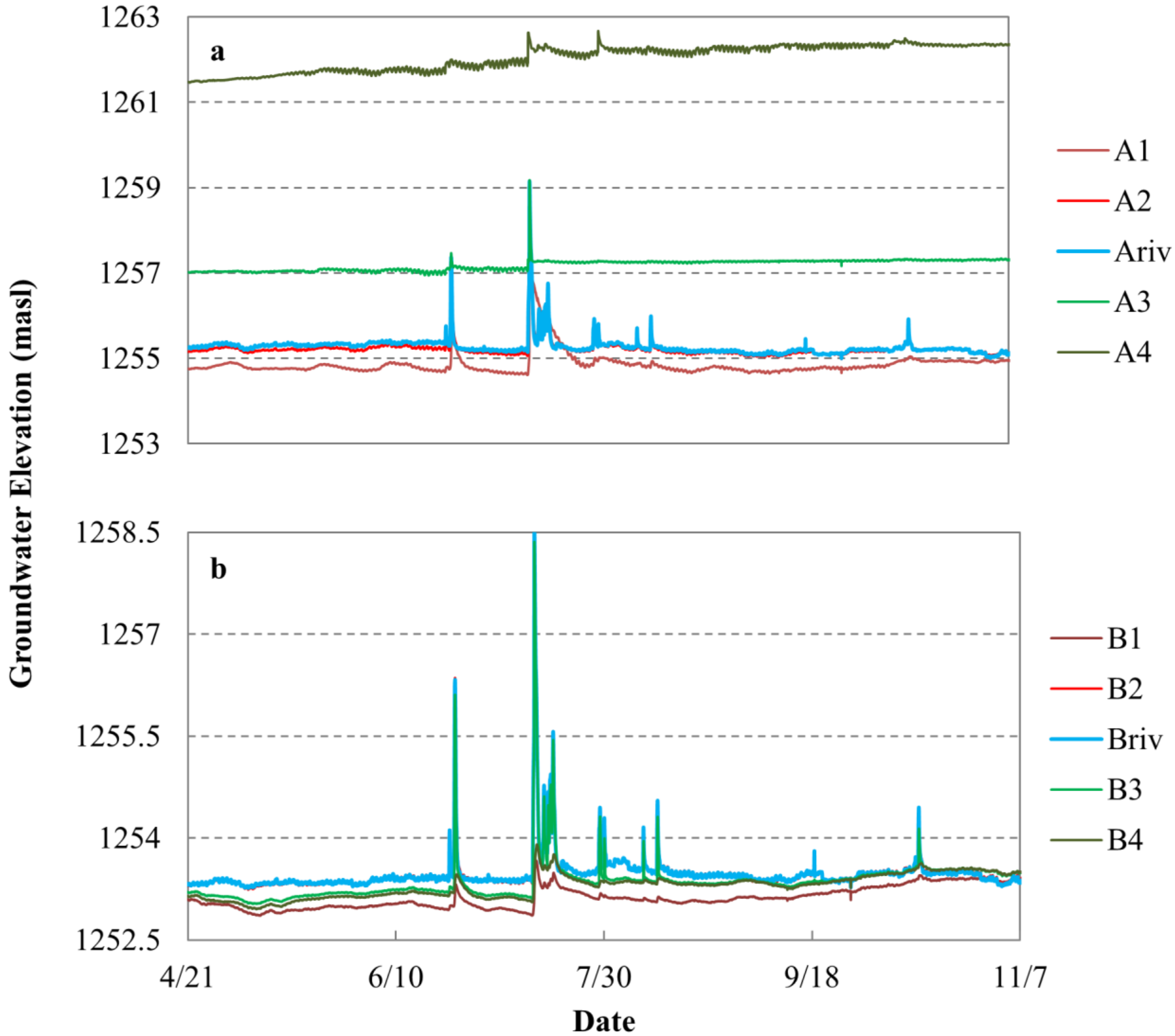

Figure 22. Growing season groundwater elevation in wells at cross section a) TIMA b) TIMB.

One problem with interpreting these gradients as shown is that it assumes a one-dimensional flow path toward or away from the creek. This same assumption was made when the wells were installed perpendicular to the creek. However, the small hydraulic head differences at cross section TIMB suggest that the wells may have been installed along a groundwater contour and therefore do not truly represent gradients away from the creek. This is supported by contour maps produced from data at two dates during the study period presented in Chapter 4.

3.2.3 Water Quality Monitoring

3.2.3.1 Arkansas River

The first basic water quality parameter monitored during the entire study period on the Arkansas River was specific conductivity. The daily averaged values at ARKU and ARKD are presented in Figure 23. The ARKU values (red line) are based on data collected at the Colorado Division of Water Resources ARKROCCO station, which were comparable to the ARKU AT installation (green line), and the ARKD values were taken from the downstream AT installation (blue line). ARKD monitoring did not occur until after May 21 due to sediment buildup around the conductivity sensor on the AT. ARKU values are presented before that date to provide a pre-monitoring estimate. Referring back to Figure 12 a negative relationship exists between specific conductivity and flow (Gali et al. 2012). The spring snowmelt provided highly diluted surface water, causing the sharp drop in specific conductivity in May. High flows through the spring and early summer maintained a lower specific conductivity value but as flows began to decrease after the spring snowmelt, values began to increase slowly until the end of the study period, with a few short-term decreases due to rain events.

The specific conductivity between ARKU and ARKD also exhibited differences beginning in early August. However, this separation is less pronounced between the ARKU AT, which was relocated in early September to replace the lost AT at TIMD, and ARKD. The specific conductivity sensor maintained by the USGS at ARKU is an YSI 600/600R 2 parameter probe and was located approximately 30 m downstream of the Aqua Troll. The difference between these two probes, calibration procedures, or placement in the water column may have resulted in slightly different readings. This is supported by the figures in Appendix D which present plots of the major dissolved ions sampled during the growing season nutrient sampling.

None of the figures show any large decreases in concentration from upstream to downstream throughout the study period.

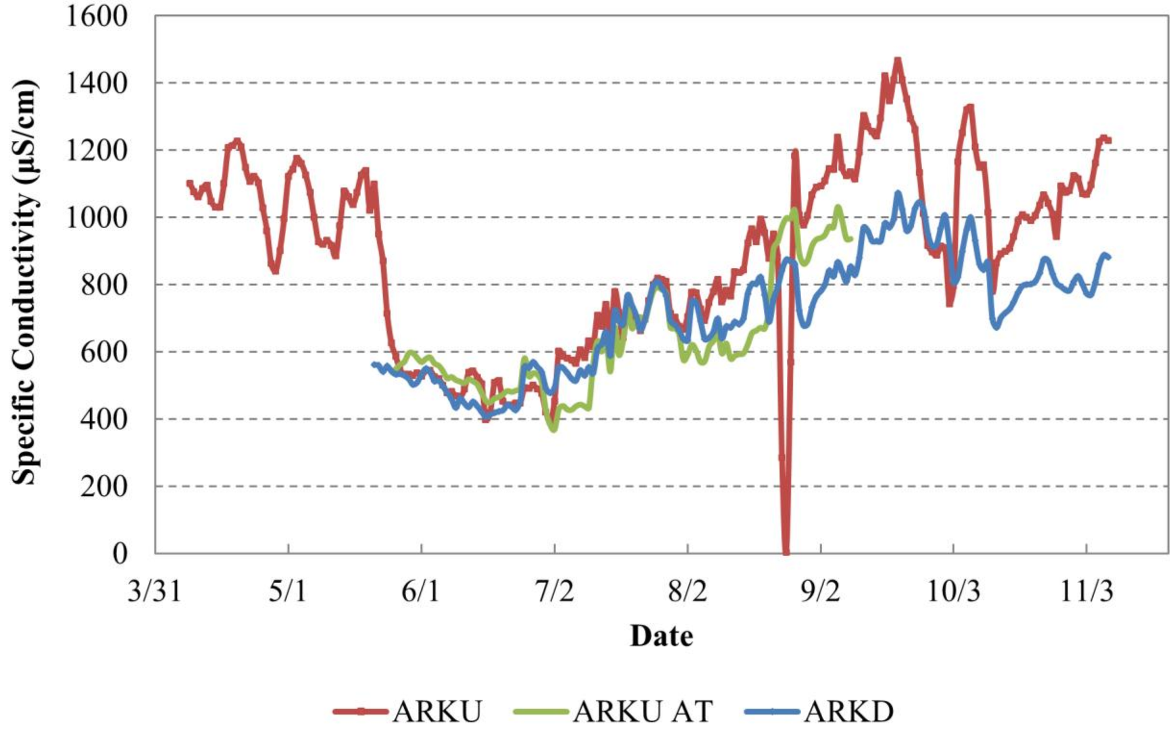

Figure 23. Comparison of specific conductivity between ARKU and ARKD during the growing season.

Water quality samples from the Arkansas River for chloride and total P are presented in Figure 24 and total N and NO_3^- as N in Figure 25. The filled in circles on the plots represent actual sample dates during the study period while dotted lines represent interpolated general trends between points. Chloride concentrations are presented with discharge to show the conservative nature of chloride in this system. There is only a small change in concentration from upstream to downstream at all dates. Total P also shows no significant differences at sample dates throughout the study period. Total N and NO_3^- as N, however, exhibit a decrease in concentration from ARKU to ARKD ranging from 35% to 66% after early to mid-August. After mid-August the total N and NO_3^- as N concentrations at ARKU steadily increase and plateau at three mg/L and two mg/L respectively. An increase of approximately 60% for total N and nearly 200% for NO_3^- as N. The concentrations of these constituents at ARKD increase only slightly to 1.9 mg/L of total N and 2 mg/L of NO_3^- as N. An increase of approximately 36% and 57% respectively.

The decrease in N species concentration corresponds with lower flows in the river after August. Low flows and slower velocities likely allowed for more residence time in the channel, increasing opportunities for interaction with river bed substrate and the exchange of surface and groundwater in the hyporheic zone (Puckett et al. 2008, McMahon and Böhlke 1996). Puckett et al. (2008) also suggested that a complex exchange due to coarse sediments and varying hydraulic gradients in the channel can create zones of denitrification in the river bed. While hydraulic gradients were not measured within the channel, the sandy river bed of the Arkansas River and water quality measurements presented later in this report suggest high amounts of exchange in these areas. However, low organic carbon percentages and low cation exchange capacity values of the river bed sediments (presented in Appendix E) suggest this is not the only mechanism for NO_3^- removal. Increased biological activity such as plant assimilation within the channel during the spring and summer months may have been a factor (Cooper 1990).

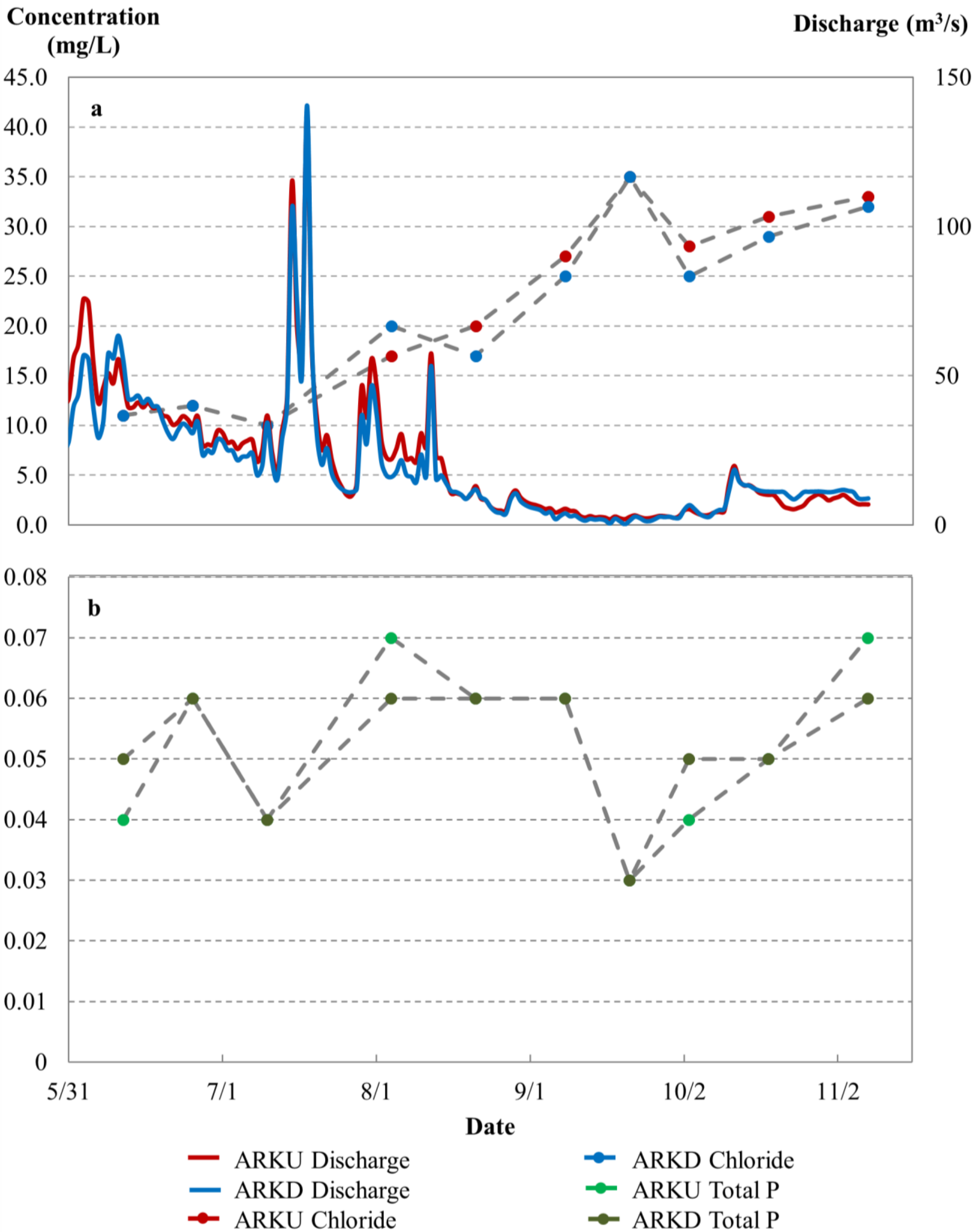

Figure 24. Growing season a) discharge and chloride concentrations b) Total P concentrations at ARKU and ARKD.

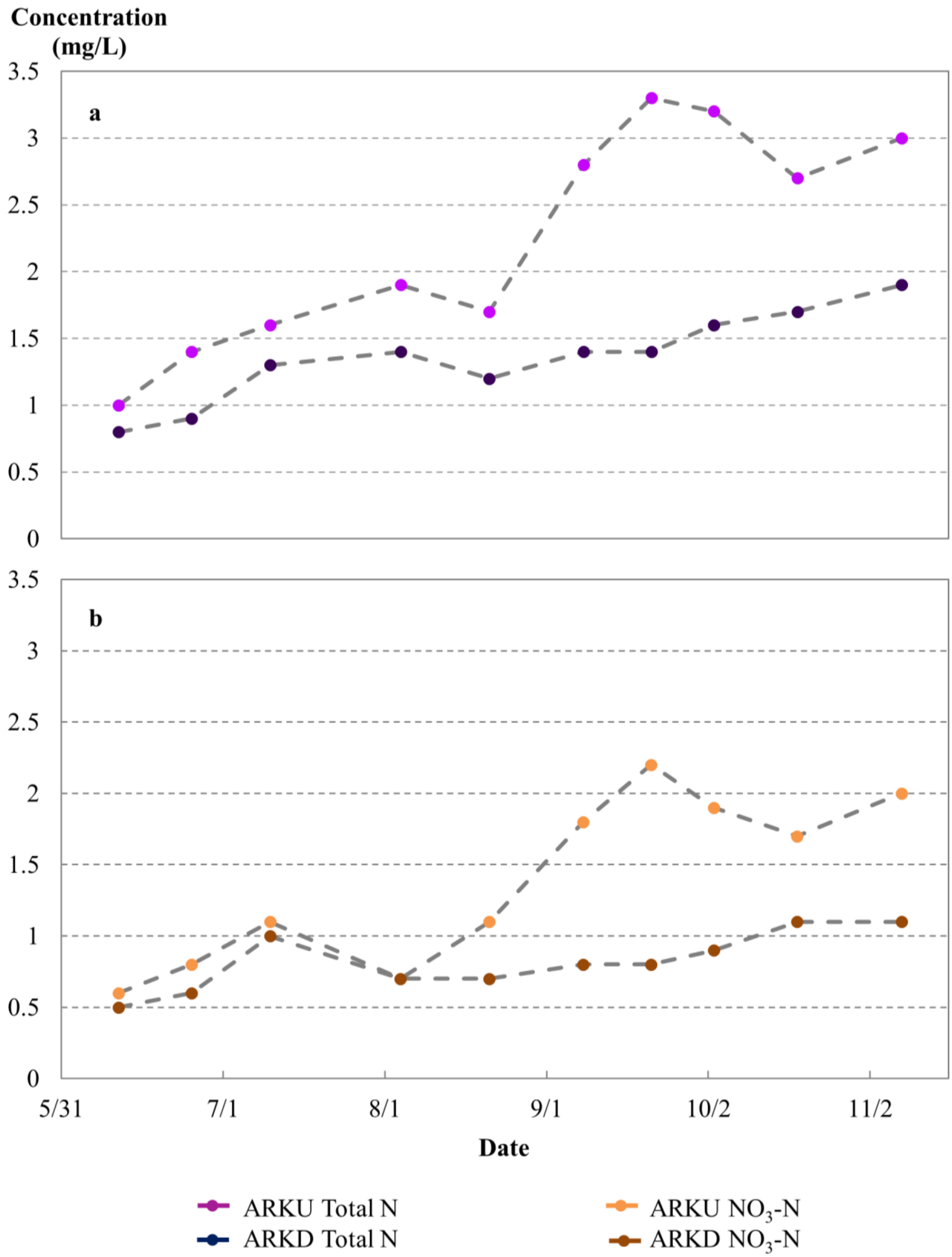

Figure 25. Growing season a) Total N concentrations and b) NO_3-N concentrations at ARKU and ARKD.

3.2.3.2 Timpas Creek

Timpas Creek was monitored for the same water quality constituents as the Arkansas River with interruptions in the specific conductivity and discharge measurements due to flooding and equipment repairs. The specific conductivity data is presented in Figure 26 and shows very little variation from upstream to downstream. The lower values at TIMD may be the result of discharges from TIM Drain causing dilution downstream. Water quality samples from Timpas Creek for chloride and total P are presented in Figure 27 and total N and NO_3^- as N in Figure 28. Once again, the chloride concentration is considered conservative in the system. In contrast to the Arkansas River all the remaining constituents show very little variation from upstream to downstream during the study period. Only one point on the total P plot (highlighted in red) shows any variation and that has been labeled as an outlier due to potential contamination during sampling.

The lack of any growing season length trends in the water quality data from Timpas Creek expected. The study reach is short and the channel has been incised from high flow velocities. As mentioned in Chapter 2 the study reach has a gravel bed underlain by a hard impenetrable layer assumed to be clay or bedrock. The high velocities and thin mixing zone of gravel suggests there is very little chance for interactions with creek bed substrate or the hyporheic zone. The low hydraulic conductivity values on the creek banks, ranging from 0.09 to 1.1 m/day, as well as groundwater water quality data presented later in this thesis (see Chapter 4, Section 4.2.2), give weight to the hypothesis that there is very little exchange of groundwater and surface water along this reach.

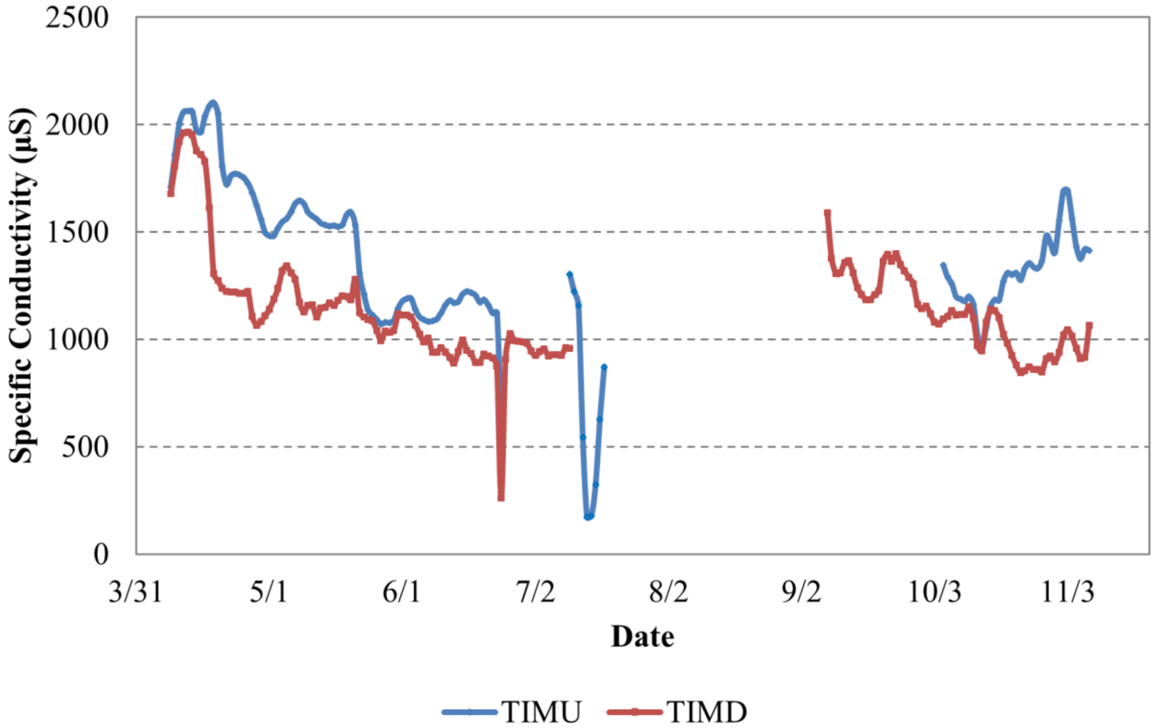

Figure 26. Comparison of specific conductivity between TIMU and TIMD during the growing season.

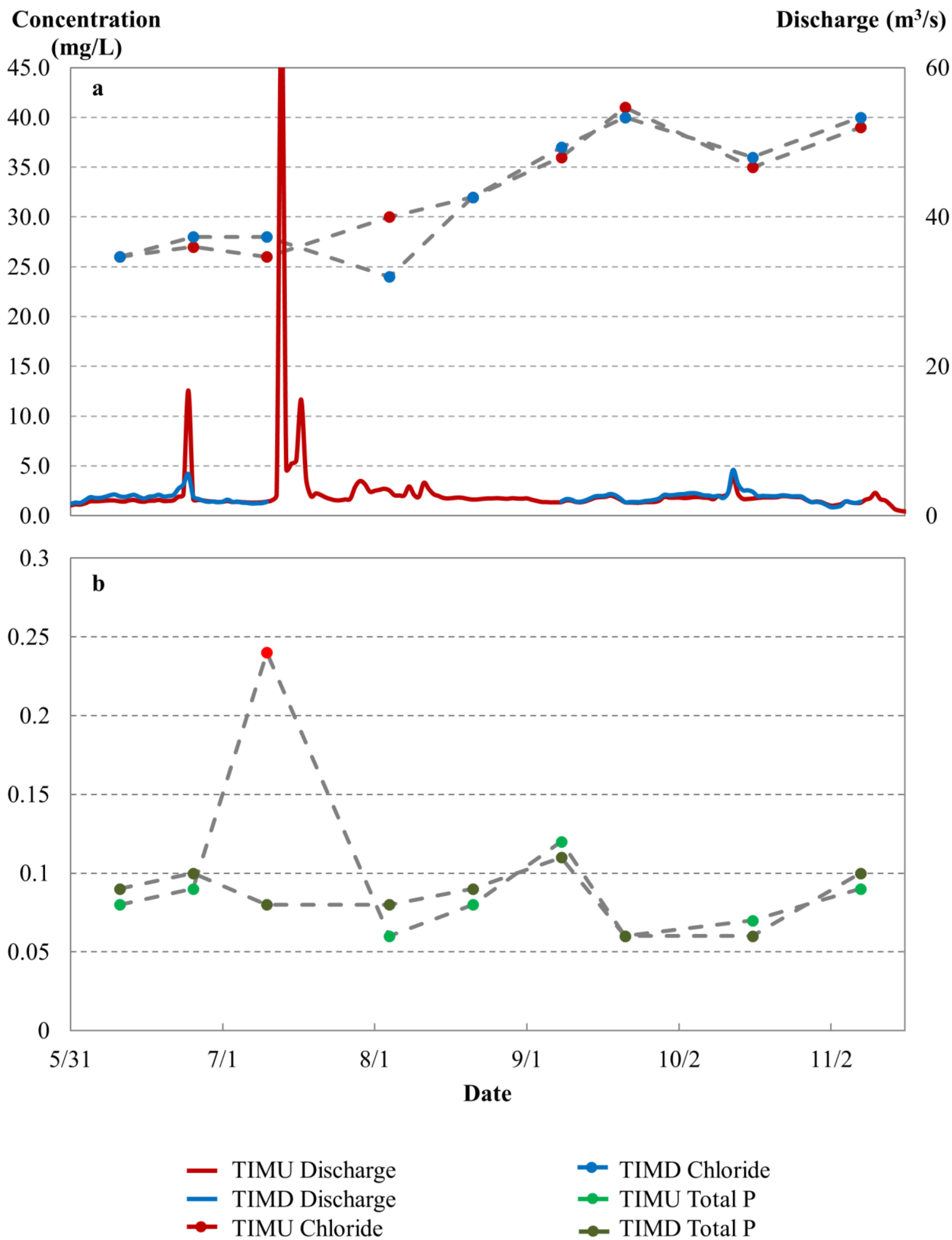

Figure 27. Growing season a) discharge and chloride concentrations b) Total P concentrations at TIMU and TIMD.

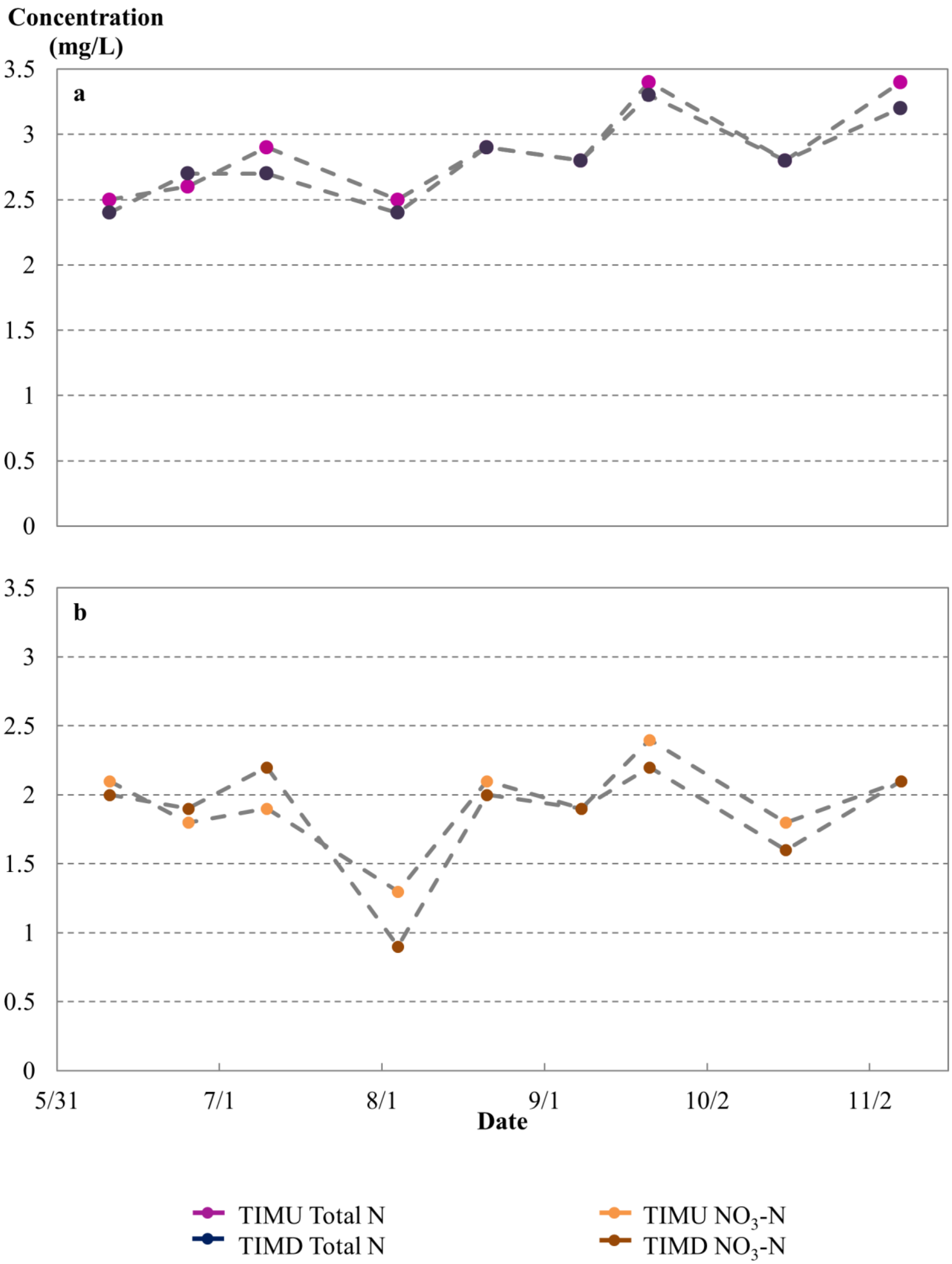

Figure 28. Growing season a) Total N concentrations and b) NO_3-N concentrations at TIMU and TIMD.

3.2.4 Arkansas River Nitrate Mass Balance

Using the specific conductivity-NO_3^- relationships and Equations 4 and 5 from section 3.1.5, and average daily flows from section 3.2.1, a growing season NO_3^- mass balance was calculated for the Arkansas River study reach. The results of the NO_3^- mass balance are presented in Figure 29. The figure shows calculated daily summations of total unaccounted for NO_3^- mass (Unmeasured Bulk) and losses of NO_3^- to the aquifer or gains to the reach through the exchange of surface and groundwater (Groundwater).

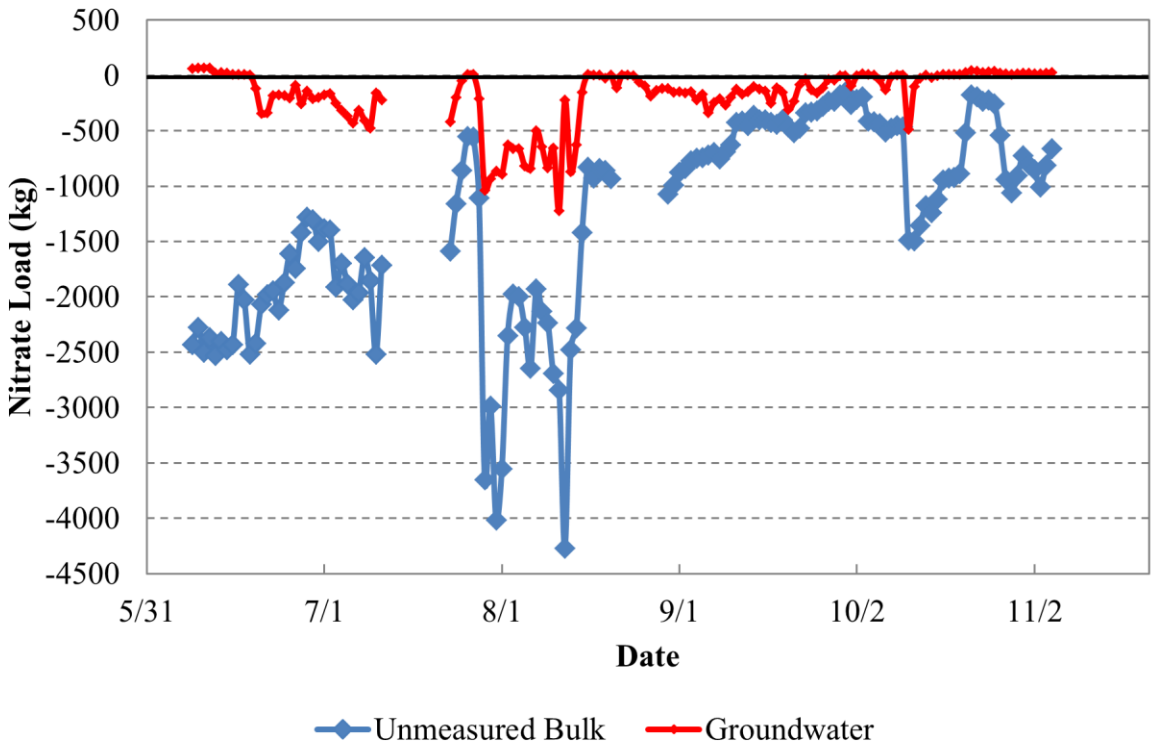

Figure 29. Unmeasured NO_3^- load from specific conductivity-NO_3^- relationships and mass balance calculations.

The figure shows that, in general, there is a net loss of NO_3^- mass during the entire growing season along this study reach. Where data existed and calculations could be performed, NO_3^- mass losses to the aquifer accounted for approximately 23% of the total loss for the entire period. The high estimated net loss of NO_3^- mass prior to mid-August is likely due to high discharges, with calculations possibly affected by uncertainty in the ARKD discharge rating curve. Inspection of the ARKU specific conductivity-NO_3^- rating curve also suggests that the relationship performs best at higher values of specific conductivity and, therefore, at lower discharges. Another issue with this period is that growing season water quality monitoring results do not support the early season results. They showed very little change in NO_3^- concentration between ARKU and ARKD until after the June and July floods.

The issues with the data prior to mid-August suggest it may not accurately represent NO_3^- loadings over the entire growing season. If the period after mid-August is considered separately, the NO_3^- losses to the aquifer account for 27% of the total unaccounted for NO_3^- mass. This suggests that 73% of the losses, observed between mid-August and November, can be attributed to in-stream and hyporheic zone processes such as biological uptake and denitrification. This amounts to nearly 37,000 kg of NO_3^- as N removed in 68 days within the 4.7 km reach. Based on the ARKU specific conductivity-NO_3^- relationship, approximately 78,000 kg was delivered to the Arkansas River study reach, which suggests that 47% of the total incoming NO_3^- load was removed by in-stream processes. However, it should be noted that the results shown in Figure 29 are uncertain due to uncertainty in discharge and loading estimates. With more data collection to strengthen the specific conductivity-NO_3^- rating curves and more accurate discharge measurements this technique could be used to determine NO_3^- loadings and NO_3^- removals in the reach at any point in time between manual sample events.

3.3 Conclusions

Water quantity and quality monitoring throughout the study period provided considerable insight into groundwater and surface water interactions and aquifer-stream nutrient mass exchange in the Arkansas River and Timpas Creek. Discharges in the Arkansas River were lower than average except during spring snowmelt in May and June and high flow events in July and October. Based on growing season monitoring of water table elevations and unaccounted for flow, during high flow events, the groundwater gradients would switch and contribute water to the aquifer. After these high flow events subsided the gradients would switch back and contribute water volume back to the river, as evidenced by the gain in flow after the snowmelt and October flow events. Contribution of flow to the river at the end of the season is also expected due to the lag of irrigation return flows contributing water volume to the aquifer and affecting the groundwater gradients around the river.

Growing season water quality sampling results in the Arkansas River suggested that there was little to no change in the concentration of the majority of dissolved ions or total P between the upstream and downstream ends of the study reach. However, NO_3^- and total N decreased in concentration between the upstream and downstream ends during low flows in the summer and fall. This is potentially due to increased reactions with river bed substrate, increased exchange with the hyporheic zone, or increased biological activity during the summer. A growing season mass balance of NO_3^- based on a relationship between NO_3^- and specific conductivity confirmed this result. Calculations suggested that in-stream processing and biological uptake account for approximately 73% of the NO_3^- mass removed in the system during this period, amounting to 47% of the total load entering the study reach. While errors in early season discharge measurements at ARKD made the data less reliable, more data collection and better methods of discharge measurement would provide a cost-effective and efficient way to track NO_3^- in this system.

Discharges in Timpas Creek were typical of the historic average for the study period, except during the high flow events in late June and July. Evidence of groundwater recharge to the creek only existed in one monitored location, however, it was determined that water table measurements elsewhere along the study reach were not representative of the regional gradients. Minimal changes in NO_3^- concentration occurred between the upstream and downstream ends of the study reach, suggesting minimal in-stream interaction with creek bed sediments, exchange with groundwater, or biological activity.

CHAPTER 4: 24-HOUR MONITORING

4.0 Introduction

Two 24-hour sampling events at each study reach occurred during the study period (June through November of 2014). Sampling events occurred once during the early growing season and again at the end of the growing season. The early season event occurred on June 9 and 10 on Timpas Creek and June 11 and 12 on the Arkansas River. The end of season event took place on October 3 and 4 on the Arkansas River and October 17 and 18 on Timpas Creek. The objective of the 24-hour monitoring was to investigate the variation in surface water quality over a 24 hour period and to try to explain those variations by determining the influence of any exchange with the aquifer or hyporheic zone. This short time period allowed for confirmation of trends discovered in the growing season monitoring. This methodology also allowed for monitoring of 24-hour variations (<24 hours) not available from the growing season monitoring. Groundwater and pore water sampling, which were not a possibility during growing season monitoring due to cost and time constraints, provided additional key information about the system.

Each 24-hour monitoring event involved two hour composite samples of surface water over the 24 hours from the auto-sampler setups, one water quality sample from each monitoring well along the reach, pore water sampling from beneath the channel bed, and samples from contributing surface water points. Each sample procedure described below occurred within the appropriate 24 hour period for each study reach with the exception of the pore water sampling. This occurred immediately after the 24 hour period to avoid disturbance of in-stream sampling by the auto-samplers. All water and soil samples were stored on ice in coolers or refrigerated with a maximum hold time of three days before being shipped overnight to Ward Laboratories, Inc. in Kearney, Nebraska for analysis.

4.1 Methods

4.1.1 Groundwater Sampling

During each sampling event, the well cross sections along the study reach were visited by two researchers to sample and to take water quality readings. At each well a low flow QED Sample Pro bladder pump, dual 0.635 cm (0.25 in) diameter polyethylene tubing, and a flow through cell were used to extract groundwater from each well. The pump was set to a flow rate between 0.10 to 0.20 L/min using a CO_2 power pack to minimize the disturbance in the flow through cell. Indicator properties of pH, electrical conductivity (EC), temperature, dissolved oxygen (DO), and oxidation reduction potential (ORP) were monitored at approximately two minute intervals using an YSI 600QS Multiparameter Sampling System (YSI), which was routinely calibrated with standard solutions. The extracted water was considered representative of the surrounding groundwater when four parameters had stabilized for two consecutive readings: +/- 0.1for pH, +/- 3% for EC, +/- 10% for DO, and +/- 10 mV for ORP.

After stabilization was reached and values were recorded, the low flow cell was removed from the end of the pump tube and the pump rate increased to between 0.20 and 0.30 L/min. Total samples for total P and total N were taken by pumping directly into the 0.25 L laboratory provided plastic sample bottle while dissolved samples for NO_2^- as N, NH_4^+ as N, NO_3^- as N, and the W-1 sample package (described in Appendix I) were filtered through a 0.45 µm filter and into another 0.25 L sample bottle. Collection of a dissolved sample is shown in Figure 30. Individual pump tubes were created for each well and the low flow pump was cleaned after each sample with acid, phosphate free detergent, and two rinses with distilled water to avoid cross contamination.

Figure 30. A researcher collects samples from a well. Pump tubing and CO_2 power pack are shown.

4.1.2 Surface Water Sampling

While the wells were sampled, continuous water sampling was performed with ISCO 6700 series automated samplers (auto-samplers) located at the upstream and downstream locations of each study reach. The auto-samplers were housed in the same shelters that the communication end of the AT cables were stored. A shelter and auto-sampler setup is shown in Figure 31. The sampling program consisted of two hour composite samples that were collected in 1 L plastic bottles and kept on ice during the entire 24 hour sample period. The two hour composite samples consisted of pumping approximately 0.10 L of water every 15 minutes. Upon completion of the 24 hour event, the water samples were capped, collected and processed within two hours. Total samples were taken by shaking the 1.0 L collection bottle to suspend all sediment and then decanted into the sample bottle. Dissolved samples were filtered through 0.45

μm filters using a peristaltic pump and collected in another sample bottle. Filters were changed for each sample and the peristaltic pump tubing was cleaned with acid, phosphate free detergent, and two rinses with distilled water.

Figure 31. Shelter and auto-sampler setup at ARKU.

YSI units were also set up at these auto-sampler locations. The probe was placed in the water at or near the intake end of the pump tubing. The data logger, connected by a communication cable, was stored in the shelter. The logger was set to record values for pH, EC, temperature, DO, and ORP every 15 minutes for the duration of the sample period.

4.1.3 Pore Water Sampling

Pore water samples were collected at each well cross section from depths of approximately 0.3 meters on Timpas Creek and one meter on the Arkansas River below the channel bed using an MHE Products PushPoint sampler. The PushPoint sampler used, consisted of a long hollow metal tube with eight, 1/8 inch slots at the bottom three centimeters ending in a point. A slender metal rod was held inside this tube when inserting the sampler into the bed sediments to provide structural support. At the desired depth, the interior metal rod was removed and silicone pump tubing was attached to the top of the hollow tube. A peristaltic pump was then used to pull water through the perforations and out the top. This process is shown in Figure 32 below.

Figure 32. Pore water sampling on the Arkansas River.

At each cross section, pore water samples were taken from three evenly spaced locations across the channel on Timpas Creek and the Arkansas River. Total samples were taken by pumping directly into the appropriate sample bottle while Dissolved samples were filtered through a 0.45 µm filter and into the sample bottle. Between each sample, distilled water was pumped in the opposite direction through the PushPoint sampler to remove debris and any of the previous sample water. Between each cross section the PushPoint sampler was cleaned with acid, phosphate free detergent, and two rinses with distilled water

4.1.4 Contributing Surface Drain Sampling

Surface drains within the study reach were checked for flow during sample events. During the growing season there were typically two surface drains contributing to Timpas Creek and two contributing to the Arkansas River as shown in Figure 3 and Figure 4 in Chapter 2. If flow was present in any of these locations; a flow measurement was taken using an ADV or filling a known volume container; YSI readings were recorded; and Total and Dissolved water samples were collected. Water samples were collected in 1.0 L plastic bottles and decanted or filtered into appropriate sample bottles. The water quality data retrieved from these locations was considered constant for the 24 hour sample period.

4.1.5 Longitudinal sampling

Total and Dissolved water samples and YSI readings were collected at seven locations on Timpas Creek and nine locations on the Arkansas River during the June sampling event and then at one point in the middle of the study reach during the October event. Sampling locations for June and October are presented in Appendix F. A 1 L plastic bottle was fitted to the end of a long metal rod to take water samples as close to the main flow as possible. Total samples were decanted directly from the 1 L bottle after shaking while Dissolved samples were pumped with a peristaltic pump through a 0.45 μm filter. YSI readings were collected as close to the main flow as possible.

4.2 Results and Discussion

4.2.1 Arkansas River

4.2.1.1 June Sampling

ARKU and ARKD Sampling

The nutrient loadings for the upstream and downstream sampling stations were calculated based on both the average flow calculated from the stage-discharge rating curves over the two hour composite sampling period and the concentration of the nutrient from that sample. Nutrient concentrations are shown in Appendix J. An auto-sampler malfunction during this event prevented sample collection during the 15-16, 17-18, 19-20, and 21-22 composites. A grab sample was taken to replace the 23-24 composite upon arrival and values for the missing samples were interpolated. Samples from surface drains were not collected due to surcharging in the ditches and lack of visible flow. Discharge increased slightly between the upstream and downstream station averaging a 13% increase from ARKU to ARKD during the entire 24 hours. Unaccounted for flow averaged 6 m^3/s over the sampling period when using average values for discharge at ARKU and ARKD, the water balance equation (Equation 5), and accounting for surface storage during the 24 hour period.

The loading for total P is presented in Figure 33 and plotted with the averaged flows during each two hour period. There is no visible difference between the upstream and downstream loadings. An average 5% increase between the loadings at ARKU and ARKD amounted to a total addition of approximately 8 kg of P. Concentrations of total P maintained a constant value between 0.04 and 0.05 mg/L at the upstream and downstream stations. Longitudinal sampling along the Arkansas River for total P also showed no changes.

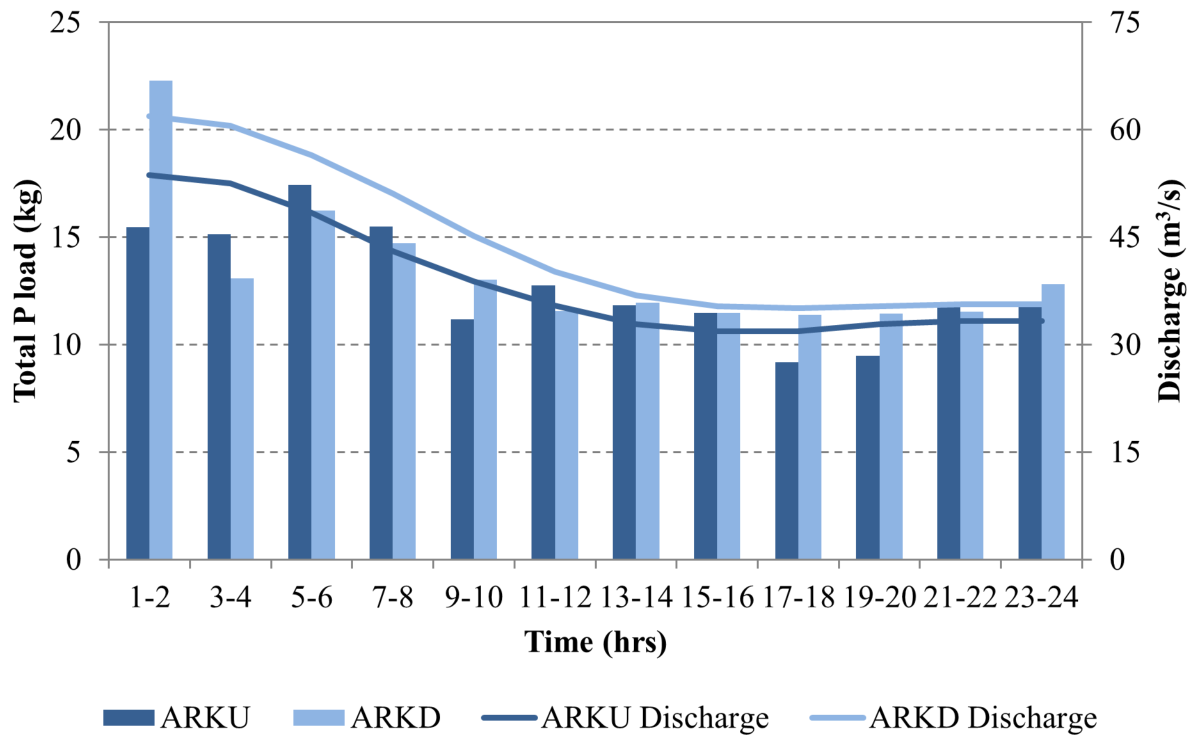

Figure 33. Two hour Total P loadings in the Arkansas River during the June sampling event.

NO_3^- as N loadings, presented in Figure 34, exhibited a small decrease from upstream to downstream. Despite higher flows downstream, the NO_3^- loadings were consistently lower than at ARKU with an average 14% decrease which amounted to a total reduction of approximately 280 kg of NO_3^-. NO_3^- concentrations at ARKU varied between 0.5 and 0.6 mg/L while concentrations at ARKD varied from 0.4 to 0.5 mg/L and longitudinal sampling showed very little variation between ARKU and ARKD. Total N sampling exhibited similar results to NO_3^- sampling. Since NO_3^- made up for more than half of the total N loading, plots for total N are not presented.

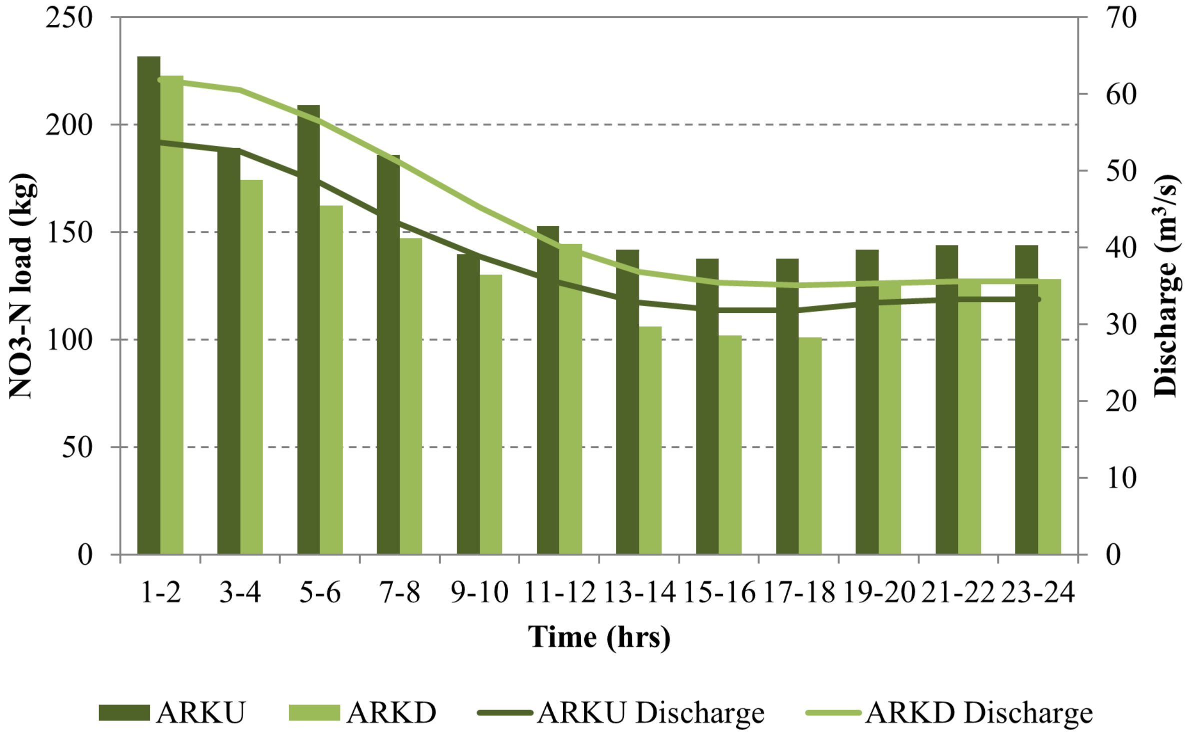

Figure 34. Two hour NO_3-N loadings in the Arkansas River during the June sampling event.

Groundwater Hydraulic Gradients

Groundwater levels were extracted from the growing season monitoring well data for the 24 hour period and are presented for cross sections ARKA, ARKB, and ARKC in Figure 35. ARKA exhibited the same general trend as its growing season monitoring equivalent. There was an average head difference of 0.1 m between A1 and A2, suggesting a gradient toward the river, and then 0.45 m between A3 and A4 away from the river. The ARKB cross section data showed a switch in gradient between B1 and B2 but averaged 0.02 m away from the river. The head difference between B4 and B3 averaged 0.08 m with a gradient toward the river. The switch in gradient was due to a decrease in river water level of approximately 20 centimeters, shown at all cross sections, and explains the decrease in water elevation in the interior wells.

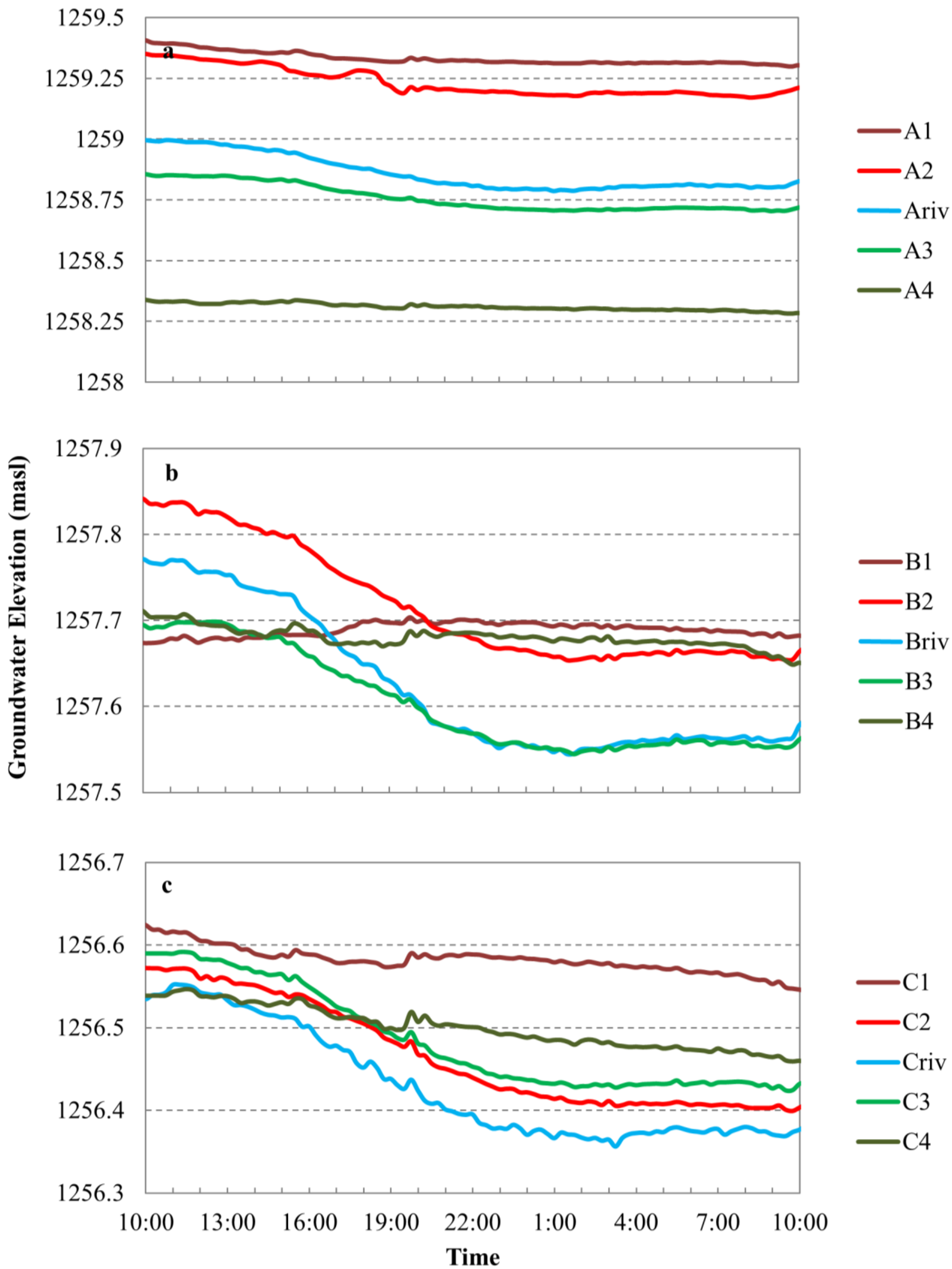

Figure 35. 24-hour well water level elevation monitoring at cross section a) ARKA b) ARKB c) ARKC.

ARKC also exhibited a decrease in water level in the interior wells. The head differences between C1 and C2 averaged 0.12 m with a gradient toward the river and another switch in gradient occurred between wells C3 and C4, where the difference averaged 0.02 m toward the river.

Up to this point, one-dimensional gradients have been assumed between monitoring wells. In order to test this assumption a two-dimensional analysis in ArcGIS was performed. Averaged well water level elevations were calculated, interpolated and, extended with ArcGIS, and then overlain onto an 8 year averaged contour plot developed from the existing MODFLOW groundwater model (Morway et al. 2013). Morway et al. (2013) used extensive regional observations of groundwater hydraulic head, groundwater return flow to streams, aquifer stratigraphy, canal seepage, evapotranspiration, and irrigation return flows as inputs to the model. The model was run over 447 weekly time steps using 250 m x 250 m grid cells, with hydraulic conductivity and specific yield modified spatially to provide matches of simulate and observed groundwater hydraulic head, groundwater discharge volumes to the Arkansas River, canal seepage rates, and ET rates. The calibrated model was then used to simulate conditions for the time period between 1999 and 2007 to be used in a comparison of alternative management scenarios. In Figure 36, grey lines are the visualized model output with 1.0 m resolution and the yellow lines are the interpolated groundwater contours estimated from well water elevations from this study with 0.25 m resolution. The model contour was used as a guide to extrapolate the groundwater elevations garnered from the wells beyond the exterior wells.

Based on the results from this exercise, it was determined that the average water levels measured in wells from cross section ARKA were an accurate measurement of the gradients. The area was both contributing to and removing water from the Arkansas River. On the other hand, the average water levels measured in cross sections ARKB and ARKC may have only represented minute changes along the same general contour line and therefore were less useful in direct measurement of gradients towards and away from the river. However, this information is still valuable because it reaffirms that the regional groundwater model is accurate near the study reach of the Arkansas River. The combination of the general model outputs and physical measurements from these wells can be used to determine areas where the river may be gaining flow from groundwater and where it may be losing flow to the aquifer. For example, the inside of large meanders of the river have the most potential for groundwater and surface water interactions. This is supported by the fact that these areas are lower in elevation, display evidence of historic channels, and are a significant portion of the river's floodplain in this reach.

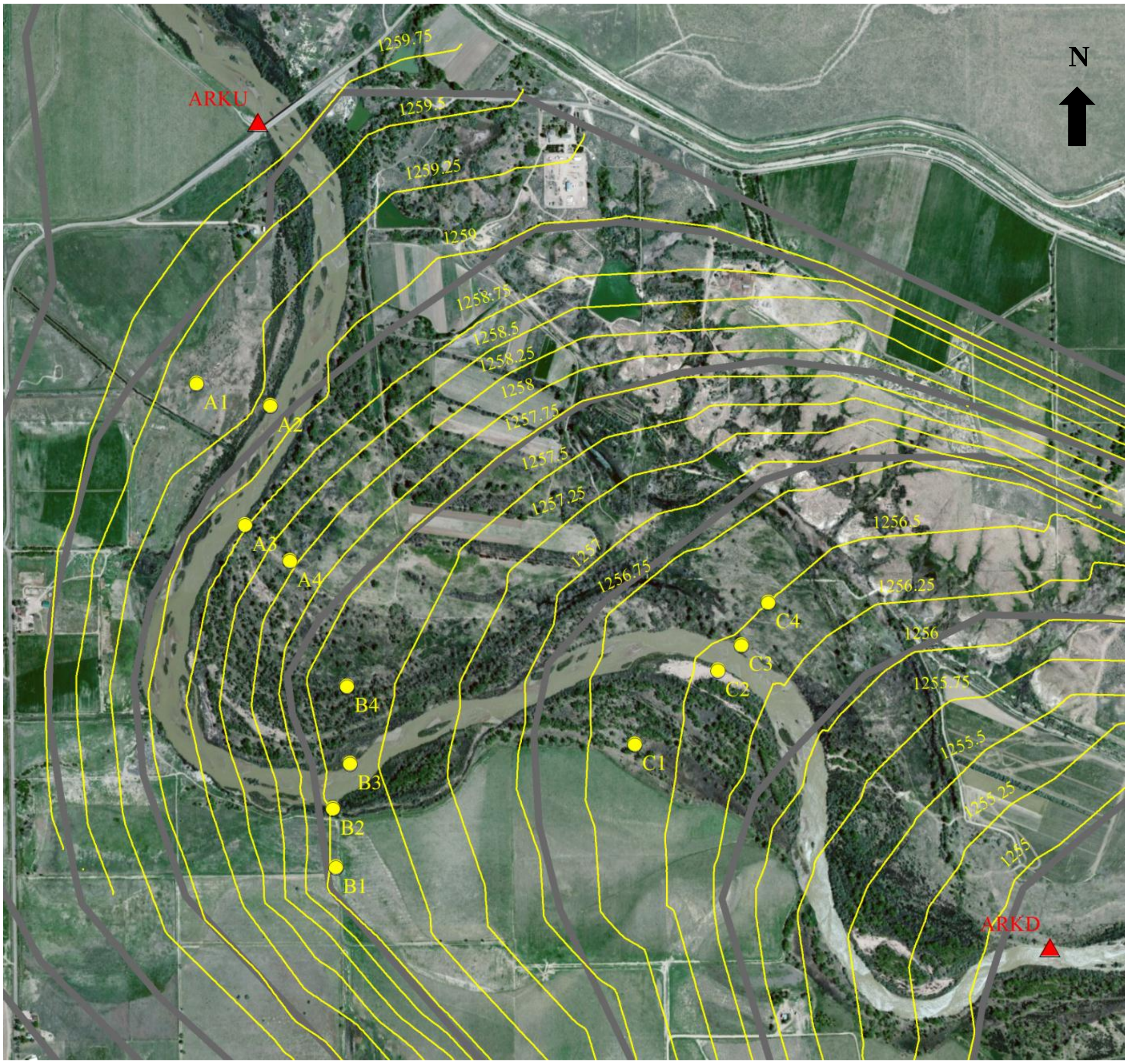

Figure 36. Water table contour plot from model results (grey lines) and Arkansas River averaged field measurements in June (yellow lines).

<u>Groundwater Quality</u>

Water quality sample results for NO_3^- as N, NH_4^+ as N and/or NO_2^- as N, total P, chloride, and electrical conductivity from each well in cross section ARKA and ARKB are presented in Figure 37 and cross section ARKC in Figure 38. The plots show a simplified cut out of each cross section of interest. Monitoring wells, pore water sample points, and a rough estimate of the direction of groundwater flow between interior and exterior wells are depicted. As stated previously, pore water samples were not collected during the June sample event in the

Arkansas River due to high flows in the river channel. Water quality concentration results in parts per million (nutrients and chloride) and mmho/cm (electrical conductivity) are shown beneath their respective wells and pore water sample points. Surface water concentrations at the cross sections for the constituents mentioned above are also presented. Chloride and electrical conductivity are presented with the nutrient data to provide a tracer for the movement and mixing of different water sources (i.e. groundwater or surface water). The use of chloride and EC as tracers in near stream environments has been used in many studies (e.g. Cox et al. 2007, Schemel et al. 2006, Haria et al. 2012).

As expected, mixing of water sources on the basis of chloride concentration and EC occurred in the interior wells. Interior wells exhibited a >50% decrease in concentration of these parameters compared to their paired exterior well in all cases except A3 (~40% decrease). Generally, the data in this plot shows lower values for N species (NO_3^- and NH_4^+) when the hydraulic gradient is only towards the river channel. Cross section ARKC did not follow this trend. NO_3^- values between wells C1 and C2 showed no change, however, their concentrations were both <0.01 mg/L. The NO_3^- concentration was higher in the interior well C3 (0.6 mg/L) than in C4 (<0.01 mg/L NO_3^-, 0.2 mg/L NH_4^+) but the hydraulic gradient switched directions part way through the 24 hour period. Total P appeared to show no consistent trend between the interior and exterior wells. Concentrations at interior wells were low (≤0.03 mg/L), with the exception of C3 (0.07 mg/L), but concentrations were both higher and lower than the paired exterior well values.

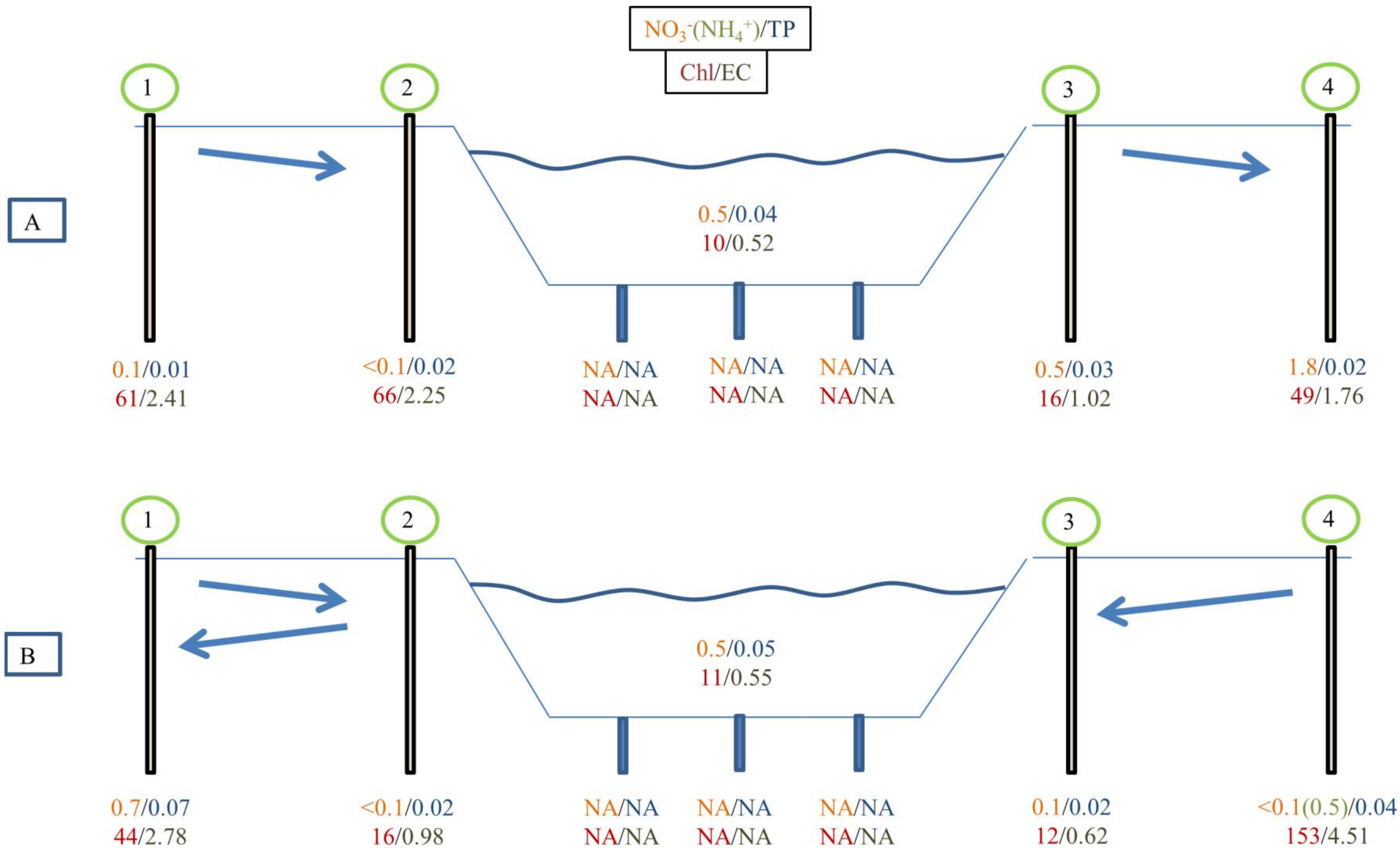

Figure 37. Well water quality results for cross sections ARKA (a) and ARKB (b) on June 12 2014. Nutrients and chloride have units of mg/L and electrical conductivity has units of mmho/cm.

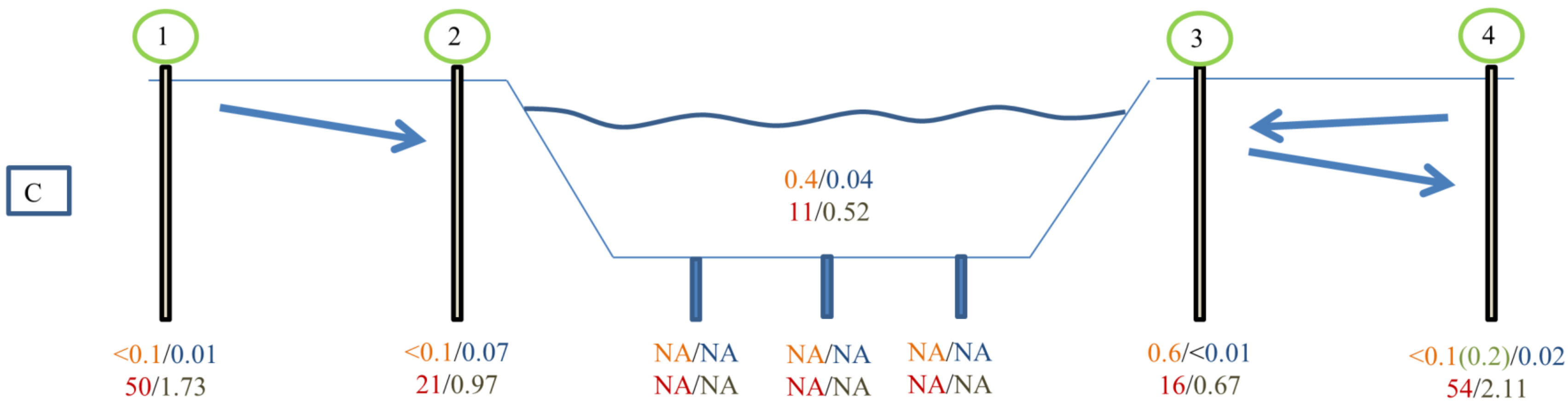

Figure 38. Well water quality results for cross sections ARKC on June 12 2014. Nutrients and chloride have units of mg/L and electrical conductivity has units of mmho/cm.

Discussion

Flows during this period were primarily due to snowmelt. High flows and velocities would inhibit any significant interactions with river bed substrate, hyporheic exchange, or biological activity (Puckett et al. 2008, McMahon and Böhlke 1996). Unaccounted for flow was assumed to be the result of groundwater contribution to the reach which was supported by the net gain in groundwater during the decline of the snowmelt flows presented in the growing season monitoring analysis (see Section 3.2.1.1), the regional water table contour map, and the one-dimensional gradients. This groundwater discharge to the river may have caused some dilution of the NO_3^- concentration based on the low NO_3^- values in the groundwater measured at the interior wells. However, the longitudinal sampling and NO_3^- loadings did not provide strong evidence of dilution from upstream to downstream.

Based on the study reach regional water table contour map (Figure 36) the only sample locations that successfully represented groundwater concentrations along a flow path are at ARKA and to some extent between ARKA4 and ARKB4. Although these zones were the only direct water quality measurements along flow paths, the other well data at ARKB and ARKC provided an estimate of concentrations in those areas. If it is assumed that flows were generally toward the river (except in the case of ARKA3 and ARKA4) and the interior wells represent groundwater that has moved through the riparian floodplain, statements can be made about the rest of the water quality results.

The well data provided no general trend in total P concentration. Regardless of whether the groundwater was moving through zones of dense riparian vegetation or areas with little riparian vegetation, there was no general resultant increase or decrease in total P concentration. This supports the results found in Lewandowski and Nützmann (2010) and Burt et al. (2002)

which suggested that groundwater P concentrations are highly variable depending on the soil substrate and environmental conditions, and may be immobilized or remobilized depending on those conditions.

NO_3^-, on the other hand, showed a marked decrease in concentration in groundwater that had moved through any distance of vegetated riparian zone in the half of the well pairs. The exceptions were wells A3 and A4 and cross section ARKC. A3 and A4 exhibited an increase in concentration as surface water moved into the groundwater. This may have been the result of varying groundwater elevation dissolving salt ions and immobilizing N in previously dry soil. A concentration of dissolved constituents, varying with depth in this area, was provided by multilevel sampling performed in the vicinity of wells A3 and A4 during each sampling period.

The methodology and results for the multilevel sampler are presented in Appendix G. In summary, higher concentrations of NO_3^- were measured at up to three meters below ground surface during a period of higher groundwater elevation in June in well A4. This concentration was nearly 10 times greater than concentrations during lower groundwater elevation in October. On the other hand, well A3 remained at a similar concentration in June and October. Another potential explanation for this increase is that minor irrigation practices occur up-gradient from well A4. An irrigation canal also flows along the northeast boundary of the wildlife refuge. Seepage from the ditch or the small irrigated fields could have contributed NO_3^- and dissolved salts to the groundwater.

Cross section ARKC also showed no decrease in NO_3^- concentration as groundwater moved toward the river. Wells C1 and C2 were both located in an area that is densely vegetated and has a shallow groundwater table. It is assumed that by the time groundwater reaches these locations, a substantial amount of NO_3^- has already been removed through denitrification or vegetative uptake. NO_3^- concentrations showed an increase from C4 to C3 as well. Based on the chloride and EC values, this may be an area of extensive groundwater and surface water mixing, which would explain the similar concentrations between surface water and groundwater in well C3.

Chloride and EC values suggested mixing between the surface and groundwater at most interior well zones. However, the decrease in NO_3^- at interior wells cannot be attributed to simple dilution because the concentration of NO_3^- in the surface water was higher than that in the groundwater, with the exception of well C3. The body of evidence from previous studies presented in Chapter 1 suggests that as the groundwater moved through the riparian zones it was intercepted by zones of denitrification and vegetative uptake.

4.2.1.2 October Sampling

ARKU and ARKD Sampling

During the October sample event, flows were higher at ARKD with an average 26% increase. Unaccounted for flow was calculated as 1.3 m^3/s using average values for discharge at ARKU and ARKD, the water balance equation (Equation 5), and accounting for surface storage during the 24 hours,. The surface drains were sampled, but results suggested a negligible contribution to flow and nutrient loadings. The loading for total P is presented in Figure 39 and plotted with the averaged flows during each two hour period. Total P loadings were consistently higher at ARKD averaging a 29% increase from ARKU, which amounts to approximately 6 kg of total added P. Total P concentrations (shown in Appendix J) at ARKU ranged from 0.04 to 0.06 mg/L and from 0.05 to 0.06 at ARKD. NO_3^- loadings, shown in Figure 40, averaged a 41% decrease from ARKU to ARKD, which amounts to a total removal of approximately 300 kg of NO_3^- over the 24 hour period. NO_3^- concentrations at ARKU varied between 1.8 and 2.1 mg/L while concentrations at ARKD maintained a constant value of 0.9 mg/L. One sample collected at the mid-point of the study reach had a total P concentration of 0.08 and a NO_3^- concentration of 1.5 mg/L.

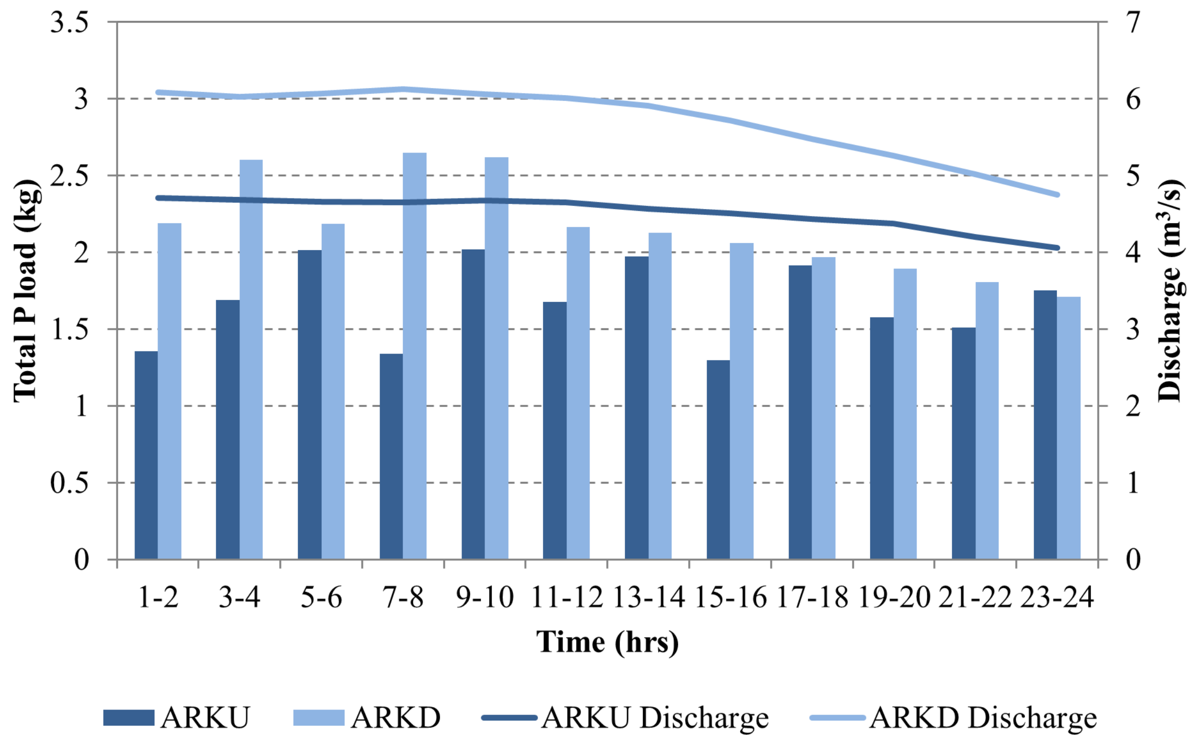

Figure 39. Two hour Total P loadings in the Arkansas River during the October sampling event.

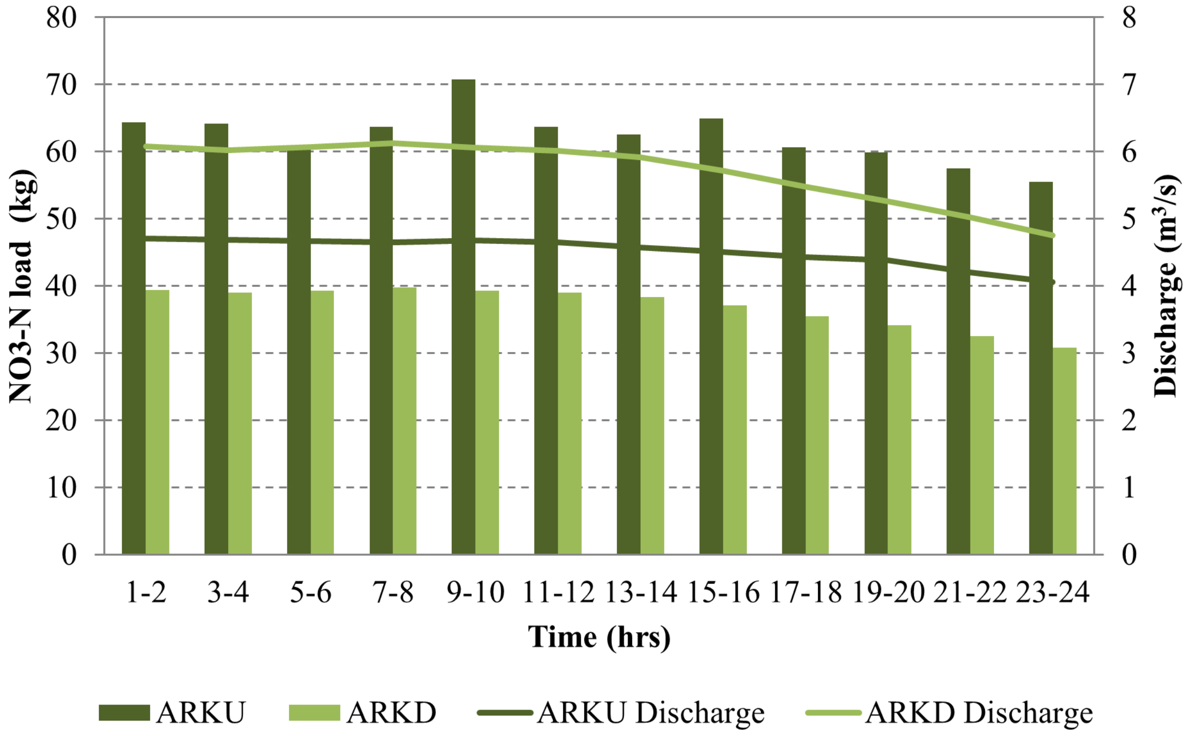

Figure 40. Two hour NO_3-N loadings in the Arkansas River during the October sampling event.

Groundwater Hydraulic Gradients

Well water levels were extracted from the growing season monitoring data for the 24 hour period and cross sections ARKA, ARKB, and ARKC are presented in Figure 41. Once again, ARKA exhibited the same general trend as its growing season monitoring equivalent. There was an average gradient of 0.23 m between A1 and A2 towards the river and an average gradient of 0.42 m between A3 and A4 away from the river. The ARKB cross section displayed consistent gradients towards the river with an average gradient of 0.17 m between B1 and B2 and 0.08 m between B4 and B3. The in-channel water level reader at cross section B was on the opposite bank and a few meters upstream of well B3, which explains why the plot shows a gradient away from the river towards B3. In this respect, the plot is incorrect. Finally, ARKC showed consistent gradients toward the river with an average gradient of 0.16 m between C1 and C2 and 0.05 m between C4 and C3.

Making the assumption that the one-dimensional gradients taken from the wells in cross sections ARKB and ARKC were not an accurate representation of the groundwater gradient, the averaged well water level elevations were calculated, interpolated and extended with ArcGIS. The contours were then overlain onto an average contour plot developed from the existing MODFLOW groundwater model and are shown in Figure 42. The methods and labels for this exercise are the same as in section 4.2.1.1. Once again, the average water levels measured in wells from cross section ARKA were an accurate measurement of the gradient in an area that is both contributing to and removing water from the Arkansas River, while cross sections ARKB and ARKC may have only represented minute changes along the same general contour line. The water table was slightly lower in October than in June, but the general groundwater flow direction was the same and flow was still through meander bends.

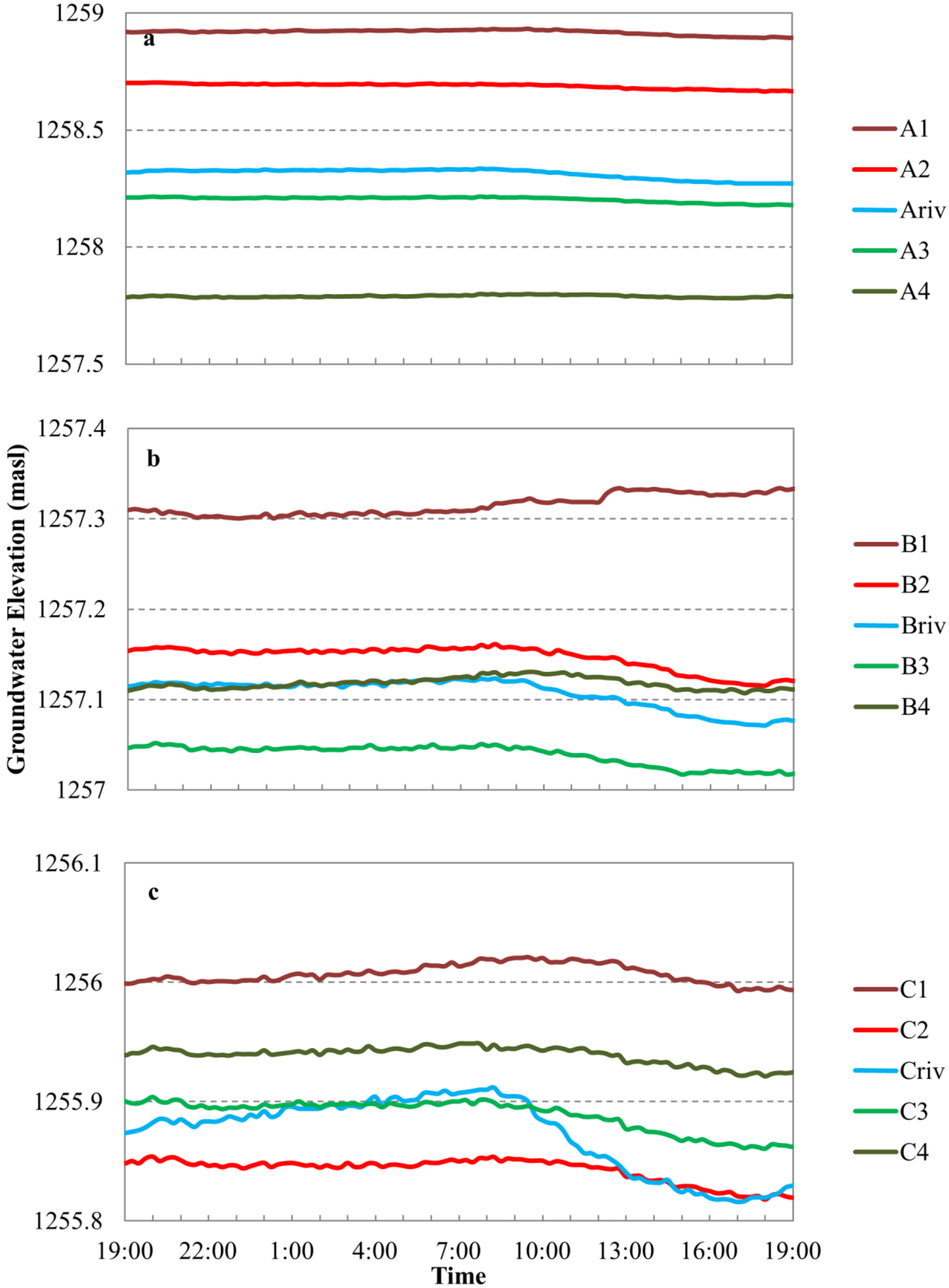

Figure 41. 24-hour well water level elevation monitoring at cross section ARKA in October.

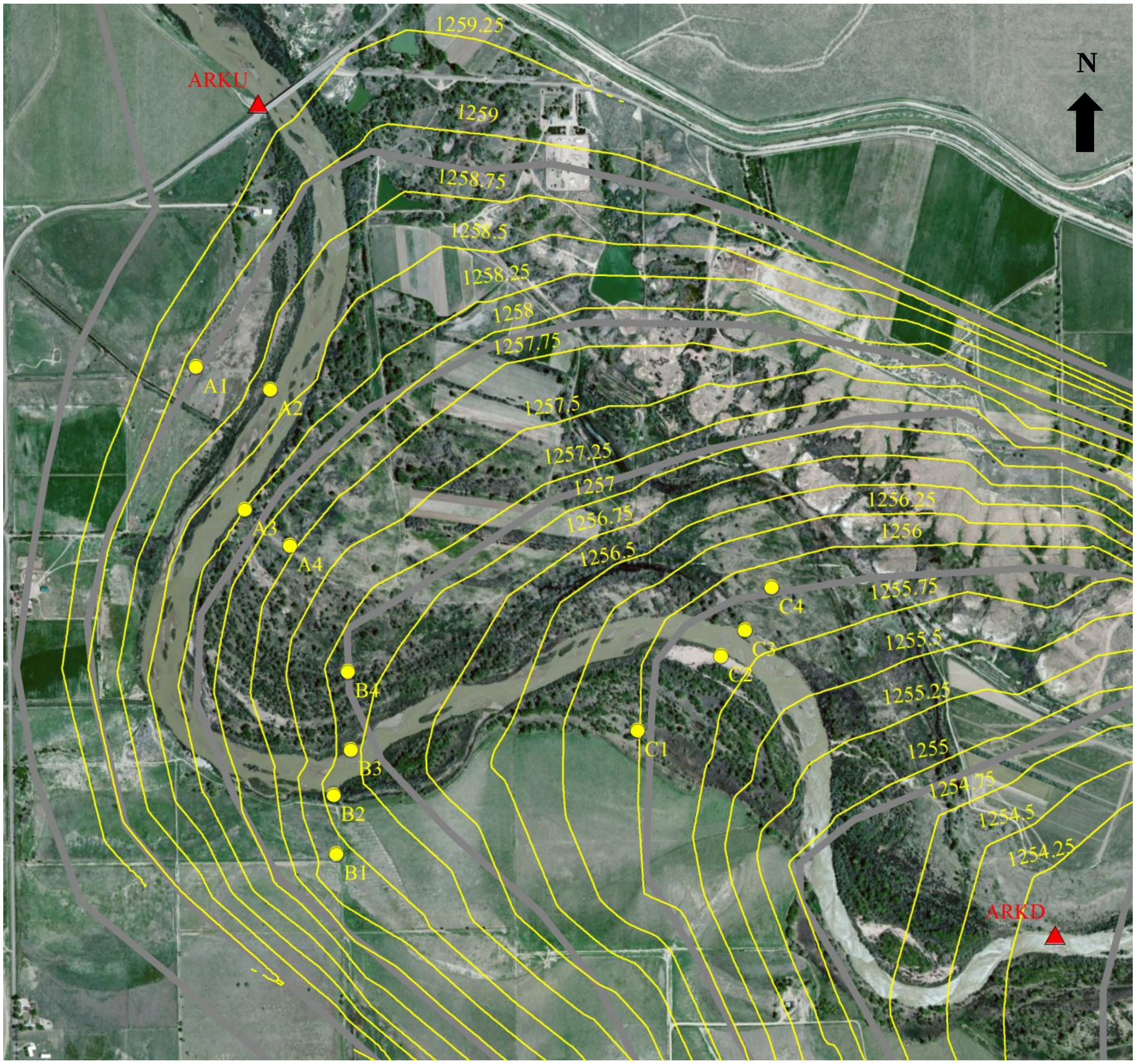

Figure 42. Water table contour plot from model results (grey lines) and Arkansas River averaged field measurements in October (yellow lines).

Groundwater Quality

Water quality sample results for NO_3^- as N, NH_4^+ as N and/or NO_2^- as N, total P, chloride, and electrical conductivity from each well in cross section ARKA and ARKB are presented in Figure 43 and cross section ARKC in Figure 44. The plots have the same setup as described in section 4.2.1.1. Groundwater and surface water mixing and nutrient concentrations were much more varied during this low flow period than during high flows in June.

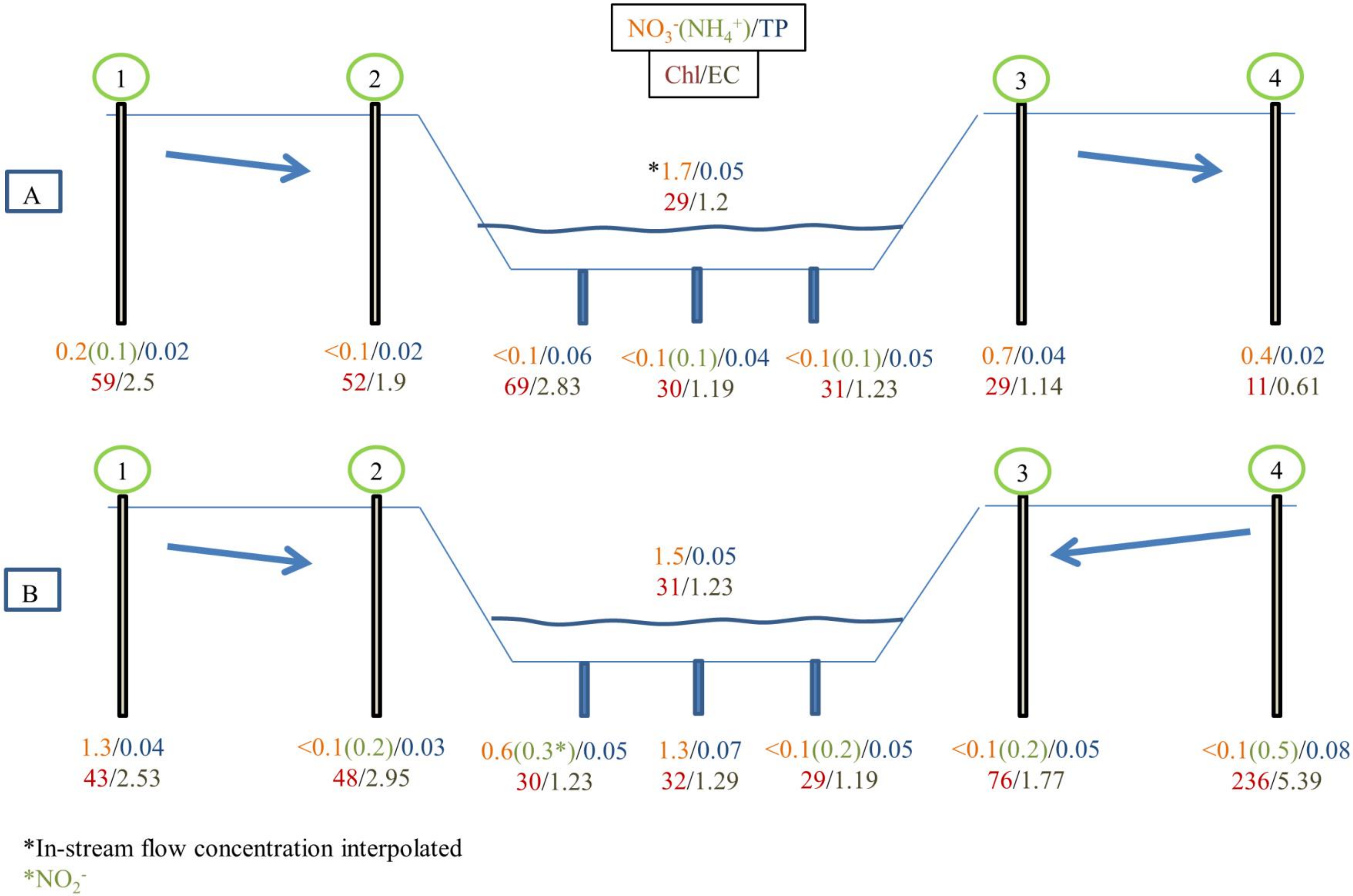

Figure 43. Well water quality results for cross sections ARKA (a) and ARKB (b) on October 4 2014. Nutrients and chloride have units of mg/L and electrical conductivity has units of mmho/cm.

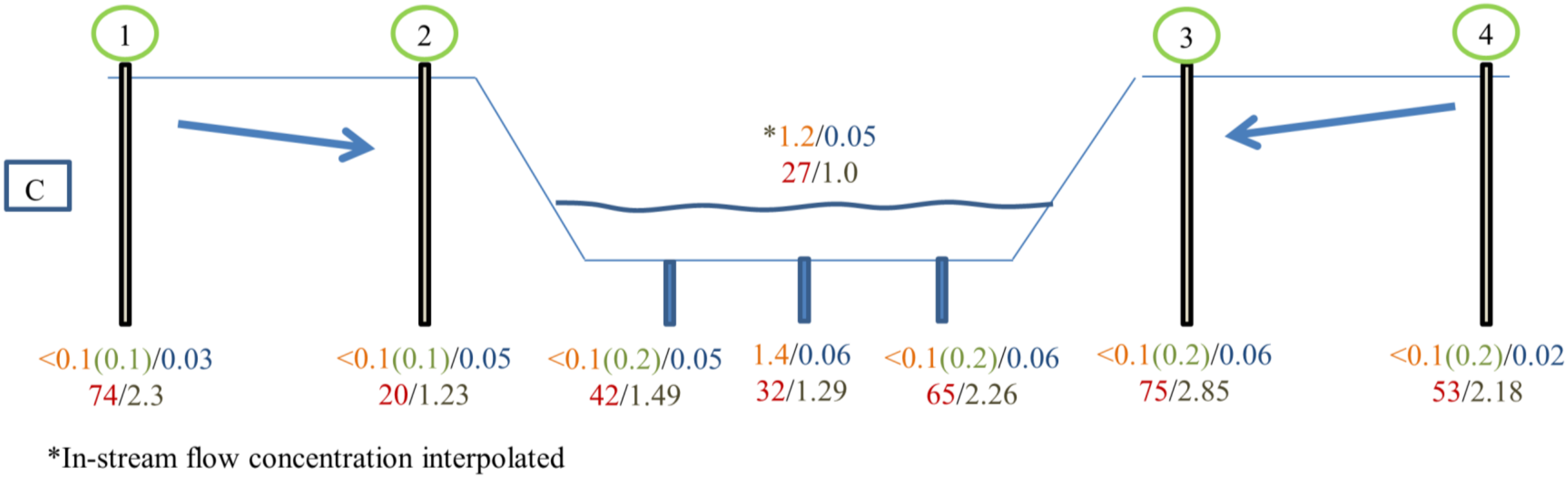

Figure 44. Well water quality results for cross sections ARKC on October 4 2014. Nutrients and chloride have units of mg/L and electrical conductivity has units of mmho/cm.

In half of the well pairs (A3-A4, B1-B2, and C3-C4), chloride and EC values were higher or showed little change in the interior wells, with no relationship to hydraulic gradient. Chloride and EC in the pore water samples in ARKA showed a relationship with hydraulic gradient. High groundwater values existed from well A1 to A2 and in the left most pore water sample point. Then at the approximate mid-point of the channel, the pore water values started to closely match the surface water. These surface water and pore water samples then matched the values found in well A3. This pattern of water quality results supports the assumed direction of groundwater movement in this area.

With regards to NO_3^-, concentrations were lower in well A2 than A1. The same low concentrations (<0.1 mg/L) were maintained in the pore water samples. Spikes in NO_3^- concentrations were observed at A3 (0.7 mg/L) and decreases were seen in A4 (0.4 mg/L). The spike in A3 may be explained by surface water infiltrating the bank since the surface water had a higher NO_3^- concentration (1.7 mg/L) than the groundwater. The decrease in NO_3^- from A3 to A4 may have been the result of movement through the riparian zone. Multilevel sampling, while less descriptive and with a lower magnitude in October, verifies the decrease in NO_3^- concentration through the entire saturated portion of the soil column. Total P showed no change between A1 (0.02 mg/L) and A2 (0.02 mg/L) and maintained a similar value to the surface water in the pore water samples (0.04 to 0.06 mg/L). In well A3, the concentration matched that of the pore water and the surface water while, by comparison, concentrations decreased in A4.

In cross section ARKB the hydraulic gradients, shown in Figure 41 and Figure 42, suggest that groundwater was consistently flowing toward the river in both well pairs. There was very little difference in chloride or EC between B1 and B2, but there was a steep reduction in NO_3^- in B2, from 1.3 mg/L to <0.01 mg/L. Total P decreased slightly between B1 to B2, from

0.04 mg/L to 0.03 mg/L. The pore water samples' chloride and EC values matched almost exactly with those of the surface water, while NO_3^- varied considerably. The left pore water sample's NO_3^- concentration was less than half of the surface water concentration (0.6 mg/L and 1.5 mg/L respectively), the middle sample had nearly the same value (1.3 mg/L), and the right sample was very low and matched the concentration in B3 (<0.01 mg/L). The total P concentration was approximately the same as that in the surface water. Data from well B3 suggested that groundwater and surface water were mixing, based on the chloride and EC values. There was also a reduction in NH_4^+ and total P concentration between B4 and B3.

In cross section ARKC, the hydraulic gradients again suggested that groundwater was flowing toward the river on both sides. The drop in chloride and EC from C1 to C2 suggested groundwater and surface water mixing in this zone. NO_3^- concentrations (<0.01 mg/L) were the same in these two wells and total P was slightly higher in C2. The left and right pore water samples had higher concentrations of chloride and EC values, but NO_3^- and total P concentrations similar to the interior wells C2 and C3. The middle pore water sample results closely matched those of the surface water (1.4 mg/L and 1.2 mg/L respectively). Well C3 had a higher total P, chloride, and EC than in C4, but the NO_3^- values remain the same.

Discussion

Flows during this period were lower than historic averages. Low flows and velocities can result in enhanced interactions with river bed substrate, hyporheic exchange, or biological activity (Puckett et al. 2008, McMahon and Böhlke 1996). Unaccounted for flow was assumed to be the result of groundwater contribution to the reach, which is supported by the growing season monitoring analysis at this date. Sampling occurred during the small peak in section 3 of Figure 16. Groundwater contribution to the reach is also supported by results from the regional water table contour map and the one-dimensional gradients. This groundwater discharge to the river may have caused some dilution of the NO_3^- concentration, based on the low NO_3^- values in the groundwater measured at the interior wells. However, the longitudinal sampling and NO_3^- loadings did not provide any strong evidence of dilution from upstream to downstream, likely due to the small contribution of groundwater volume to overall stream discharge.

The Arkansas River October sampling event provided 24-hour water quality data that support the results presented for the growing season sampling period. Surface water sampling suggested a substantial decrease in NO_3^- loadings and a slight increase in total P loadings. It can be assumed that the primary modes of NO_3^- decrease were in-stream processes and groundwater-surface water exchange in the hyporheic zone, based on the results from well and pore water sampling. Pore water sampling presented evidence of extensive groundwater-surface water mixing based on EC and chloride values. While no measurements of biological activity were collected in this study, it is possible that this also contributed to losses of NO_3^-.

The increase in total P loadings was likely caused by a combination of groundwater contributions, enrichment of fine sediments being transported downstream, and pickup of sediment bound P from the channel banks. Bank sediment results for the Arkansas River, presented in Appendix E, suggested that these areas could be sources of sediment bound P because they were higher in concentration than bed sediments. Bed sediments ranged in total P concentration from 200 ppm to 250 ppm while bank sediments ranged between 400 ppm and 700 ppm. Since no substantial increase in P concentration occurred in the surface water from upstream to downstream it is likely, based on groundwater concentrations, that any contribution from groundwater was of a similar concentration to the surface water.

The ARKA cross section showed a distinct difference between zones of the river being fed by groundwater and zones of the aquifer being fed by surface water. Consistently low NO_3^- concentrations in the pore water samples suggested denitrification occurring in the hyporheic zone before being mixed with surface water in well A3. These zonal changes in the cross section also closely matched the water table gradients. Cross section ARKB, with groundwater contributing to the reach from both sides of the channel, displayed a mixing of groundwater and surface water in the pore water samples closest to the banks. Data from the middle pore water sample suggested that the dominant source of water was the infiltration of surface water into the hyporheic zone, based on NO_3^- concentrations matching those in the surface water. Cross section ARKC presented a similar mixing pattern in the pore water. The two outside pore water samples indicated mixing between groundwater and surface-water, while the middle pore water sample was a close match to surface water concentrations, based on NO_3^-, chloride, and EC values.

Similar to the June sampling event, groundwater concentrations in October suggested decreases in NO_3^- concentrations as the groundwater moved through the riparian zone and no distinguishable trend in total P. In all cross sections except ARKC, NO_3^- concentration decreased as groundwater moved down-gradient through the aquifer and through the riparian zone. It is likely that the wells in ARKC showed no decrease because the NO_3^- and NH_4^+ concentrations were already so low. Again, the decrease cannot be attributed to dilutions because the surface water concentrations were often higher than the interior well concentrations.

4.2.2 Timpas Creek

4.2.2.1 June Sampling

<u>TIMU and TIMD Sampling</u>

The same process used to determine nutrient loadings in the Arkansas River was used to determine loadings into and out of the Timpas Creek study reach. An auto-sampler malfunction also occurred during this sample period at the TIMU monitoring station which resulted in no sample collection during the 19-20 and 21-22 composites. A grab sample was taken to replace the 23-24 composite and values for the missing samples were interpolated. The loadings for total P during the study period are presented in Figure 45 and plotted with the averaged flows during each two hour period. The TIM Drain flow was consistently between 0.25 and 0.3 m^3/s throughout the 24 hour period, which accounted for less than half of the difference between the TIMU and TIMD discharges. The TIM Drain two hour loadings are also included in this plot. Discharges and loadings from the second surface drain were found to be negligible. Using average values for discharge at TIMU, TIM Drain, TIMD, and the water balance equation (Equation 6), unaccounted for flow was calculated as 0.45 m^3/s averaged over the 24 hour period. Approximately 20% of the average flow in the channel.

Generally the TIM Drain loadings did not account for the full difference between TIMU and TIMD total P loadings. Total P loadings averaged a 59% increase from TIMU to TIMD, which amounts to 10 kg of added P. TIM Drain accounted for approximately 60% of this increase, or 6 kg. Concentrations of total P (shown in Appendix J) at TIMU ranged from 0.08 to 0.10 mg/L during the sampling period and 0.10 to 0.13 mg/L at TIMD. However, longitudinal sampling, which terminated just upstream of the confluence of TIM Drain with Timpas Creek, showed no variation from the upstream concentrations.

NO_3^- as N loadings, presented in Figure 46, exhibited similar results from upstream to downstream. The loading difference of NO_3^- between TIMU and TIMD is not fully explained by the TIM Drain loading. NO_3^- loadings averaged a 55% increase, which amounts to approximately 160 kg of added NO_3^-. TIM Drain accounted for 48% of this increase, or about 77 kg. Concentrations of NO_3^- at TIMU ranged from 1.3 to 2.1 mg/L, while concentrations at TIMD were consistently between 2.0 and 2.2 mg/L. Longitudinal sampling showed very little variation from the upstream concentrations until the last longitudinal sample point (sample point 1 in Figure F- 2 in Appendix F) above the confluence with TIM Drain which increased from 1.8 mg/L at point 2 to 2.3 mg/L at point 1.

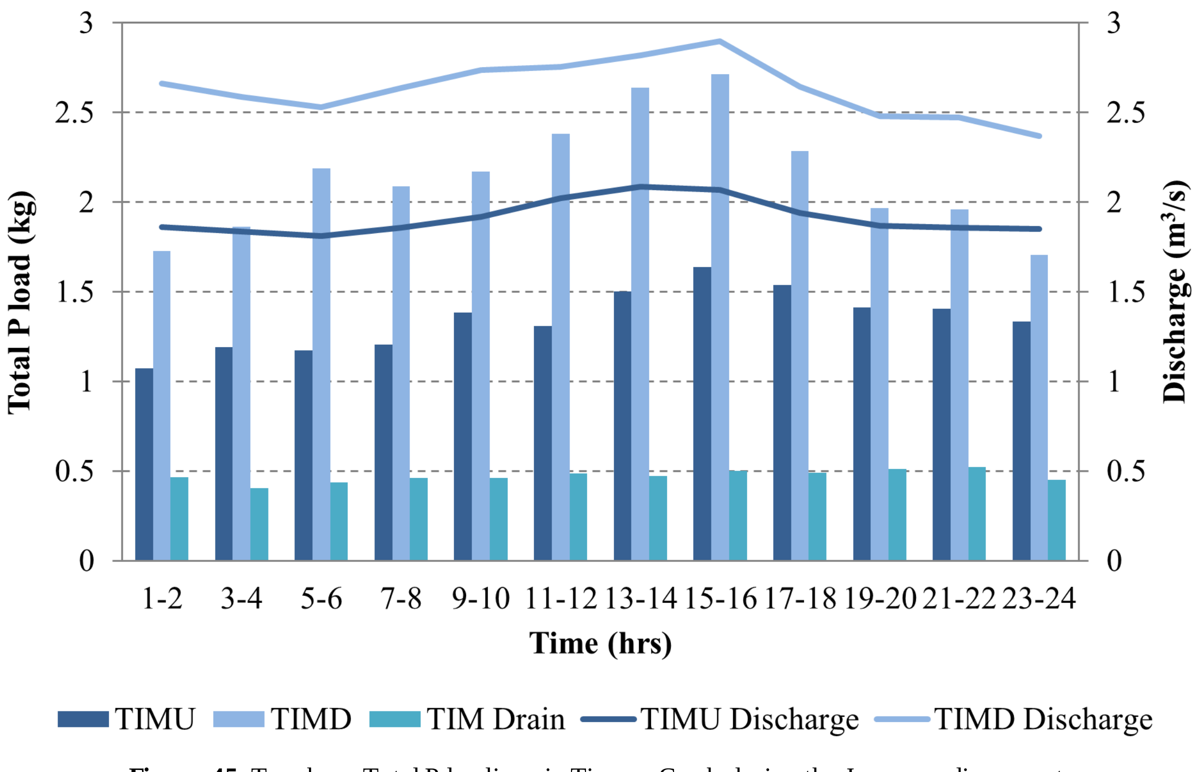

Figure 45. Two hour Total P loadings in Timpas Creek during the June sampling event.

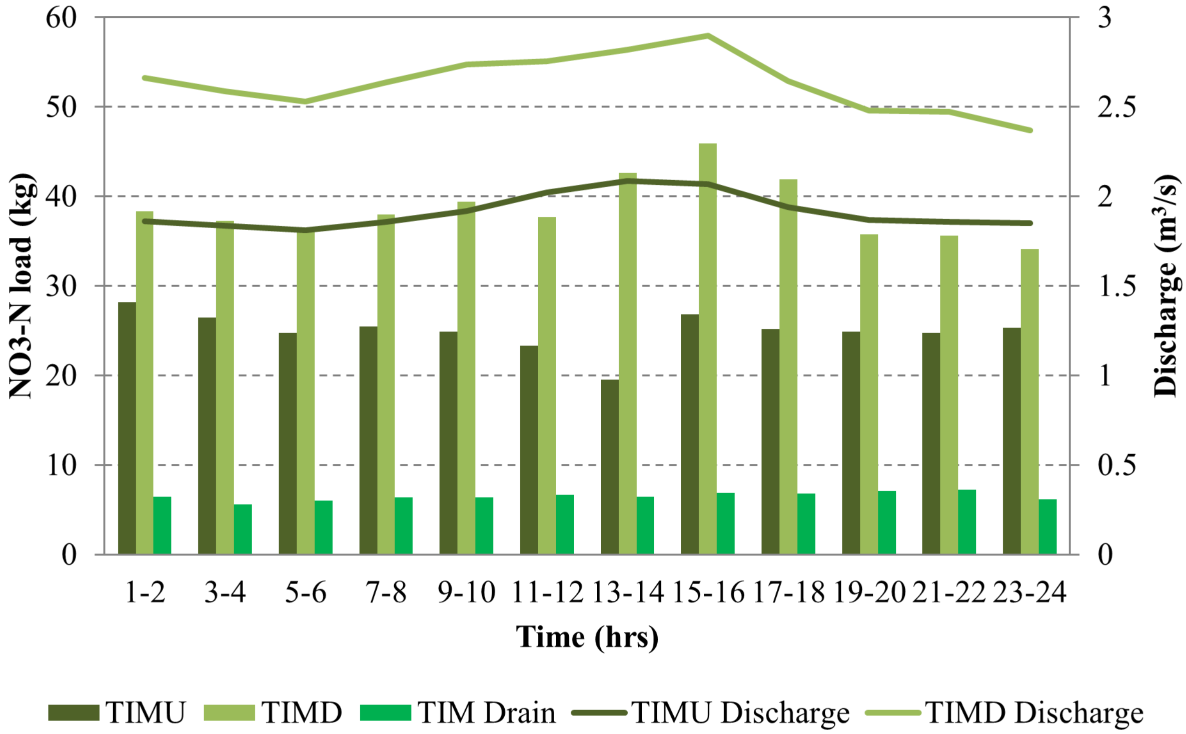

Figure 46. Two hour NO_3-N loadings in Timpas Creek during the June sampling event.

Groundwater Hydraulic Gradients

Well water levels were extracted from the growing season monitoring data for the 24 hour sampling period and cross sections TIMA and TIMB are presented in Figure 47 and Figure 48 respectively. As stated in section 2.2.2, a substantial head difference, which averaged 4.7 m during the 24 hours, existed between wells A4 and A3 towards the creek. A smaller head difference, which averaged 0.4 m, existed between A1 and A2 away from the creek. Similar to the growing season well results, TIMB exhibited gradients away from the creek on both sides. The head difference between B1 and B2 averaged 0.37 m away from the creek and the difference between B3 and B4 averaged 0.05 m away from the creek.

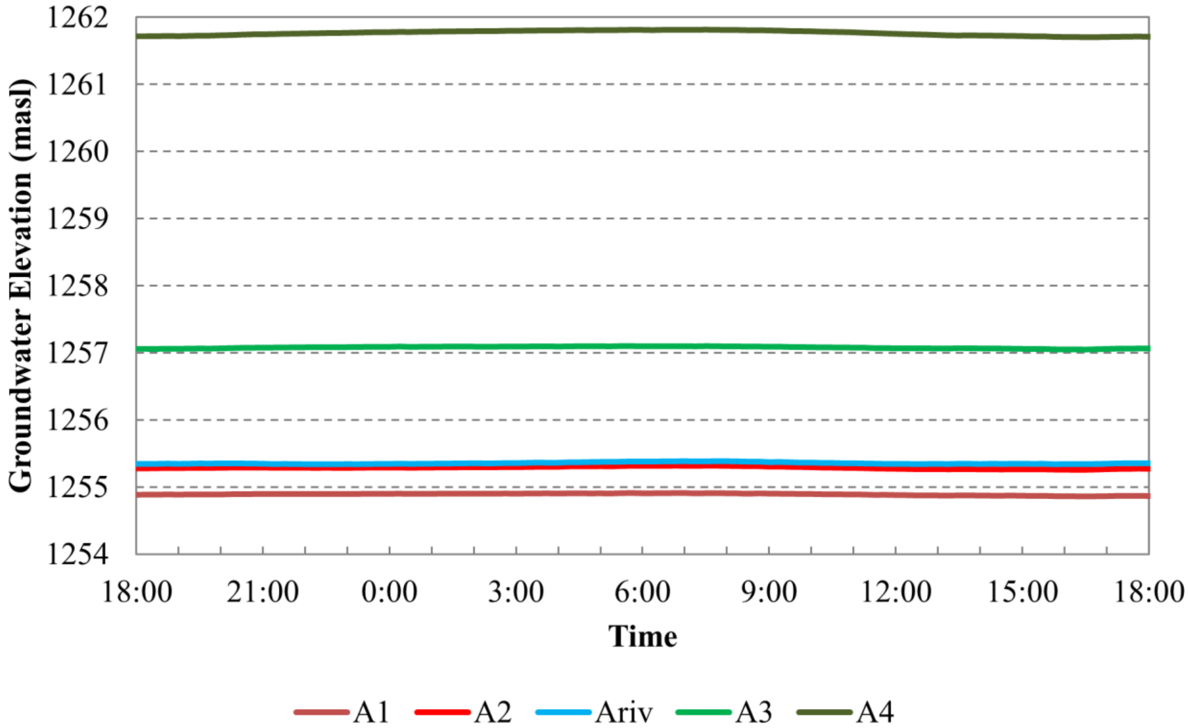

Figure 47. 24-hour well water level elevation monitoring at cross section TIMA in June.

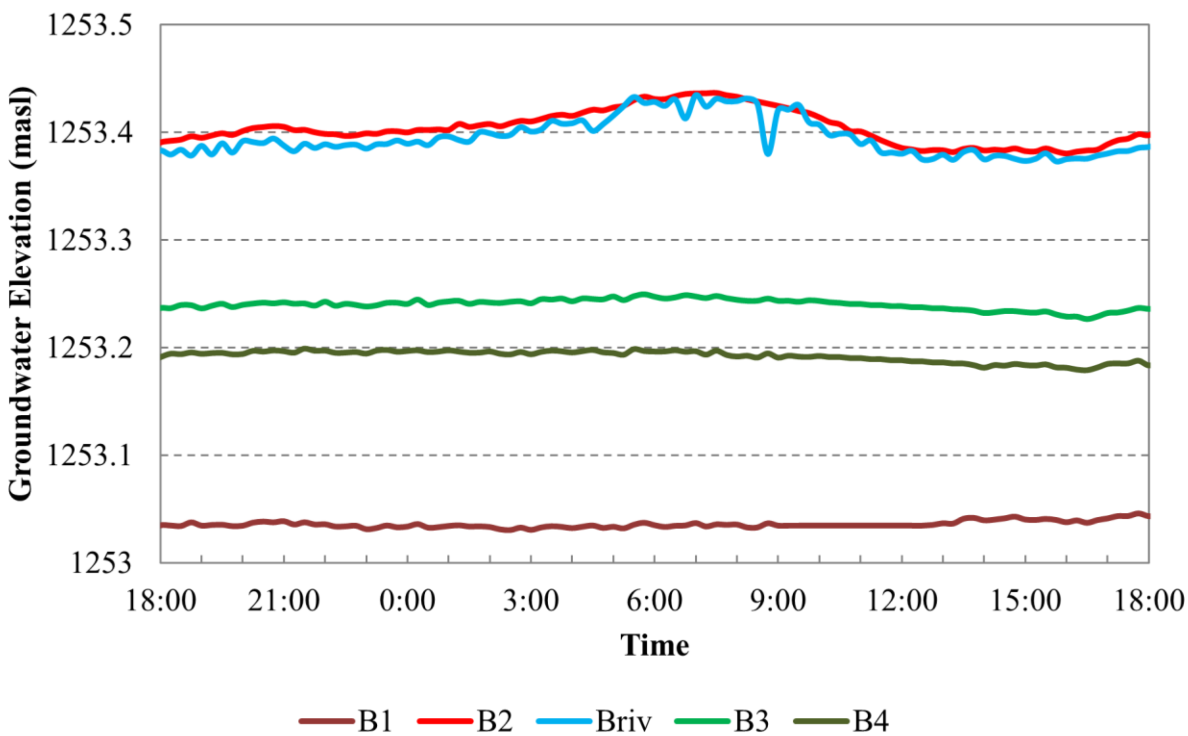

Figure 48. 24-hour well water level elevation monitoring at cross section TIMB in June.

Averaged well water level elevations were calculated, interpolated and extended with ArcGIS, and overlain onto an average contour plot developed from the existing MODFLOW groundwater model, shown in Figure 49. In this plot, grey lines are the visualized model output with 1.0 m resolution and the yellow lines are the interpolated groundwater contours estimated from well water elevations with 0.5 m resolution. Based on the results from this exercise, it was determined that the average water levels measured in wells A3 and A4 were an accurate measurement of the gradients to the southeast of the creek. This area was contributing groundwater to the creek. On the other hand, the average water levels measured in wells A1 and A2, as well as cross section TIMB, may have only represented small changes along the same general contour line and therefore were less useful in direct measurement of gradients towards and away from the creek. Again, this information is still valuable because it reaffirms that the general direction and shape of the regional groundwater model water table developed by Morway et al. (2013) is accurate in these areas along Timpas Creek.

However, the regional groundwater model output differs from the results of this study in the steepness of the gradients along the study reach. To the south of the creek there was over a 6.0 m gradient between well A4 and the creek, while the regional model shows, at most, a 1.0 m gradient in that area. As the contours from this study moved north, the measured gradients started to decrease but were still two times greater than the regional groundwater model at cross section TIMB. The decrease in groundwater gradient, moving from south to north can be explained, in part, by changes in hydraulic conductivity and soil type as seen in the soil maps for the area in Appendix A and hydraulic conductivity values in Table 2. In this study, the areas of lower measured hydraulic conductivity corresponded with the steep gradients in the southern portion of the study reach while the areas of higher measured hydraulic conductivity then corresponded with moderate gradients.

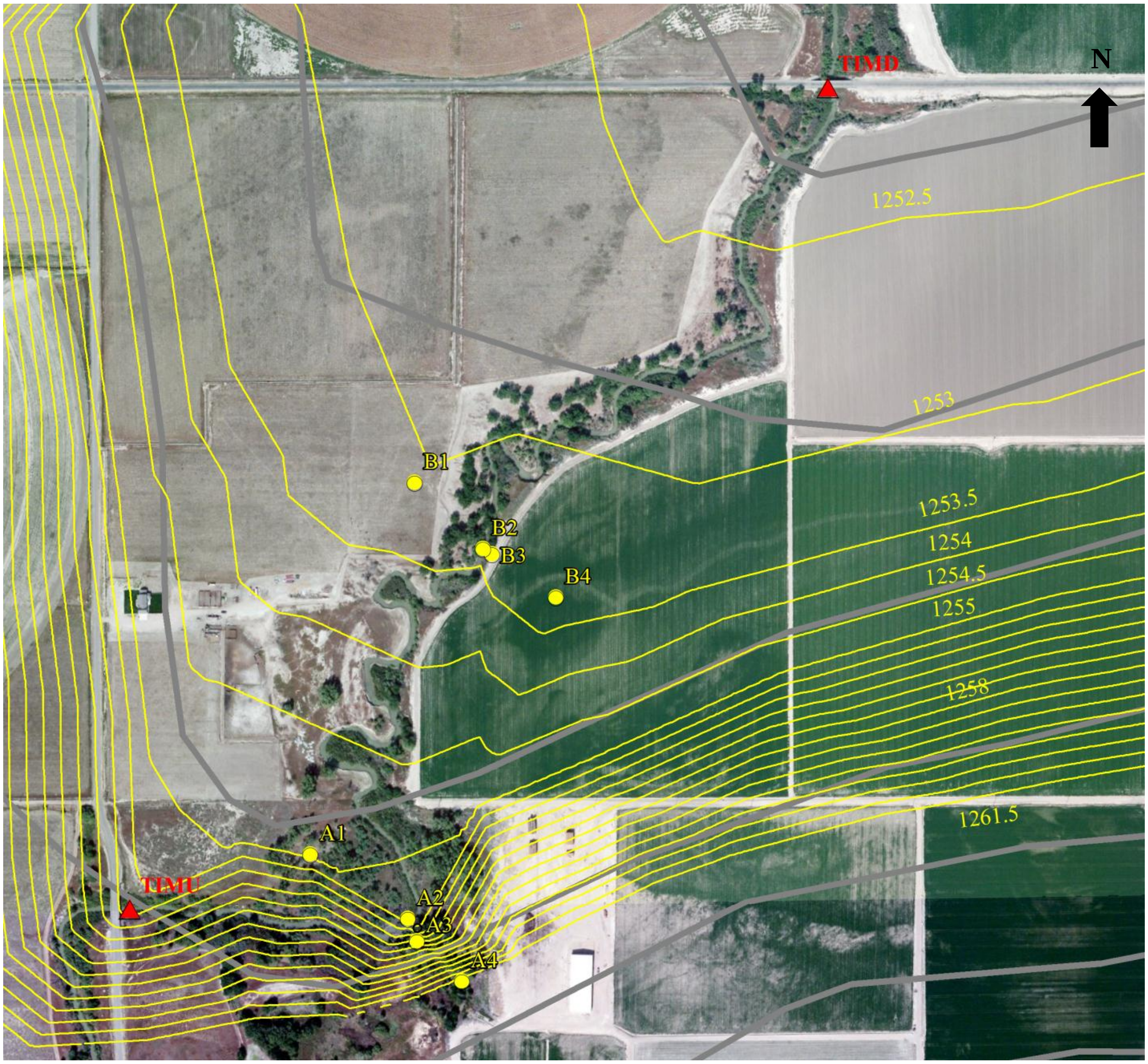

Figure 49. Water table contour plot from model results (grey lines) and Timpas Creek averaged field measurements in June (yellow lines).

Groundwater Quality

Water quality sample results for NO_3^- as N, NH_4^+ as N and/or NO_2^- as N, total P, chloride, and electrical conductivity from each well in cross section TIMA and TIMB are presented in Figure 50. The plots have the same setup as described in section 3.2.1.1. Chloride concentrations and EC in interior wells showed less mixing between surface and groundwater than the Arkansas River. Parameter values had a <30% difference for EC and <40% difference for chloride between paired wells. Chloride and EC values were higher closer to the creek in half of the well pairs. Results from two locations, wells A2 and B2, indicated some mixing of groundwater and surface water, based on EC and chloride values. However, the hydraulic conductivity at well B2 was one of the lowest recorded values (0.09 m/d), which suggested very little mixing between surface and groundwater. On the other hand, well A2 had a measured hydraulic conductivity value of 1.1 m/day. Its low elevation, location in the floodplain of the creek, and the direction of the gradients (presented in Figure 49) strongly supported groundwater movement and mixing with surface water in this area. Chloride and EC values in the pore water samples matched the surface water values almost exactly at all points, suggesting extensive surface water mixing in the bed sediments, but little infiltration of groundwater into the hyporheic zone.

N species were lower in all interior wells despite varying hydraulic gradient directions. Pore water NO_3^- concentrations also decreased and averaged approximately half of the surface water concentrations (~1.0 mg/L and ~2.0 mg/L respectively). The pore water sample adjacent to well A3 displayed the lowest NO_3^- concentration (0.1 mg/L) suggesting that the area in the creek may have been a zone of high denitrification rates. Total P showed no consistent trend between paired wells. However, concentrations in the pore water sample points (~0.05 mg/L) were approximately half that of surface water samples (~0.1 mg/L).

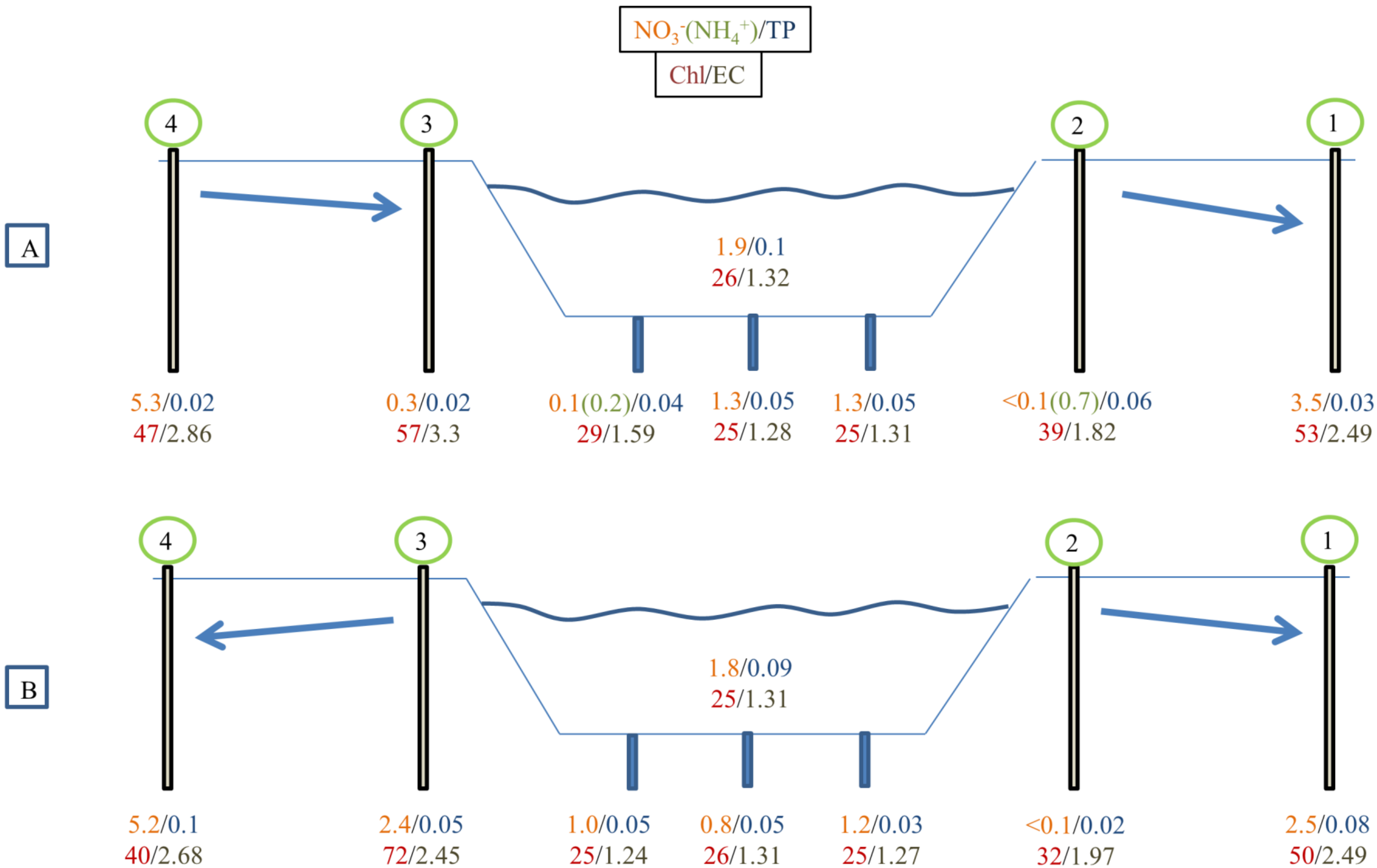

Figure 50. Well water quality results for cross sections TIMA (a) and TIMB (b) on June 10 2014. Nutrients and chloride have units of mg/L and electrical conductivity has units of mmho/cm.

Discussion

Flows during this period were likely due to irrigation ditches flowing into Timpas Creek, as well as irrigation return flow from fields upstream, based on the moderate nutrient concentrations and high specific conductivity values. This hypothesis is strengthened by the knowledge that snowmelt does not significantly affect Timpas Creek and no rain events had occurred prior to the sampling event. Unaccounted for flow was assumed to be the result of groundwater contribution to the reach, which is supported by the growing season monitoring analysis at this date. In addition, the TIM Drain discharge could only account for approximately half of the difference between TIMU and TIMD.

Groundwater-surface water interactions along this study reach were complex and difficult to determine. Groundwater contribution to the reach varied and, based on the one-dimensional gradients provided by the water table elevations in the wells and the study reach's interpolated groundwater contour results, there may be areas of water volume loss from the creek to the aquifer. The high gradients toward the creek near A3 and A4 suggested that any groundwater contribution to the creek likely came from the steep gradient section to the south of the study reach, with minor contributions from groundwater as the creek flows north, as well as zones of loss to the aquifer. Since there were only two cross sections providing water table elevations, the contour plot could not provide the level of detail needed to delineate specific zones of loss or gain in the creek. However, the relative homogeneity of the soils at the middle and northern sections of the study reach, and the low hydraulic conductivity values at the interior wells, suggested that these areas of the creek were losing water to the aquifer but at very slow rates.

The water quality results in wells A3 and A4 were similar to previous results (Jacobs and Gilliam 1985). Groundwater movement through a vegetated riparian zone has caused a decrease in NO_3^- concentration due to vegetative uptake or zones of denitrification (Jacobs and Gilliam 1985, Peterjohn and Correll 1984). The area was heavily vegetated and the high water table and low hydraulic conductivity values suggested a reduced environment where denitrification could occur. Low hydraulic conductivity values in the region raise the issue of groundwater age. It could be argued that the concentration difference was merely the result of older groundwater with lower concentrations having moved closer to the creek, while newer groundwater with a higher concentration had just moved from its location in the aquifer below the irrigated field. However, a rough calculation of transit time using the measured hydraulic conductivity at A4 suggested that movement of groundwater from A4 to A3, a distance of approximately 65 m, would take approximately 60 days. That transit time would put the water reaching the creek within the period when irrigation began.

The very low hydraulic conductivity at well A1 indicated that groundwater movement through this area was limited, while there was obvious evidence of groundwater-surface water interactions at well A2. Pore water samples in this area suggested denitrification of surface water in the creek bed sediments because EC and chloride values showed little evidence of mixing. The higher concentrations of total P in the surface water compared to the concentrations in the pore water may have been the result of a P source upstream of the study reach, such as a surface drain. The high velocity of the creek may have kept P bound clays and silts in suspension, while coarser sediments settled to the creek bed (Novotny 2002).

Water quality results for NO_3^- at cross section TIMB were less intuitive to interpret. The well results showed a higher concentration in B2 and a lower concentration in B3 than in the surface water. If the gradient at these locations is assumed to be correct, then it can be inferred that NO_3^- concentrations increase as flows move away from the creek. Total P was also higher in the exterior wells. However, the low hydraulic conductivity value at well B2 indicated that very little water volume was lost to the aquifer in this area. Therefore, the higher concentrations further from the creek may have been the result of concentrated groundwater below irrigated fields flowing north, rather than the increase in concentration of flows away from the creek. The hydraulic conductivity value at B3, approximately 0.6 m/day, was more moderate and suggested that some water was lost to the aquifer in this area. The movement of surface water through the creek bank may have resulted in the decrease of NO_3^- as it moved through a reduced zone and was denitrified. This is supported by the low dissolved oxygen concentration of 0.21 mg/L in B3 at the time of sampling. The NO_3^- and total P concentrations in the pore water samples indicated both a similar denitrifying environment and similar suspended sediment bound P processes to those observed in TIMA.

Surface water sampling suggested a substantial increase in both NO_3^- and total P loadings. Approximately half of both of these loadings could be explained by discharges from TIM Drain. The other half of the total P loading was likely from enrichment and pickup of P bound sediment as flows traveled downstream. The lack of longitudinal concentration increase that would mirror this enrichment may have been masked by the small contributions of low total P concentration groundwater to the creek over the study reach. Based on the groundwater concentrations of NO_3^- near the creek it seems unlikely that contributions from NO_3^- rich groundwater caused the increase in NO_3^- loadings. However, the spike in concentration at the last longitudinal sample point suggested that there was some NO_3^- source between longitudinal sample point 2 and 1. No surface drains or seeps were detected between these two sampling points, which points toward a groundwater source.

4.2.2.2 October Sampling

<u>TIMU and TIMD Sampling</u>

The TIM Drain flow was consistently between 0.16 and 0.21 m^3/s throughout the 24 hour period, which accounted for approximately 75% of the difference between TIMU and TIMD. Discharges and loadings from the second surface drain were found to be negligible. Using average values for discharge at TIMU, TIM Drain, TIMD, and the water balance equation (Equation 6), unaccounted for flow was calculated as 0.06 m^3/s averaged over the 24 hour period.

The loadings for total P during the study period are presented in Figure 51 and plotted with the averaged flows during each two hour period. The TIM Drain two hour loadings are also included in this plot. Generally, these loadings did not account for the full difference between TIMU and TIMD total P loadings. Total P loadings averaged a 17% increase from TIMU to TIMD, which amounted to a total addition of 2 kg. TIM Drain accounted for approximately 40% of the increase. Concentrations of total P (shown in Appendix J) at TIMU ranged from 0.05 to 0.07 mg/L during the sampling period and 0.05 to 0.07 mg/L at TIMD. A mid reach sample also displayed no variation from the upstream concentrations.

NO_3^- as N loadings, presented in Figure 52, increased from TIMU to TIMD by an average of 10%, amounting to a total addition of approximately 39 kg. The average NO_3^- load from TIM Drain made up this entire difference, suggesting very little contribution of NO_3^- from groundwater. Concentrations of NO_3^- at TIMU and TIMD ranged from 1.6 to 1.9 mg/L. A mid-reach sample also showed no variation from the upstream concentrations.

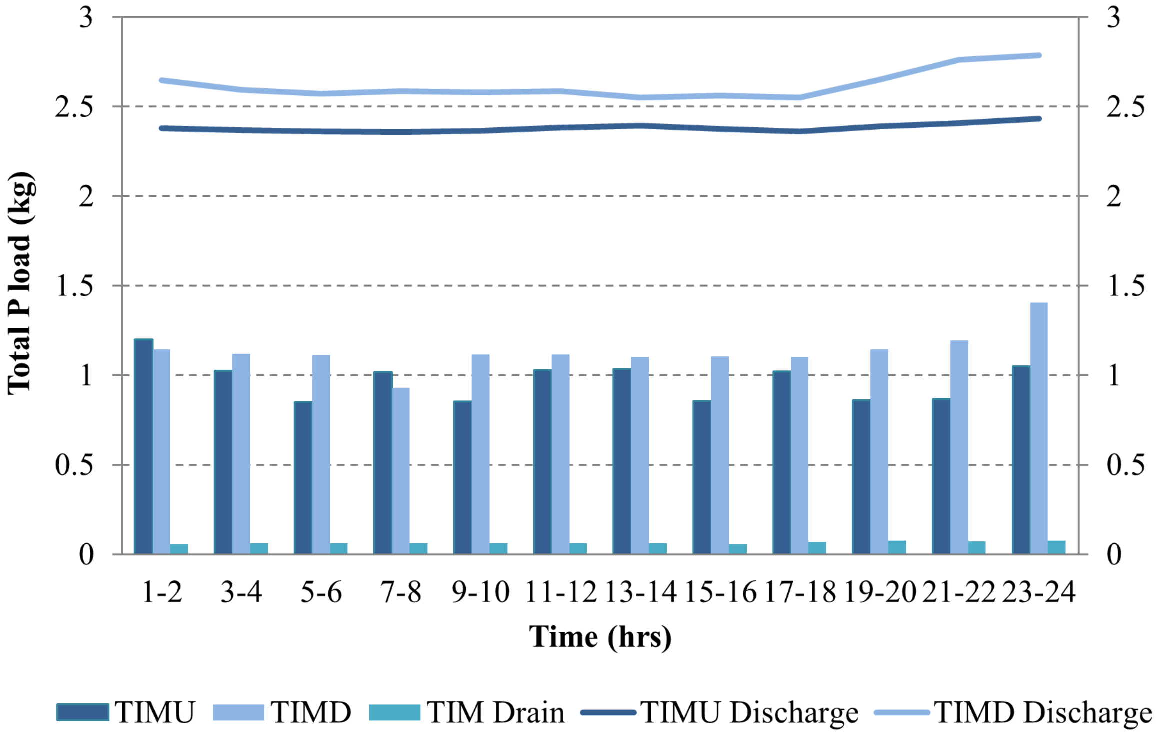

Figure 51. Two hour Total P loadings in Timpas Creek during the October sampling event.

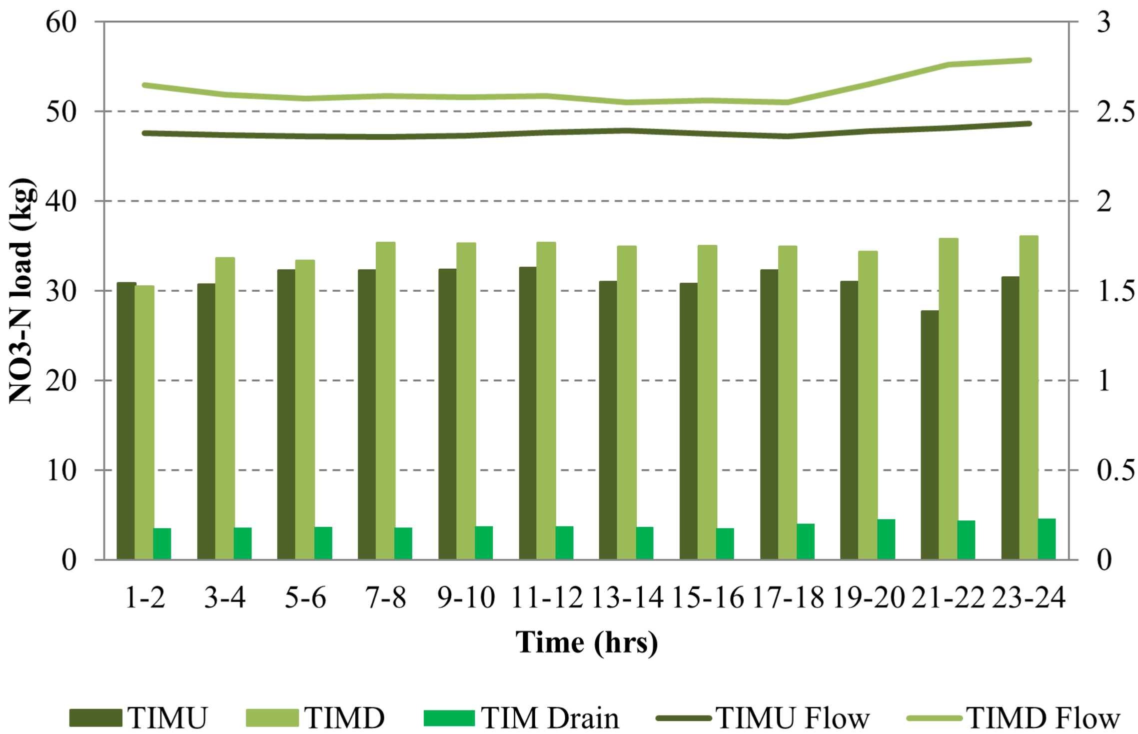

Figure 52. Two hour NO_3-N loadings in Timpas Creek during the October sampling event.

Groundwater Hydraulic Gradients

Well water levels were extracted from the growing season monitoring data for the 24 hour sampling period and cross sections TIMA and TIMB are presented in Figure 53 and Figure 54 respectively. As stated in section 2.2.2, a substantial head difference, which averaged over 5 m, existed between wells A4 and A3 towards the creek. A smaller difference, which averaged 0.26 m, existed between A1 to A2 away from the creek. Similar to the growing season well results, TIMB exhibited gradients away from the creek on both sides. The head differences between B1 and B2 averaged 0.12 m, while the head differences between B4 and B3 averaged 0.01 m.

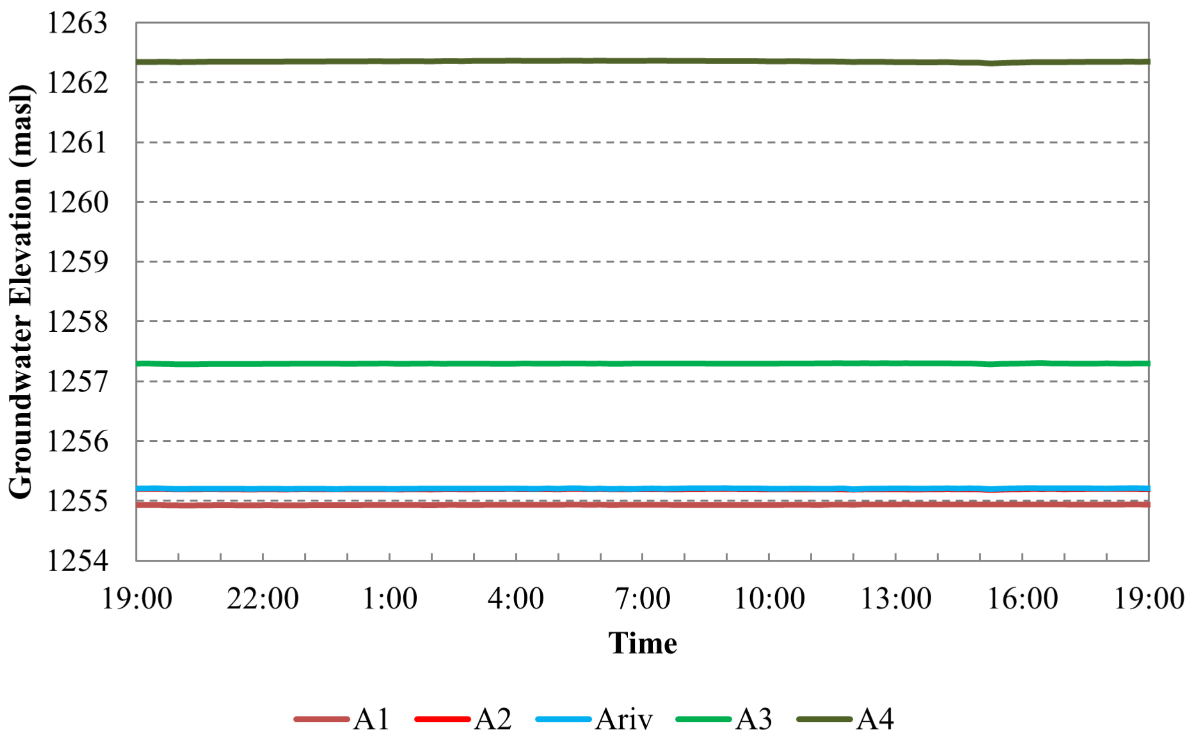

Figure 53. 24-hour well water level elevation monitoring at cross section TIMA in October.

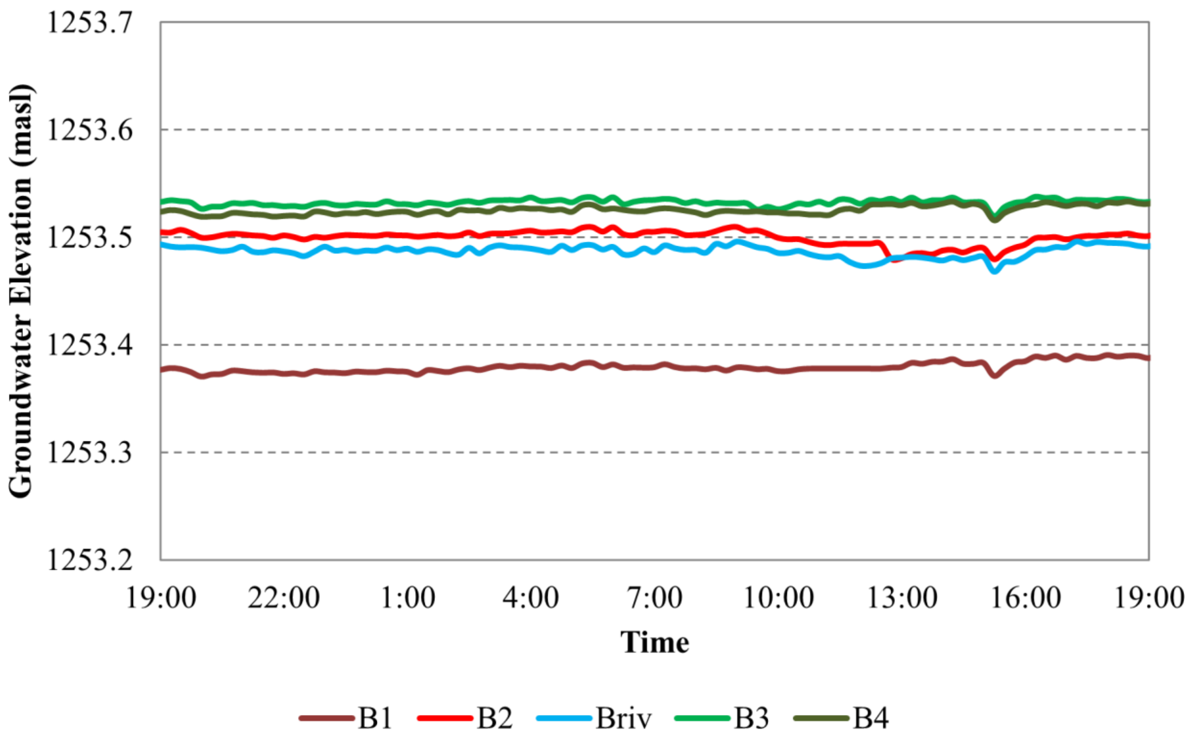

Figure 54. 24-hour well water level elevation monitoring at cross section TIMA in October.

Averaged well water level elevations were calculated, interpolated and extended with ArcGIS. The water level elevations were then overlain onto an average contour plot developed from the existing MODFLOW groundwater model and are shown in Figure 55. The methods and labels for this exercise were the same as those described in section 4.2.1.2. The results of this exercise were similar to the results seen in June. The average water levels measured in wells A3 and A4 were an accurate measurement of the gradients to the southeast of the creek, an area that is contributing water. On the other hand, the average water levels measured in wells A1 and A2, as well as in cross section TIMB, may have only represented minute changes along the same general contour line. The water table was approximately 0.5 m higher in October than it was in June, but the general flow direction was the same.

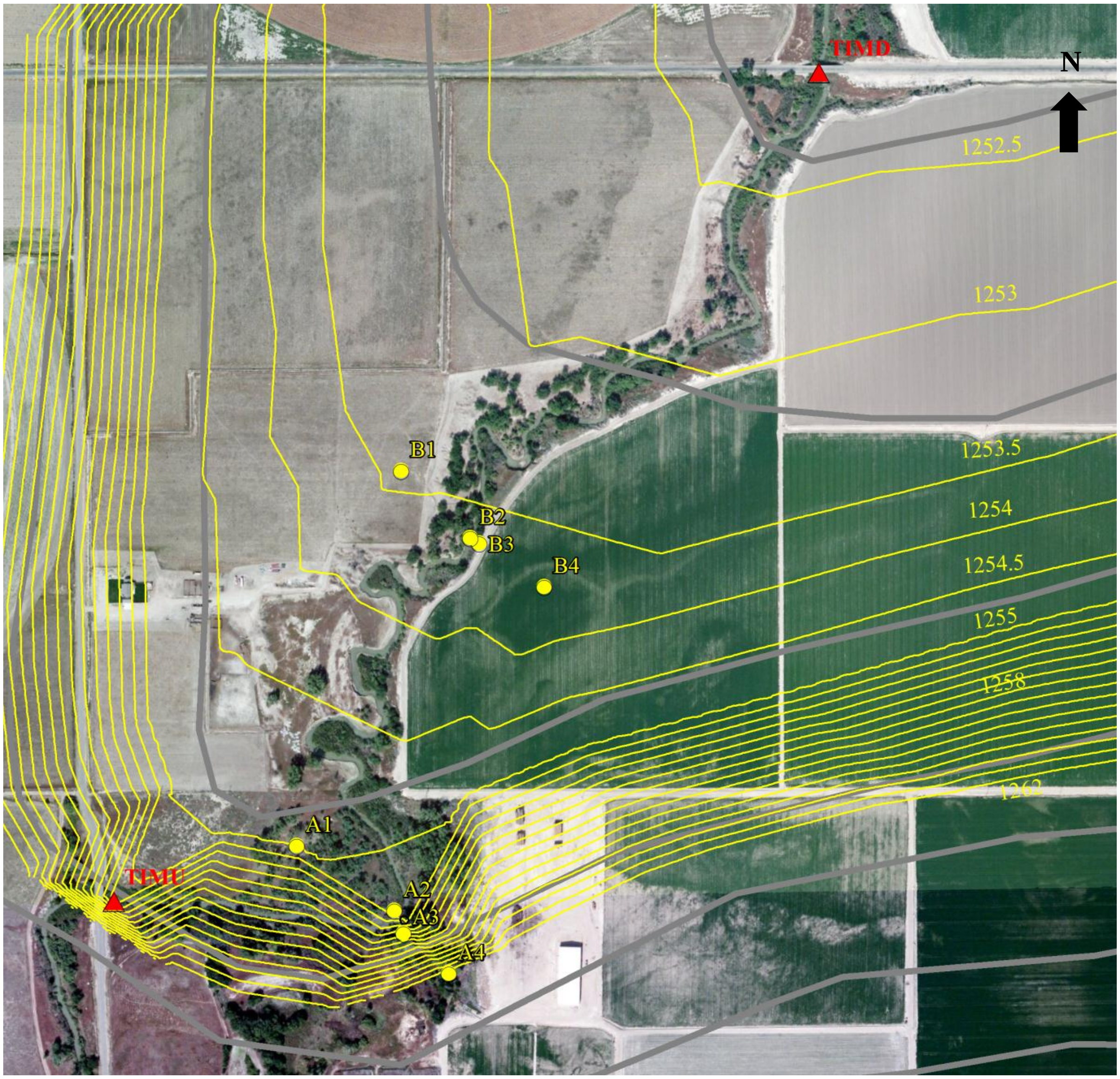

Figure 55. Water table contour plot from model results (grey lines) and Timpas Creek averaged field measurements in October (yellow lines).

Groundwater Quality

Water quality sample results for NO_3^- as N, NH_4^+ as N and/or NO_2^- as N, total P, chloride, and electrical conductivity from each well in cross section TIMA and TIMB are presented in Figure 50. The plots have the same setup as described in section 3.2.1.1. Once again, chloride concentrations and EC values in interior wells displayed little evidence of mixing between surface and groundwater. In contrast to the June sample event, in October the chloride and EC values were similar to the groundwater values in the pore water in cross section TIMA (approximately 60 mg/L and 3.0 mmho/cm). While chloride and EC values were consistent at almost every pore water sample point, the NO_3^- concentration in the left pore water sample (1.3 mg/L) was slightly lower than the surface water concentration (1.5 mg/L). However, it was still comparable to the surface water concentration. The NO_3^- concentration in the middle pore water point (0.8 mg/L) was approximately half of the concentration in the surface water. The NO_3^- concentration at the right point was even lower (<0.1 mg.L), with an increased concentration of NH_4^+ (0.4 mg/L). The right sample point and well A3 had very similar values for NO_3^-, EC, and chloride. Well A2 had a similar concentration of N species to those observed in A1, but in the reduced NH_4^+ form. During this sample event there was no difference in NO_3^- concentration between wells A3 and A4 (0.5 mg/L). Total P concentrations showed little variation between sample points in TIMA, except at the pore water sample point adjacent to well A3 where it was double the other values (0.15 mg/L).

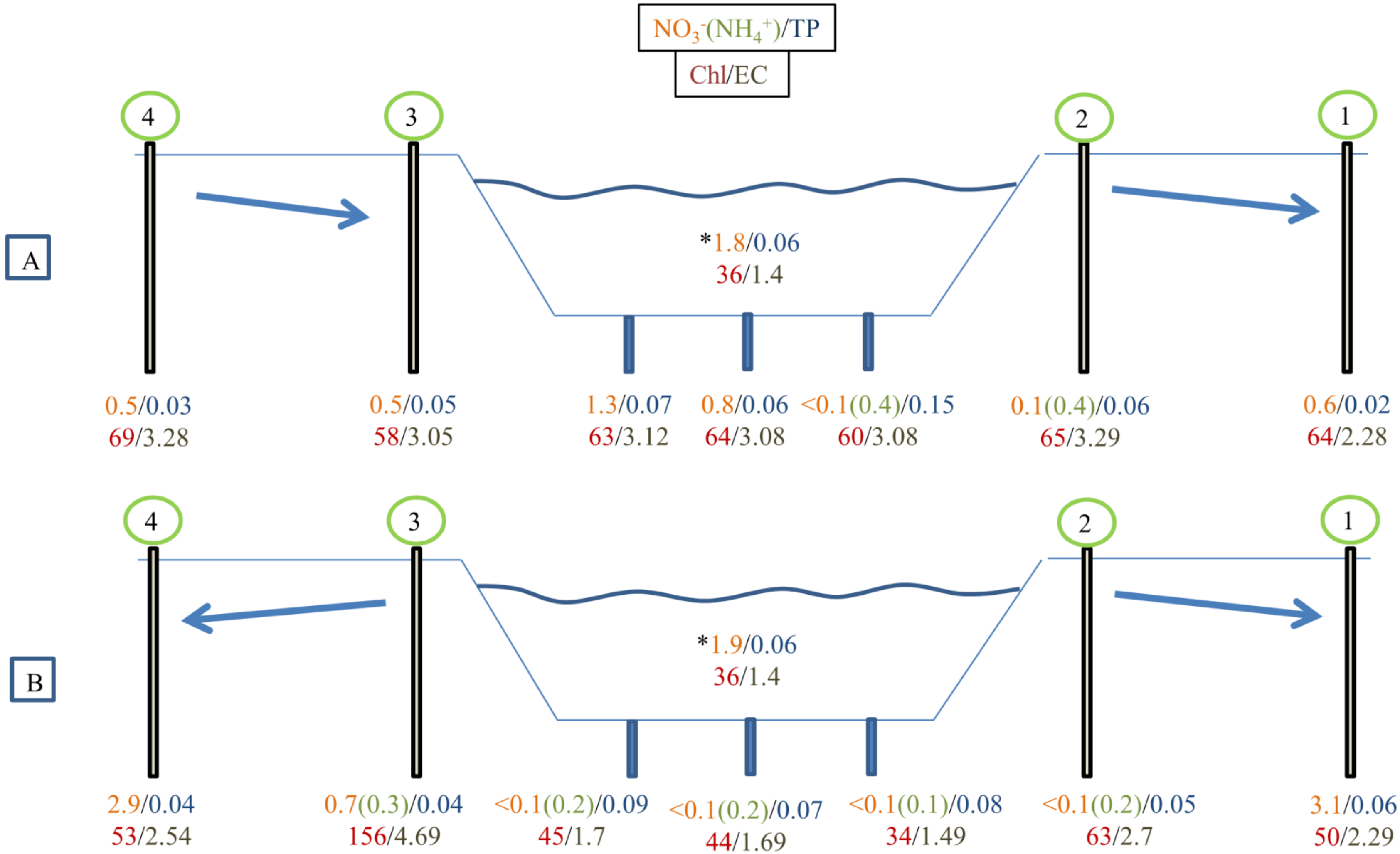

*In-stream flow concentration interpolated

Figure 56. Well water quality results for cross sections TIMA (a) and TIMB (b) on October 17 2014. Nutrients and chloride have units of mg/L and electrical conductivity has units of mmho/cm.

Cross section TIMB had the highest chloride and EC values in the interior wells B2 and B3. The pore water chloride and EC values were higher in the left and middle sample points, while the right sample point approximately matched the surface water values. Similar to the June sample event, in October the interior wells had the lowest NO_3^-/NH_4^+ concentrations in the well pairs and N species concentrations in the pore water samples were consistently lower than in the surface water. The total P concentration was relatively constant at all sampling locations with slightly higher values in the pore water samples.

Discussion

The October sampling event occurred less than one week after a high flow event on October 13. The average discharge on that date was over two times the historic average for TIMU, as shown in Figure 19. The measured peak flow that day was approximately 10.9 m^3/s. While this flow was not unprecedented for Timpas Creek, it was out of season based on the historic average. This high flow late in the year may have disturbed bed sediments and any biological communities in the creek and therefore is less representative of the conditions typically present at this time of year. Unaccounted for flow was assumed to be the result of groundwater contribution to the reach, which is supported by the growing season monitoring analysis at this date. In addition, the TIM Drain discharge did not account for the difference between TIMU and TIMD.

Groundwater-surface water interactions along the study reach displayed some variation from the June sample event. This is to be expected due to the multiple flooding events between sampling periods and the high flow event directly before. The one-dimensional hydraulic gradients were similar to those measured during the June event. The one major difference was that the head differences between wells in TIMB decreased.

The cross section water quality results for October also showed some differences from the June sampling event. The biggest difference was that there was no change in NO_3^- concentration between wells A4 and A3 and NO_3^- concentrations in well A4 decreased nearly 10 times between the June and October sampling events. There are multiple explanations for this change and the following hypotheses were considered the most feasible.

The high NO_3^- concentrations at A4 in June were likely due to increased fertilizer application on the adjacent agricultural field at the beginning of the growing season. The fertilizer may have been applied in excess of the crop requirements at that time and bacterial communities that could degrade the excess had not fully established or were overwhelmed. The high concentration groundwater may have then flowed through the vegetated riparian zone where denitrification and vegetative uptake reduced the NO_3^- load approaching the creek. It is likely that toward the end of the growing season in October, fertilizer application had ceased and agricultural crops had been harvested or were close to harvesting. This would have reduced NO_3^- concentrations in groundwater below the fields and in areas adjacent to the fields. This is supported by decreased concentrations reported in October at well B4, located directly in an irrigated field.

Another explanation for the lack of decrease between well A4 and A3 could have been the low NO_3^- concentration itself. NO_3^- concentrations have been shown to be a limiting factor of denitrification along with organic carbon sources and dissolved oxygen concentrations (Cavari and Phelps 1977, Wang et al. 1995). Therefore, it is likely that the low groundwater concentration was not acted upon by denitrifying zones in the riparian zone. Furthermore, biological uptake of NO_3^- may have also been reduced due to N saturation of the vegetative material because it was the end of the growing season. The riparian zone in this area had been intercepting NO_3^- rich groundwater for five months and had potentially reached its capacity for assimilation.

In addition, the pore water results in TIMA changed from June to October. The pore water samples in TIMA appeared to reverse the high and low NO_3^- concentration locations observed in June. In June, the lowest concentration of NO_3^- was found in the pore water sample adjacent to well A3, whereas in October the lowest concentration was found adjacent to A2. The water source of the pore water samples also appears to have changed from June to October. In June it was evident that the pore water sample was composed primarily of surface water. However, based on chloride and EC values, it became apparent that in October the pore water sample consisted primarily of groundwater. The changes in NO_3^- concentration may have been the result of shifting sediment during high flows or changes in areas of denitrification in the hyporheic zone.

Well water quality results in cross section TIMB for October were similar to results from the June sampling event. Low concentrations of NO_3^- existed at the interior well locations, while higher concentrations were found at the exterior wells. The big difference at this cross section was found in the pore water samples. Similar to the June event, the chloride and EC values indicated that the primary water source was surface water in October. However, the pore water NO_3^- concentrations were much lower than both the surface water and groundwater concentrations. Again, the spatially variable nature of denitrification in the hyporheic zone of this study reach is evident.

Total P concentrations in the pore water samples at both cross sections were equal to, or higher than, concentrations in the surface water or groundwater. This suggests that the low oxygen environments that were reducing NO_3^- in the pore water were creating zones of P mobility in the hyporheic zone, as shown by Lewandowski and Nützmann (Lewandowski and Nützmann 2010). However, the low concentration differences between pore water and surface water make it difficult to draw concrete conclusions.

4.3 Conclusions

24-hour water quality sampling provided considerable insight into the variation and trends in groundwater and surface water interactions in the Arkansas River and Timpas Creek. During the June sample event in the Arkansas River, 24-hour surface water sampling supported the hypothesis that high flows and velocities inhibit any significant nutrient interactions with river bed substrate, hyporheic exchange, or biological activity. On the other hand, data collected during low flows in the October sample event displayed a substantial decrease in NO_3^- loadings and an increase in total P loadings. The primary modes of NO_3^- load reduction were assumed to be in-stream processes such as vegetative assimilation and groundwater-surface water exchange in denitrification areas within the hyporheic zone, based on the results from well and pore water sampling. The increase in total P loadings was attributed to contribution from groundwater flows and in stream enrichment.

Groundwater samples collected along the banks of the Arkansas River suggested that groundwater movement through any amount of riparian zone produces a reduction in NO_3^- concentration. The exact mechanisms of this reduction were not analyzed in this study but the overwhelming body of evidence in the literature points to vegetative uptake and zones of denitrification. No distinguishable trend was observed for groundwater concentrations of total P. This result has also been well documented in the literature and can be summarized by stating that P mobilization and immobilization in the groundwater aquifer is a variable and complex process which requires a more thorough understanding of the system and more spatially and temporally frequent measurements to provide any meaningful analysis.

24-hour water quality sampling in Timpas Creek revealed a similarly complex mosaic of groundwater and surface water mixing and exchange. Water mass balance calculations suggested small contributions to surface flow from groundwater and was supported by the low hydraulic conductivity floodplain surrounding the creek. However, analysis of well water elevations and groundwater contours indicated that the creek had both areas of groundwater contribution and areas of surface water loss to the aquifer.

24-hour surface water sampling showed increases in total P and NO_3^- from upstream to downstream in June, but very little change in October. The increases in June can be explained by total P enrichment in the surface water and isolated areas of NO_3^- loading contribution from groundwater. The lack of change during the October sampling event was likely due to high flows prior to the sampling period, which may have disturbed biological communities and bed sediments. The disturbed sediments from flows in October, as well as in July, may have affected the pore water sample results as well, which indicated large changes in the function of the hyporheic zone during the study period. Between June and October, areas of denitrification shifted; cross sections where little denitrification occurred switched to denitrification "hot spots" and the source of water in the hyporheic zone also showed some variation.

Results from groundwater sampling showed high spatial and temporal variation over this short study reach. Only one well pair (TIMA3 and A4) showed removal of NO_3^- as groundwater moved through a vegetated riparian zone. However, this process was not repeated during the October sampling event. The other well pairs appeared to be located in areas where water was lost from the creek to the aquifer. Groundwater and surface water exchanges were shown to be most prevalent at the A2 and B2 well locations, as evidenced by moderate hydraulic conductivity values and chloride and EC values. In all cases, the interior well results reported the lowest NO_3^- concentrations and low hydraulic conductivity values suggesting that denitrification may have been the primary mechanism of NO_3^- loss. One-dimensional gradients supported evidence of flow away from the creek at cross section TIMB and from well A2 to A1. However, the interpolated groundwater contours, low hydraulic conductivities at the creek banks, and the higher concentrations of NO_3^- suggest that the exterior wells were more representative of groundwater from below irrigated fields flowing north than an increase in NO_3^- concentration as water from the creek flows through the aquifer.

CHAPTER 5: CONCLUSIONS AND RECOMMENDATIONS

5.1 Conclusions from Monitoring Efforts

Monitoring hydro-chemical processes on study reaches in the Arkansas River and Timpas Creek has enriched the knowledge of nutrient dynamics on small spatial and temporal scales in the Lower Arkansas River Valley. Previous regional monitoring and modeling studies in the study region provided insights into large-scale scale processes, however, very little data for reach scale processes existed prior to this study. Growing season and 24-hour monitoring between April and November 2014 has shown the variable nature of nutrient dynamics within a single growing season. By measuring discharges, groundwater gradients, and water quality throughout the growing season, in-stream processing and nutrient loads were estimated.

Nutrient loadings in the Arkansas River exhibited evidence of increased in-stream NO_3^- processing after the initial high discharges in the spring, while nutrient loadings in Timpas Creek suggested point sources of NO_3^- contribution from groundwater and displayed minimal evidence of significant groundwater-surface water exchanges. Total P showed little growing season variation in both study reaches but slight increases in surface water loadings during the 24 hour sample events were likely due to groundwater contributions and enrichment of fine sediments in the channel. Water quality sampling in the hyporheic zone and groundwater in the riparian corridor supported common themes in the literature of NO_3^- reduction by vegetative assimilation and denitrification. The effectiveness of riparian zones in NO_3^- removal was shown by decreased NO_3^- concentrations along approximate groundwater flow paths at many of the monitored cross sections. However, these removals were spatially and temporally variable, particularly along the short reach on Timpas Creek. Hyporheic zone sampling also suggested high spatial and temporal variation within the study reaches. Results for total P in this study supported statements in the literature that mobilization and immobilization of P is a spatially variable process in both groundwater and the hyporheic zone.

Being one of the first small scale, high frequency nutrient monitoring studies in the region this research enriched the knowledge base of reach-scale processes. However, certain aspects of the research method could have been improved. The lack of high flow discharge measurements at the ARKD monitoring station may have reduced the accuracy of loading and water balance calculations during the first half of the study period. The chosen location made discharge measurements difficult and dangerous at high flows but there were few alternatives. One option to consider for future studies in the area is to double the length of the study reach to use the bridge crossing on County Road 24.5 as the downstream monitoring station. This would have made high discharge measurements easier to perform from the safety of the bridge. One drawback to this change is that the confluence of Timpas Creek and the Arkansas River is just upstream of CR 24.5 and would require another set of discharge measurements. Another issue with the placement of the Arkansas River study reach is that it does not include any irrigated fields directly adjacent to the river channel. Most of the land to the southwest of the reach was left fallow for the study period. Groundwater concentrations and nutrient dynamics from irrigated fields adjacent to the river would have been useful in comparing to the vegetated riparian zones.

The Timpas Creek study area includes irrigated agriculture directly adjacent to the creek channel. However, in addition to the lack of high flow measurements at TIMD, the complicated geology and groundwater gradients in the area made drawing conclusions about groundwater-surface water interactions very difficult. More wells would be required to infer the true nature of the water table and gradients along the study reach.

Issues common to both study areas included lack of high flow measurements as well as instability of the AT installations. The initial intent of the in-stream installations was to be impermanent and easy to move in case changes needed to be made and to keep costs low. The downside to this impermanence was that the installations were highly susceptible to damage and displacement during high flows. This would not have been an issue during an average precipitation and flow year, however, the flashy flood events in June and July caused significant damage to in-stream sensors and AT installations. The unpredictable nature of extreme flow events in the area makes the author urge future monitoring efforts to make in-stream installations more permanent or to use bridge mounted, non-contact water level sensors such as radar or ultrasonic devices.

Both sites also lacked a 24 hour sample event during the middle of the growing season. This was primarily due to recovery from high flow damages and budget restrictions. This resulted in the two sampling events on the Arkansas River coinciding with the only two time periods when the river was gaining water volume from the aquifer. Based on the 24 hour auto-sampler results, the same information could have been gathered with fewer samples. Therefore it is the opinion of the author that more of the budget could be used for higher frequency groundwater and pore water sampling if future monitoring campaigns are attempted.

5.2 Applications of Gathered Data and Avenues for Future Research

The data gathered during this study will be used in the development of small scale, hydro-chemical, groundwater-surface water exchange models. The models will create a platform from which broader conclusions can be drawn about the study reaches. For example, seasonal variations in regional groundwater elevations and gradients, nutrient and salt dynamics, hydraulic conductivity interpolation, and mass loading calculations are all aspects that can be explored through model development.

Continued monitoring of well water elevations and water quality data collection past this study period will allow for calibration and validation of these models. Other avenues for future research could include:

1) Monitoring seasonal variation in hydraulic conductivity. In this study, hydraulic conductivity was only measured at the end of the growing season. Factors such as water temperature and saturation of the soil column can affect this parameter spatially and temporally. While it was not a key component to the conclusions drawn in this study, seasonal variation may be necessary for future modeling efforts and mass loading calculations.
2) Extensive monitoring of the hyporheic zone using pore water sampling. Pore water samples collected in this study hinted at the highly variable nature of the hyporheic zone in both study reaches. Sample collection from multiple depths below the channel bed and more frequently throughout the growing season would clarify those variations.
3) Acquiring estimates of denitrification and P immobilization/mobilization capacity in riparian soils and channel bed sediments through lab experiments. Without these estimates, a true quantification of the losses and gains of nutrients in the study reaches cannot be completed. If estimates existed of these values under various conditions clearer distinctions could be made between in-stream processes such as denitrification and vegetative uptake.
4) Focus efforts on one intensively monitored area. For example, take a single cross section of the study reach and intensively monitor every aspect of it. The multi-level sampler results in

this study suggest significant differences in concentration of NO_3^- at various levels in the soil column. This could be explored further by installation of more multi-level samplers in a small area and a more frequent sampling schedule.

5) Perform an uncertainty analysis on all aspects of data collection and management. Conclusions and statements were made in this study with little quantitative attention paid to the uncertainty involved in many of the measurements. Flow measurements, variations in water quality due to depth or location, water table depth measurements, and laboratory testing are all sources of error that could be quantified to determine the precision and accuracy of the results presented.

5.3 Conclusions Regarding Nutrients in Irrigated Agriculture

Results from this study support past research on the benefit of riparian zones as areas of N removal and suggest that in-stream processing can also play a major role in the reduction of N loadings. P loadings on the other hand were shown to be variable and often unaffected by movement through the riparian zone and that in-stream sediments can act as a source. Excess loadings of these nutrients from agricultural diffuse pollution are a primary cause of eutrophication in rivers, lakes, estuaries, and coastal ocean waters. Eutrophication then leads to toxic algal blooms, oxygen depletion, and loss of aquatic life. Nutrients will continue to be of particular concern in agriculture because as the demand for food increases, irrigated agriculture and fertilizer use will continue to increase. This, in turn, will rapidly deteriorate the world's waterways unless conservation and mitigation practices are adopted. Monitoring and modeling of the riparian environment will continue to be necessary to assess how riverine systems react to increased nutrient loads.

WORKS CITED

Alexander, R. B., Smith, R. A., Schwarz, G. E., Boyer, E. W., Nolan, J. V., and Brakebill, J. W. (2008). Differences in Phosphorus and N Delivery to The Gulf of Mexico from the Mississippi River Basin. *Environmental Science and Technology, 42*, 822-830.

Bailey, R. T. (2012). *Regional selenium cycling in an irrigated agricultural groundwater system: Conceptualization, modeling, and mitigation*. Dissertation, Colorado State University.

Bailey, R. T., Hunter, W. J., and Gates, T. K. (2012). The influence of NO_3^- on selenium in irrigated agricultural groundwater systems. *Journal of Environmental Quality, 41*, 783-792.

Birgand, F. R., Skaggs, R. W., Chescheir, G. M., and Gilliam, J. W. (2007). N removal in streams of agricultural catchments-a literature review. *Critical Reviews in Environmental Science and Technology, 37*, 381-487.

Burkart, M. R., and James, D. (1999). Agricultural-N Contributions to Hypoxia in the Gulf of Mexico. *Journal of Environmental Quality, 28*, 850-859.

Burt, T. P., Pinay, G., Matheson, F. E., Haycock, N. E., Butturini, A., Clement, J. C., . . . Maitre, V. (2002). Water table fluctuations in the riparian zone: comparative results from a pan-European experiment. *Journal of Hydrology, 265*, 129-148.

Butler, J. J. (1998). *The Design, Performance, and Analysis of Slug Tests.* Boca Raton, Florida: CRC Press LLC.

Carpenter, S. R., Caraco, N. F., Correll, D. L., Howarth, R. W., and Sharpley, A. N. (1998). Nonpoint pollution of surface waters with phosphorus and N. *Ecological Applications*, 559-568.

Cavari, B., and Phelps, G. (1977). Denitrification in Lake Kinneret in presence of oxygen. *Freshwater Biology, 7*, 385-391.

Cooper, A. B. (1990). NO_3^- depletion in the riparian zone and stream channel of a small headwater catchment. *Hydrobiologia, 202*, 13-26.

Cox, M. H., Su, G. W., and Constantz, J. (2007). Heat, Chloride, and Specific Conductance as Ground Water Tracers near Streams. *Groundwater, 45*, 187-195.

Cunningham, W., Schalk, C., and comps. (2011). *Groundwater technical procedures of the U.S. Geological Survey: U.S. Geological Survey Techniques and Methods 1-A1.* U.S. Geological Survey.

Duff, J. H., Tesoriero, A. J., Richardson, W. B., Strauss, E. A., and Munn, M. D. (2008). Whole-Stream Response to NO_3^- Loading in Three Streams Draining Agricultural Landscapes. *Journal of Environmental Quality, 37*, 1133-1144.

Erisman, J. W., Sutton, M. A., Galloway, J., Klimont, Z., and Winiwarter, W. (2008). How a century of ammonia synthesis changed the world. *Natural Geoscience, 1*, 636-639.

Fernandez-Cirelli, A., Arumi, J. L., Rivera, D., and Boochs, P. W. (2009). Environmental effects of irrigation in arid and semi-arid regions. *Chilean Journal of Agricultural Research, 69*, 27-40.

Gali, R. K., Soupir, M. L., and Helmers, M. J. (2012). Electrical Conductivity as a tool to estimate chemical properties of drainage water quality in the Des Moines Lobe, Iowa. *American Society of Agricultural and Biological Engineering Annual International Meeting*. Dallas: American Society of Agricultural and Biological Engineers.

Gates, T. K., Cody, B. M., Donnelly, J. P., Herting, A. W., Bailey, R. T., and Price, J. M. (2009). Assessing selenium contamination in the irrigated stream-aquifer system of the Arkansas River, Colorado. *Journal of Environmental Quality, 38*, 2344-2356.

Gates, T. K., Garcia, L. A., Hemphill, R. A., Morway, E. D., and Elhaddad, A. (2012). *Irrigation Practices, Water Consumption, and Return Flows in Colorado's Lower Arkansas River Valley: Field and Model Investigations.* Colorado Water Institute.

Gijzen, H. J., and Mulder, A. (2001, August). The N cycle out of balance. *Water21*(3.4), pp. 38-40.

Halford, K. J., and Kuniansky, E. L. (2002). *Documentation of Spreadsheets for the Analysis of Aquifer-Test and Slug-Test Data.* Carson City: U.S. Geological Survey.

Haria, A. H., Shand, P., Soulsby, C., and Noorduijn, S. (2012). Spatial delineation of groundwater-surface water interactions through intensive in-stream profiling. *Hydrological Processes, 27*, 628-634.

Heathwaite, A. L., and Dils, R. M. (2000). Characterising phosphorus loss in surface and subsurface hydrological pathways. *Science of the Total Environment, 251-252*, 523-538.

Holman, I. P., Whelan, M. J., Howden, N. J., Bellamy, P. H., Willby, N. J., Rivas-Casado, M., and McConway, P. (2008). Phosphorus in groundwater-an overlooked contributor to eutrophication? *Hydrological Proccesses, 22*, 5121-5127.

House, W. A., and Warwick, M. S. (1998). A mass-balance approach to quantifying the importance of in-straem processes during nutrient transport in a large river catchment. *Science of the Total Environment, 210-211*, 139-152.

Iwanyshyn, M., Ryan, M., and Chu, A. (2009). Cost-Effective Approach for Continuous Major Ion and Nutrient Concentration Estimation in a River. *Journal of Environmental Engineering, 135*, 218-224.

Jacobs, T. C., and Gilliam, J. W. (1985). Riparian losses of NO_3^- from agricultural drainage waters. *Journal of Environmental Quality, 14*, 472-478.

Jain, C. K. (1996). Application of chemical mass balance to upstream/downstream river monitoring points. *Journal of Hydrology, 182*, 105-115.

Jarvis, S. C., and Hatch, D. J. (1994). Potential for denitrification at depth below long-term grass swards. *Soil Biology and Biochemistry, 26*, 1629-1636.

Jaworski, N. A., Groffman, P. M., Keller, A. A., and Prager, J. C. (1992). A watershed N and phosphorus balance: The Upper Potomac River Basin. *Estuaries, 15*, 1706-1715.

Jiao, P., Xu, D., Wang, S., Wang, Y., Lin, K., and Tang, G. (2012). N loss by surface runoff from different cropping systems. *Soil Research, 50*, 58-66.

Jordan, T. E., and Weller, D. E. (1996). Human Contributions to Terrestrial N Flux. *BioScience, 46*, 655-664.

Khalid, R., Patrick, W. J., and DeLaune, R. (1977). Phosphorus sorption characteristics of flooded soils. *Soil Science Society of Americal Journal, 41*, 305-310.

Lewandowski, J., and Nutzmann, G. (2010). Nutrient retention and release in a floodplain's aquifer and in the hyporheic zone of a lowland river. *Ecological Engineering, 36*, 1156-1166.

Logan, T. (1982). Mechanisms for release of sediment-bound phosphate to water and the effects of agricultural land management on fluvial transport of particulate and dissolved phosphate. *Hydrobiology, 92*, 219-231.

Martin, C., and Gates, T. (2014). Uncertainty of canal seepage losses estimated using flowing water balance with acoustic Doppler devices. *Journal of Hydrology*, 746-761.

McDowell, R. W., and Sharpley, A. N. (2003). Uptake and release of phosphorus from overland flow in a stream environment. *Journal of Environmental Quality, 32*, 937.

McMahon, P. B., and Bohlke, J. K. (1996). Denitrification and mixing in a stream-aquifer system: effects on NO_3^- loading to surface water. *Journal of Hydrology, 186*, 104-128.

Mellander, P.-E., Melland, A. R., Jordan, P., Wall, D. P., Murphy, P. N., and Shortle, G. (2012). Quantifying nutrient transfer pathways in agricultural catchments using high temporal resolution data. *Environmental Science and Policy, 24*, 44-57.

Monteagudo, L., Moreno, J. L., and Picazo, F. (2012). River eutrophication: Irrigated vs. non-irrigated agriculture through different spatial scales. *Water Research, 46*, 2759-2771.

Morway, E. D., Gates, T. K., and Niswonger, R. G. (2013). Regional-scale appraisal of options to enhance groundwater flow conditions in an irrigated alluvial aquifer system. *Journal of Hydrology*, in review.

Mueller, D. K., Hamilton, P. A., Helsel, D. R., Hitt, K. J., and Ruddy, B. C. (1992). *Nutrients in Ground Water and Surface Water of the United States-An Analysis of Date Through 1992*. USGS Water-Resources Investigations Report 95-4031.

Nolan, B. T., Ruddy, B. C., Hitt, K. J., and Helsel, D. R. (1998). A National Look at NO_3^- Contamination of Ground Water. *Water Conditioning and Purification, 39*, 76-79.

Novotny, V. (2002). Water Quality: Diffuse Pollution and Watershed Management. Hoboken, NJ: John Wiley and Sons, Inc.

Peterjohn, W. T., and Correll, D. L. (1984). Nutrient dynamics in an agricultural watershed: Observations on the role of a riparian forest. *Ecology, 65*, 1466-1475.

Puckett, L. J., Zamora, C., Essaid, H., Wilson, J. T., Johnson, H. M., Brayton, M. J., and Vogel, J. R. (2008). Transport and fate of NO_3^- at the ground-water/surface-water interface. *Journal of Environmental Quality, 37*, 1034-1050.

Reddy, K. R., Kadlec, R. H., Flaig, E., and Gale, P. M. (1999). Phosphorus retention in streams and wetlands: a review. *Critical Reviews in Environmental Sciences and Technology, 29*, 83-146.

Schemel, L. E., Cox, M. H., Runkel, R. L., and Kimball, B. A. (2006). Multiple injected and natural conservative tracers quantify mixing in a stream confluence affected by acid mine drainage near Silverton, Colorado. *Hydrological Processes, 20*, 2727-2743.

Sharpley, A. N., Chapra, S. C., Wedepohl, R., Sims, J. T., Daniel, T. C., and Reddy, K. R. (1994). Managing Agricultural Phosphorus for Protection of Surface Waters: Issues and Options. *Journal of Environmental Quality, 23*, 437-451.

Sharpley, A. N., Foy, B., and Withers, P. (2000). Practical and Innovative Measures for the Control of Agricultural Phosphorus Losses to Water: An Overview. *Journal of Environmental Quality, 29*, 1-9.

Simmard, R. R., Beauchemin, S., and Haygarth, P. M. (2000). Potential for preferential pathways of phosphorus transport. *Journal of Environmental Quality, 29*, 97-105.

Soil Survey Staff, Natural Resources Conservation Service, United States Department of Agriculture. (n.d.). Web Soil Survey. Retrieved March 23, 2014, from http://websoilsurvey.nrcs.usda.gov/

Stelzer, R. S., Bartsch, L. A., Richardson, W. B., and Strauss, E. A. (2011). The dark side of the hyporheic zone: depth profiles of N and its processing in stream sediments. *Freshwater Biology, 56*, 2021-2033.

Stelzer, R. S., Drover, D. R., Eggert, S. L., and Muldoon, M. A. (2011). NO_3^- retention in a sand plains stream and the importance of groundwater discharge. *Biogeochemistry, 103,* 91-107.

Strange, E. M., Fausch, K. D., and Covich, A. P. (1999). Sustaining ecosystem services in human-dominated watersheds: Biohydrology and ecosystem processes in the South Platte River Basin. *Environmental Management, 24*, 39-54.

Swaney, D. P., Hong, B., Ti, C., Howarth, R. W., and Humborg, C. (2012). Net anthropogenic N inputs to watersheds and riverine N export to coastal waters: a brief overview. *Current Opinion in Environmental Sustainability, 4*, 203-2011.

Teissier, S., Sauvage, S., Vervier, P., Garabetian, F., and Sanchez-Perez, J. (2008). A mass-balance approach to estimate in-stream processes in a large river. *Hydrological Processes, 22*, 420-428.

Tilman, D. (1999). Global environmental impacts of agricultural expansion: the need for sustainable and efficient practices. *Proceedings of the National Academy of Sciences, 96,* pp. 5995-6000.

United States Environmental Protection Agency. (1986). *Quality criteria for water 1986.* Washington, DC: Office of Water.

United States Environmental Protection Agency. (2007). *Hypoxia in the Northern Gulf of Mexico*. Washington, DC: EPA Science Advisory Board.

Vaneck, V. (1991). Riparian zone as a source of phosphorus for a groundwater-dominated lake. *Water Research, 25*, 409-418.

Wang, J., Baltzis, B., and Lewandowski, G. (1995). Fundamental denitrfication kinetic-studies with pseudomonas-denitrificans. *Biotechnology and Bioengineering, 47*, 26-41.

APPENDICES

APPENDIX A: SOIL MAPS OF EACH STUDY REACH

Soils data was collected from the USDA Web Soil Survey (http://websoilsurvey.sc.egov.usda.gov/App/HomePage.htm). The extent and map unit label of each soil type is presented in the figures below. More detailed soils data is available upon request

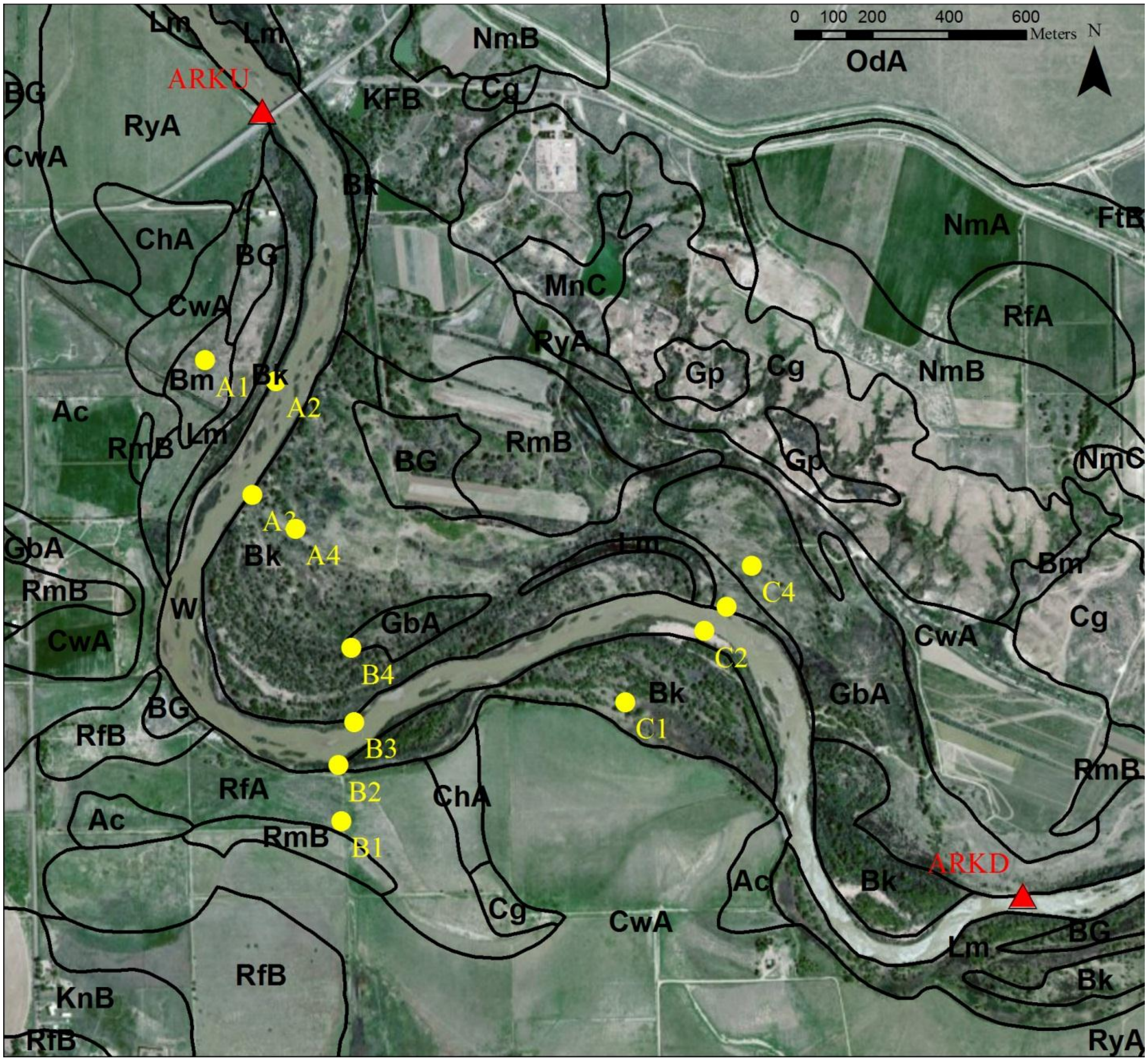

Figure A- 1. Soil map of the Arkansas River study reach.

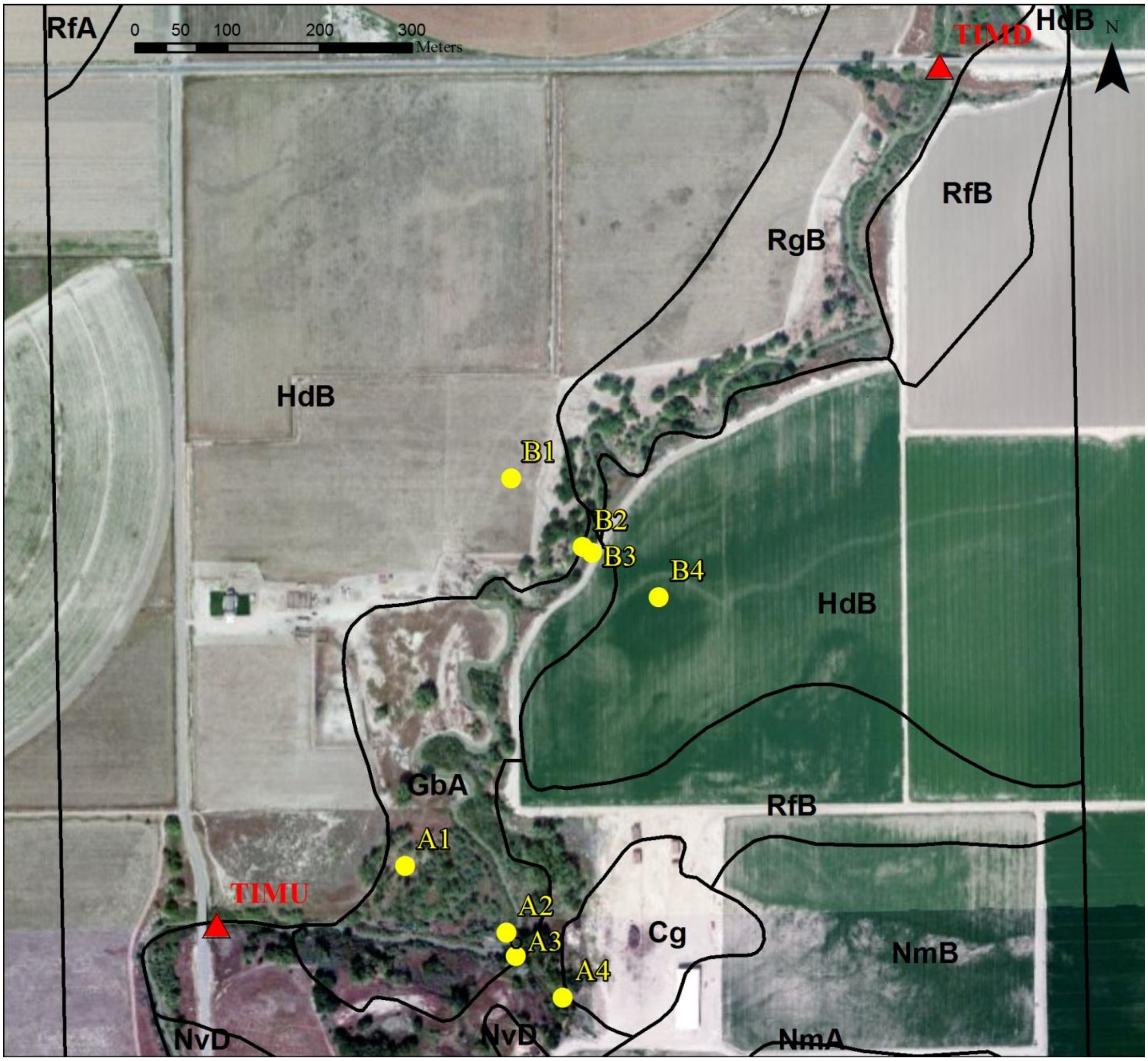

Figure A- 2. Soil map of the Timpas Creek study reach.

APPENDIX B: SLUG TESTING PROCEDURE AND USGS HYDRAULIC CONDUCTIVITY CALCULATION TOOL

Hydraulic conductivity was measured once at every well from November 6 to 7 using slug tests and bailer removal methods. Using an In-Situ Aqua Troll 700 (AT 700) multiparameter probe, a 0.3 m cylindrical slug, and a 1.0 m bailer, three slug in-slug out tests and three bailer removals were performed at each well with the exception of well B2. At B2, six slug tests and one bailer removal were performed due to slow groundwater recharge at this site.

Procedure

A step by step process of the field methods is presented below. Images of the materials required and a slug test in action are presented in Figure B- 1. The methodology is adapted from descriptions in Butler 1998 and the procedures described in USGS Groundwater Procedure 17 (Cunningham and Schalk 2011).

1) Attach the AT 700 communication cable to the field computer.
2) Place the AT 700 in the well below the level of where the slug will be submerged.
3) Anchor AT 700 to top of well casing.
4) Measure the maximum length of slug line that will allow the slug to completely submerge to about 0.3 m below the water surface.
5) Allow the transducer to adjust to new pressure and temperature.
6) Prepare slug to be lowered and raised in the well by lowering the decontaminated slug to a point just above the water level.
7) Note the starting water level as shown on the field computer.

8) Prepare the field computer to log depth data as frequently as possible at the beginning of the test. The Aqua Troll 700 allowed for a logarithmic recording time scale starting with 0.25 second increments.

Figure B- 1. a) Materials required for slug testing procedure and b) a slug test in action.

Slug In Test

9) Begin the test by starting the data logging capability on the field computer and simultaneously submerging the slug quickly and gently into the water. Secure the slug cord to maintain its position.

10) Monitor the water level on the live data display on the field computer.

11) When the water level is equal to the initial water level, or the readings change less than 0.3 cm per 10 minutes, stop the test.

Slug Out Test

12) Establish a new starting water level.

13) Begin the test by starting the data logging capability on the field computer and simultaneously withdrawing the slug quickly and gently out of the water. Secure the slug cord so it remains out of the water.
14) Monitor the water level on the live data display on the field computer.
15) When the water level is equal to the initial water level, or the readings change less than 0.3 cm per 10 minutes, stop the test.
16) Review the data for completeness and accuracy; paying special attention to unaccounted for peaks, missing data, or a significant change in initial water levels.
17) Perform this procedure three times so that three complete tests of falling and rising head test data are collected (six tests)

Bailer Removal Test

18) After the three sets of slug tests have performed, establish a new starting water level.
19) Begin the test by starting the data logging capability on the field computer and nearly simultaneously dropping the bailer into the water, allowing it to fill as much as possible, and removing the bailer completely out of the well.
20) If the bailer was not completely filled, pour the water into a 1.0 L graduate cylinder to measure amount removed.
21) Monitor the water level on the live data display on the field computer.
22) When the water level is equal to the initial water level, or the readings change less than 0.3 cm per 10 minutes, stop the test.
23) Review the data for completeness and accuracy; paying special attention to unaccounted for peaks, missing data, or a significant change in initial water levels.
24) Perform this procedure three times, or as many as time permits.

Data Analysis and Post Processing

The data collected in the field was processed and hydraulic conductivity values calculated using a Bouwer-Rice method based spreadsheet tool developed by the U.S. Geological Survey. The Bouwer-Rice method was chosen because the wells are screened across the water table (Butler 1998). Only the rising head tests were used in the tool as suggested by the U.S. Geological Survey (Halford and Kuniansky 2002). The methods for using the spreadsheet tool are outlined in the report referenced above but not presented here. An example output of the spreadsheet tool is shown in

WELL ID: ARKA1

Local ID:
Date: 11/6/2014
Time: 16:51

INPUT

Construction:

Casing dia. (d_c)	2.5	Inch
Annulus dia. (d_u)	2.5	Inch
Screen Length (L)	6	Feet

Depths to:

water level (DTW)	2.19	Feet
top of screen (TOS)	1.2	Feet
Base of Aquifer (DTB)	25	Feet

Annular Fill:

across screen -- Fine Sand
above screen -- Bentonite

Aquifer Material -- Fine Sand

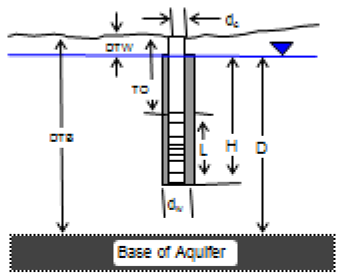

COMPUTED

L_{wetted}	5.01	Feet
D =	22.81	Feet
H =	5.01	Feet
L/r_u =	48.10	
$y_{0\text{-DISPLACEMENT}}$ =	0.31	Feet
$y_{0\text{-SLUG}}$ =	0.34	Feet

From look-up table using L/r_u

Partial penetrate A =	3.048	
B =	0.489	
ln(Re/rw) =	2.502	
Re =	1.27	Feet
Slope =	0.02832	$\log_{10}$/sec
$t_{90\%}$ recovery =	35	sec

Input is consistent.

K =	15	Feet/Day

Adjust slope of line to estimate K

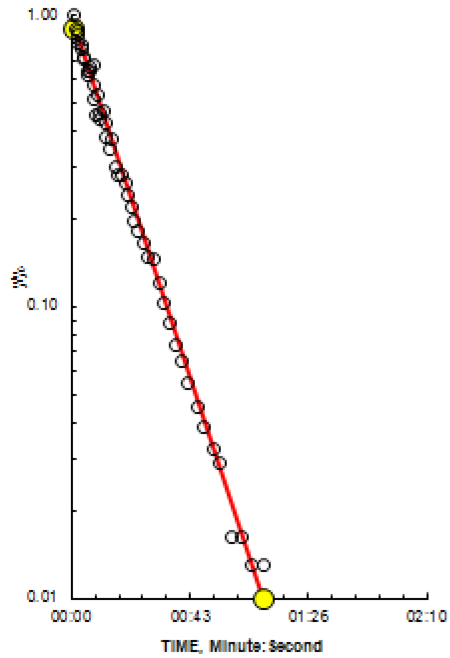

Reduced Data

Entry	Time, Hr:Min:Sec	Water Level
1	16:51:35.7	5.04
2	16:51:37.0	5.01
3	16:51:37.2	5.00
4	16:51:37.5	4.99
5	16:51:37.7	4.98
6	16:51:39.0	4.98
7	16:51:39.2	4.97
8	16:51:39.5	4.95
9	16:51:39.7	4.95
10	16:51:41.0	4.92
11	16:51:41.2	4.93
12	16:51:41.5	4.93
13	16:51:41.7	4.93
14	16:51:43.0	4.91
15	16:51:43.2	4.94
16	16:51:43.5	4.89
17	16:51:43.7	4.87
18	16:51:45.0	4.90
19	16:51:45.2	4.87
20	16:51:45.6	4.87
21	16:51:46.9	4.88
22	16:51:47.4	4.86
23	16:51:47.8	4.85
24	16:51:49.2	4.84
25	16:51:49.7	4.85
26	16:51:51.2	4.82
27	16:51:51.7	4.82
28	16:51:53.3	4.82
29	16:51:54.9	4.81
30	16:51:55.5	4.81
31	16:51:57.2	4.80
32	16:51:57.9	4.79
33	16:51:59.7	4.79
34	16:52:01.4	4.78
35	16:52:03.3	4.78
36	16:52:05.2	4.78
37	16:52:07.1	4.77
38	16:52:09.1	4.76
39	16:52:11.2	4.76
40	16:52:13.3	4.75
41	16:52:15.5	4.75
42	16:52:17.8	4.75
43	16:52:21.1	4.74
44	16:52:23.5	4.74
45	16:52:27.0	4.74

REMARKS:

Bouwer and Rice analysis of slug test, WRR 1976

Slug test was conducted in an alluvial aquifer in the Lower Arkansas Valley.

Figure B- 2. Example output from Bouwer-Rice spreadsheet tool.

APPENDIX C: CROSS SECTION GROUND SURFACE SURVEYS AND STAGE-TOP WIDTH RELATIONSHIPS

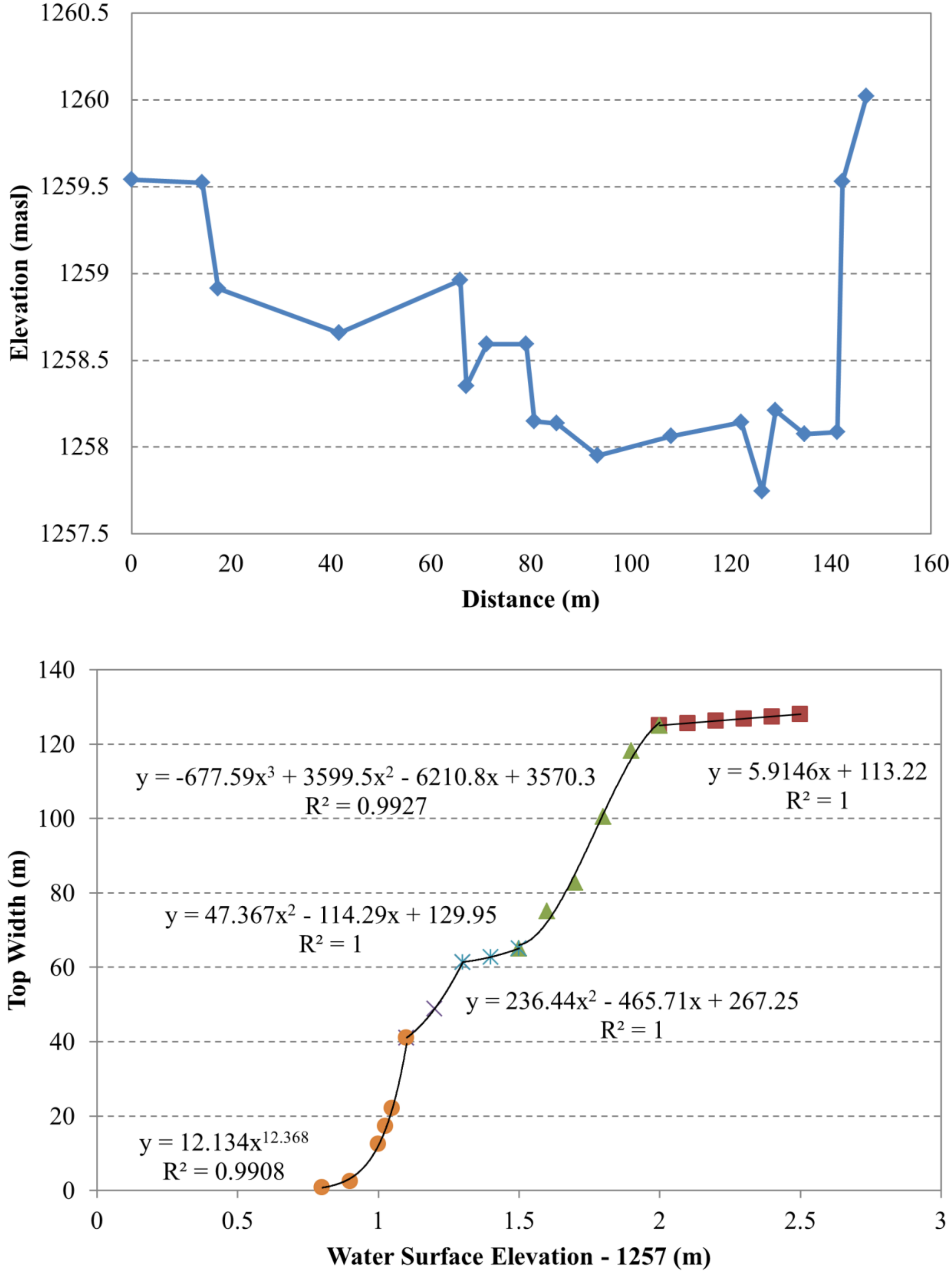

Figure C- 1. ARKA cross section survey and stage-top width relationship.

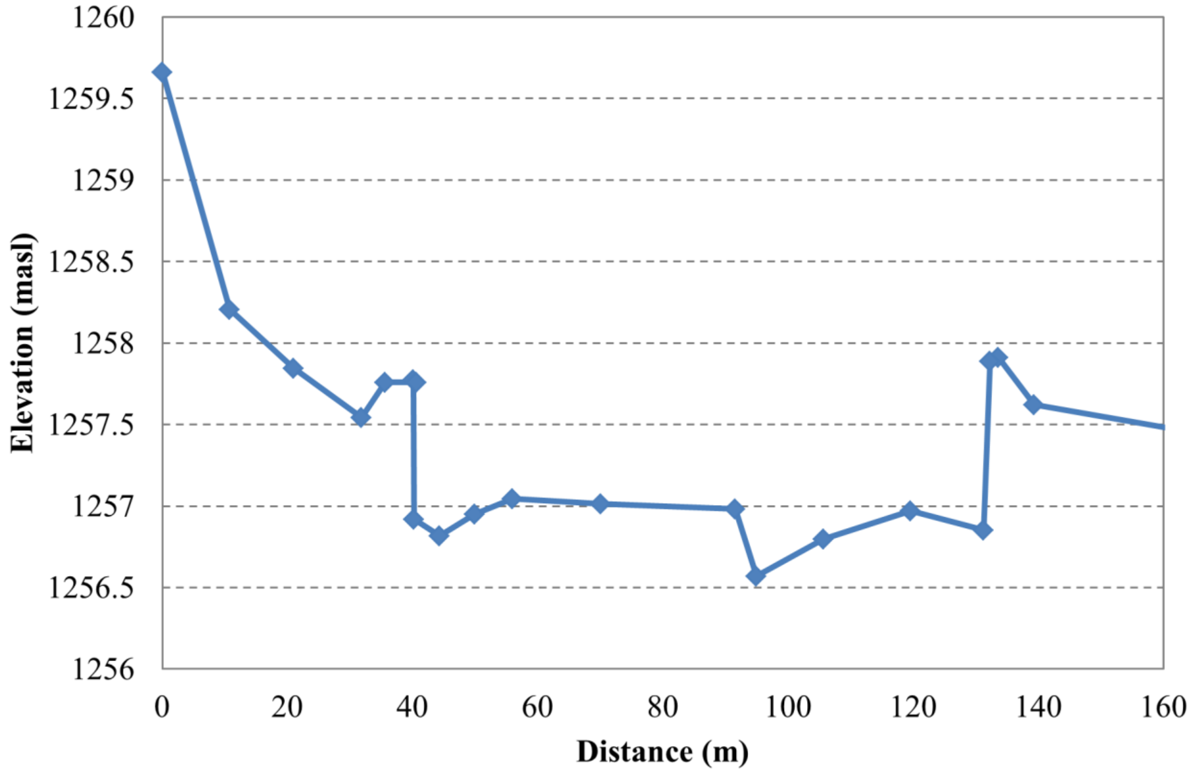

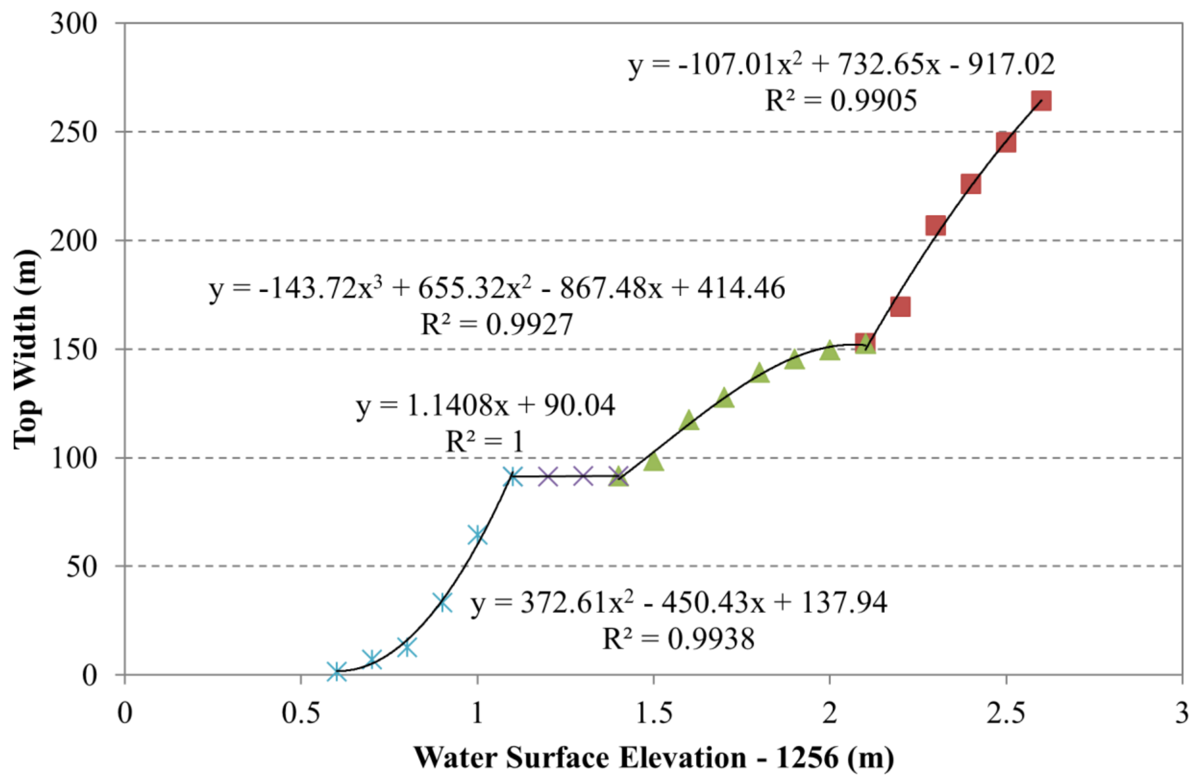

Figure C- 2. ARKB cross section survey and stage-top width relationship.

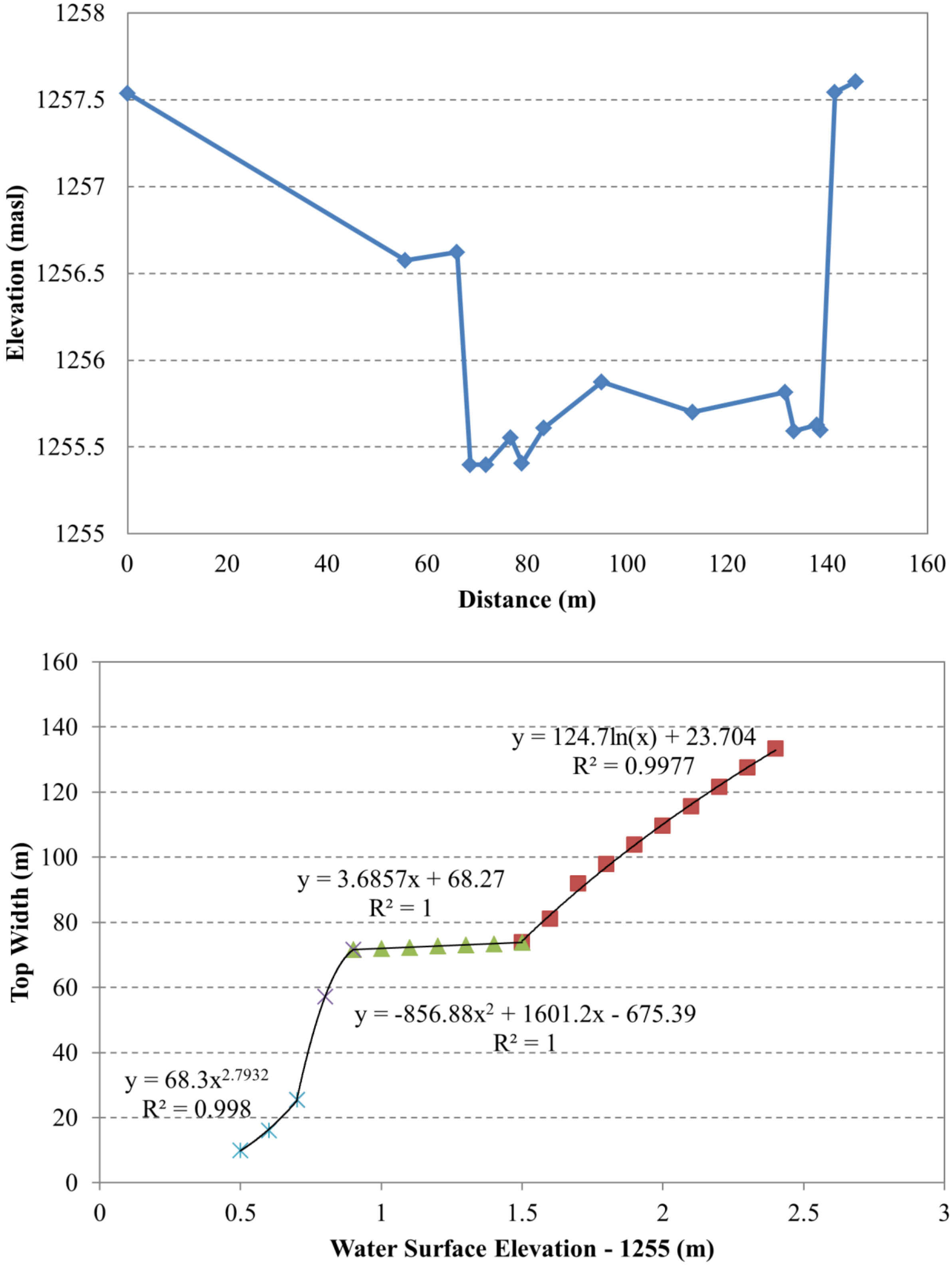

Figure C- 3. ARKC cross section survey and stage-top width relationship

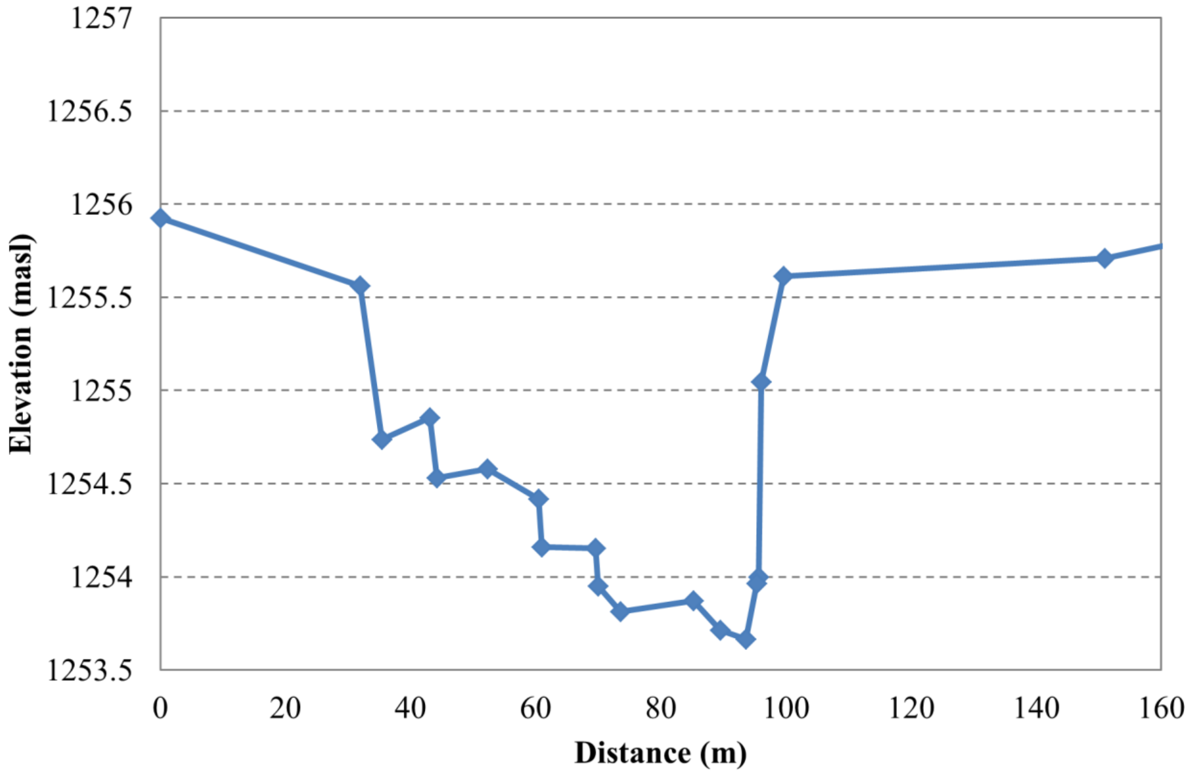

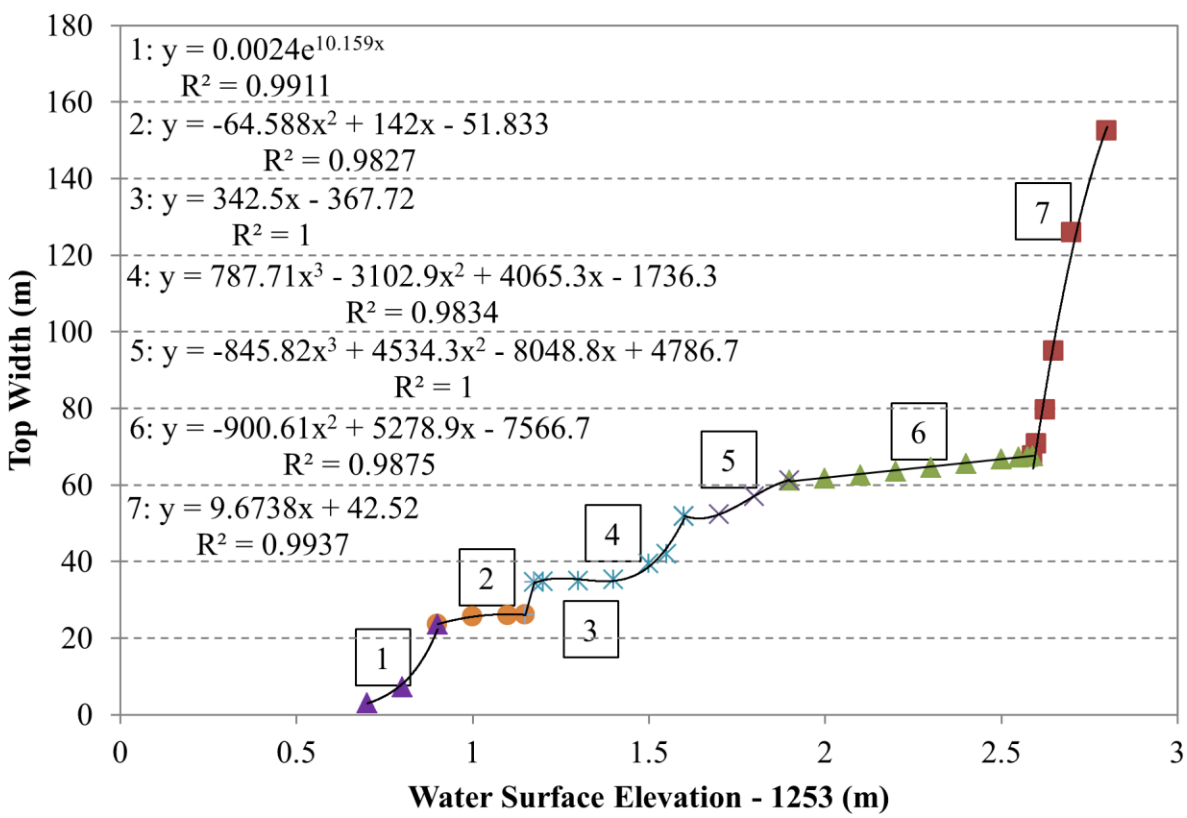

Figure C- 4. ARKD cross section survey and stage-top width relationship

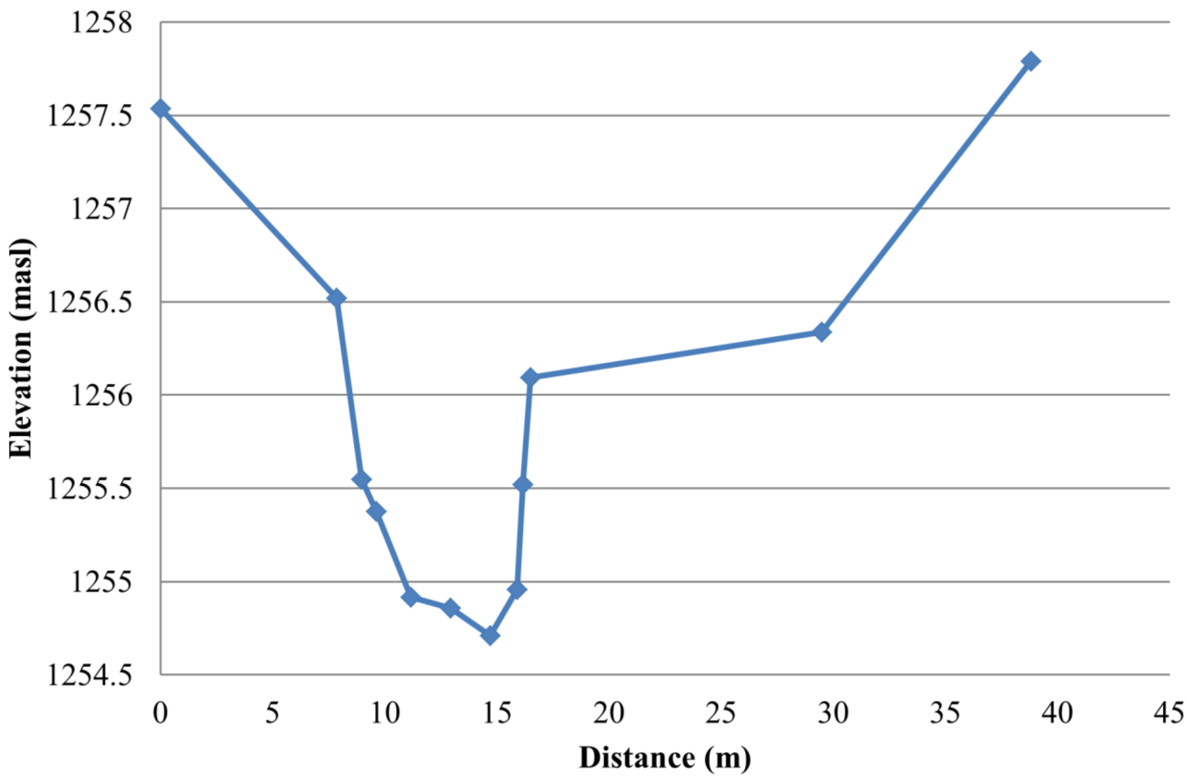

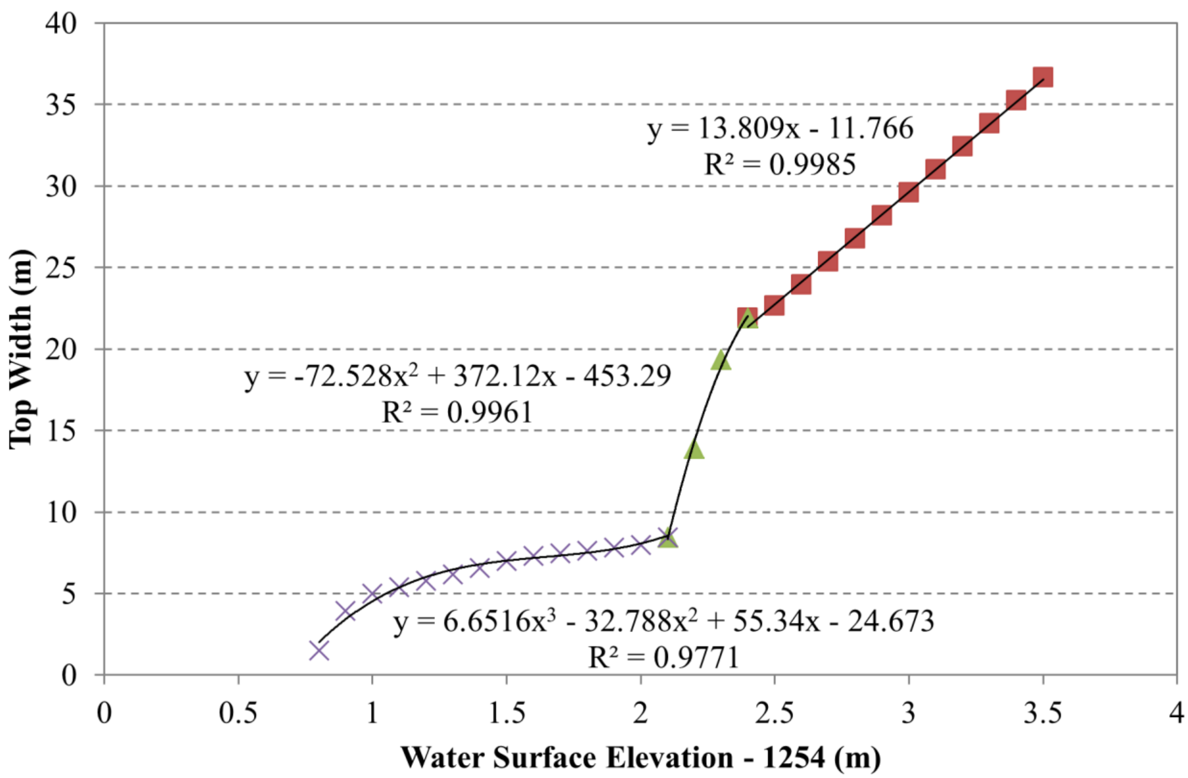

Figure C- 5. TIMU cross section survey and stage-top width relationship

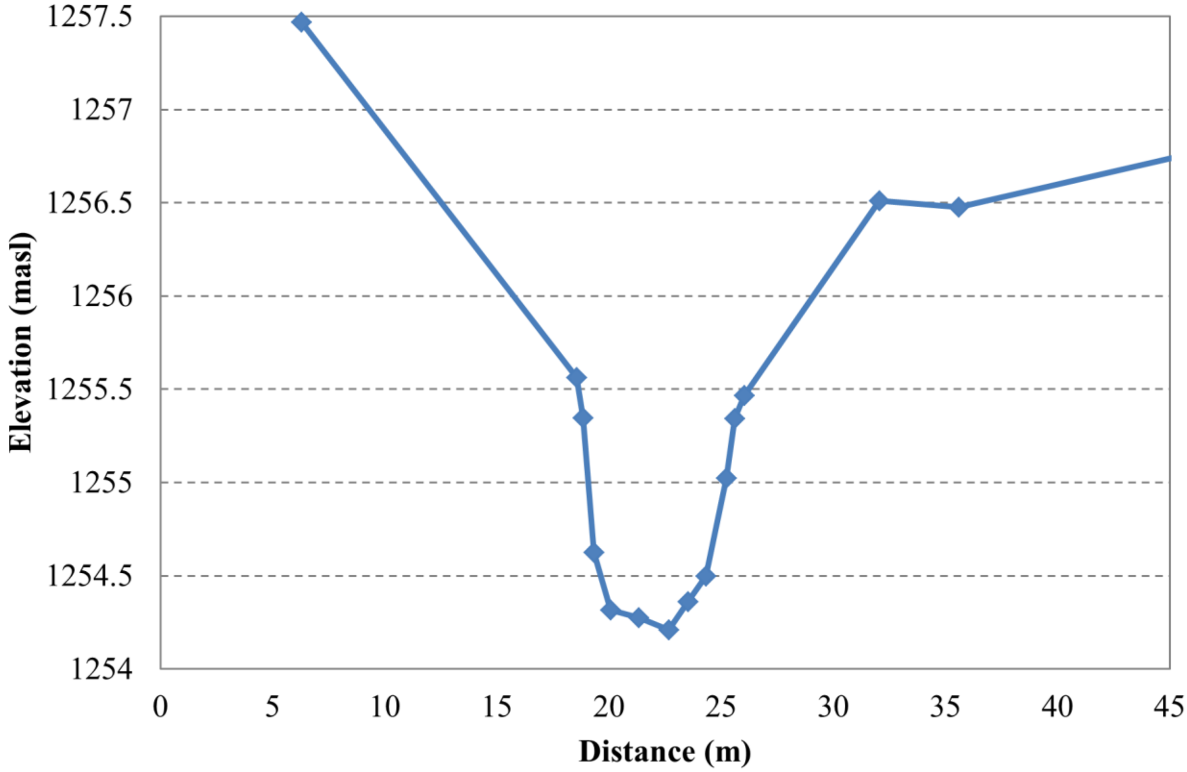

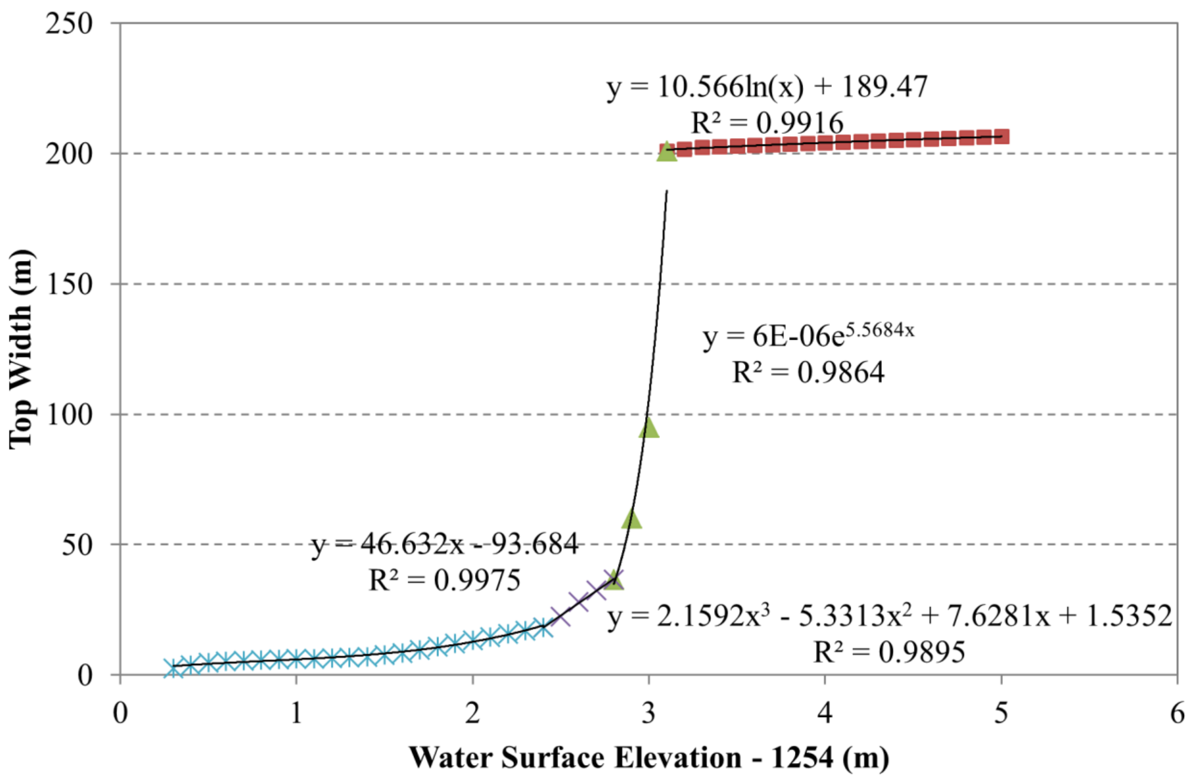

Figure C- 6. TIMA cross section survey and stage-top width relationship

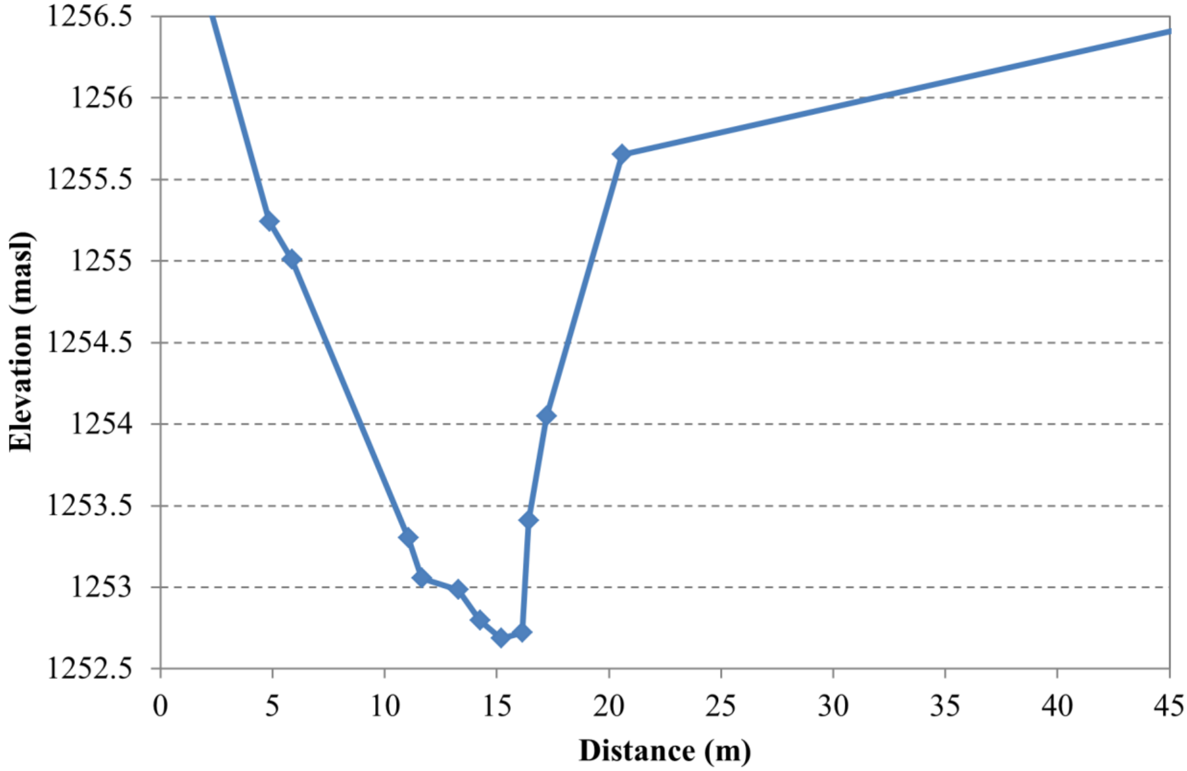

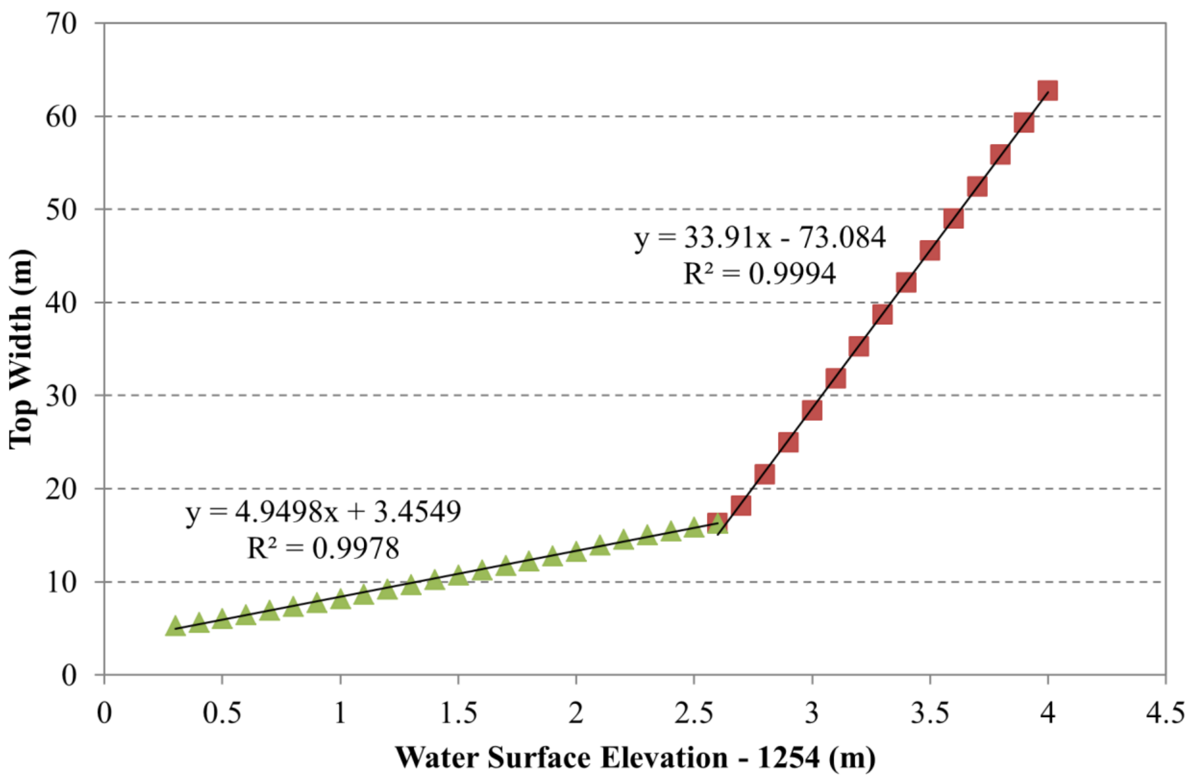

Figure C- 7. TIMB cross section survey and stage-top width relationship

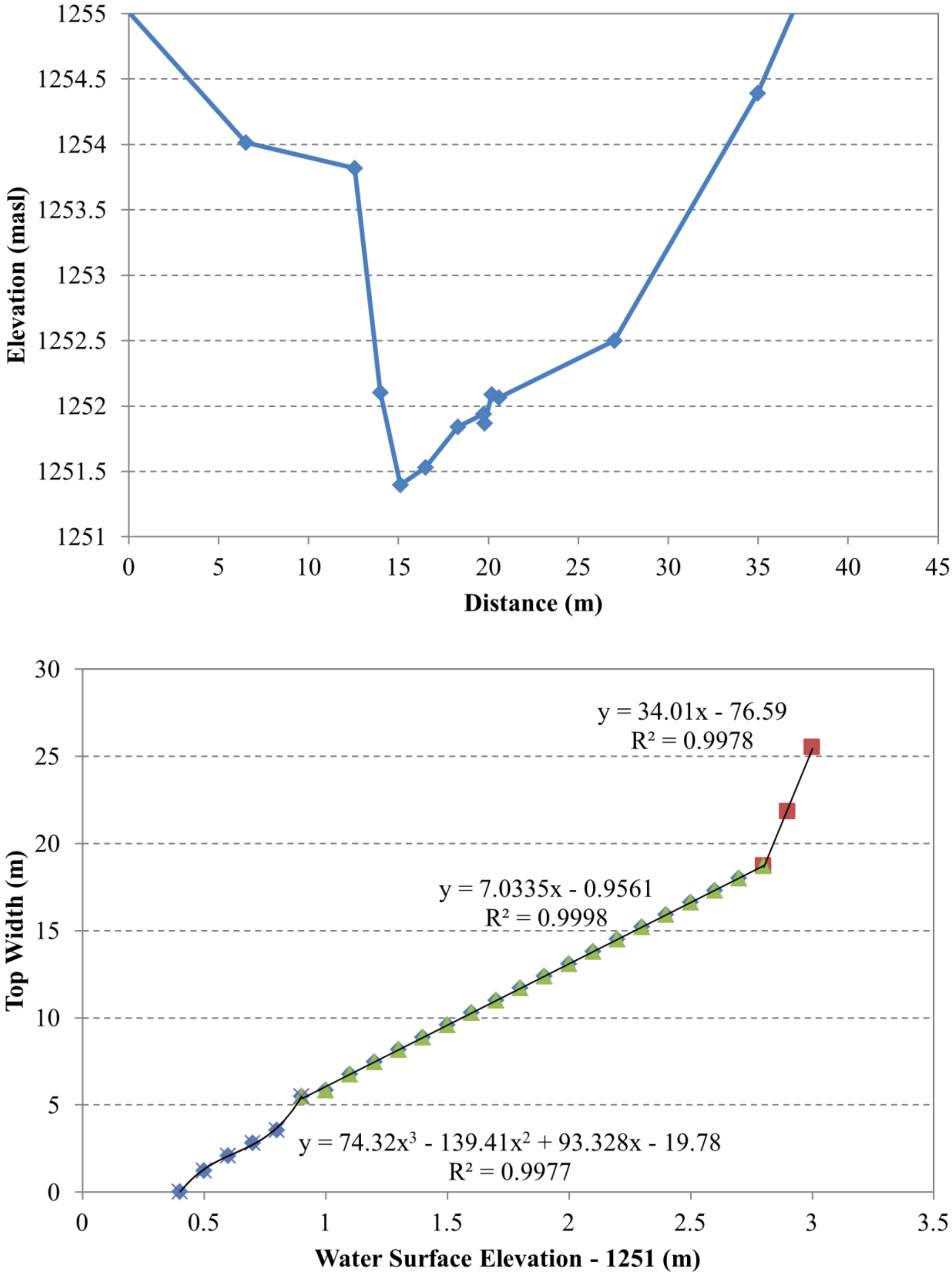

Figure C- 8. TIMD cross section survey and stage-top width relationship

APPENDIX D: CONCENTRATIONS OF TOTAL DISSOLVED SOLIDS AND MAJOR CATIONS AND ANIONS FOR THE ARKANSAS RIVER TO SUPPORT SPECIFIC CONDUCTIVITY EXPLANATION

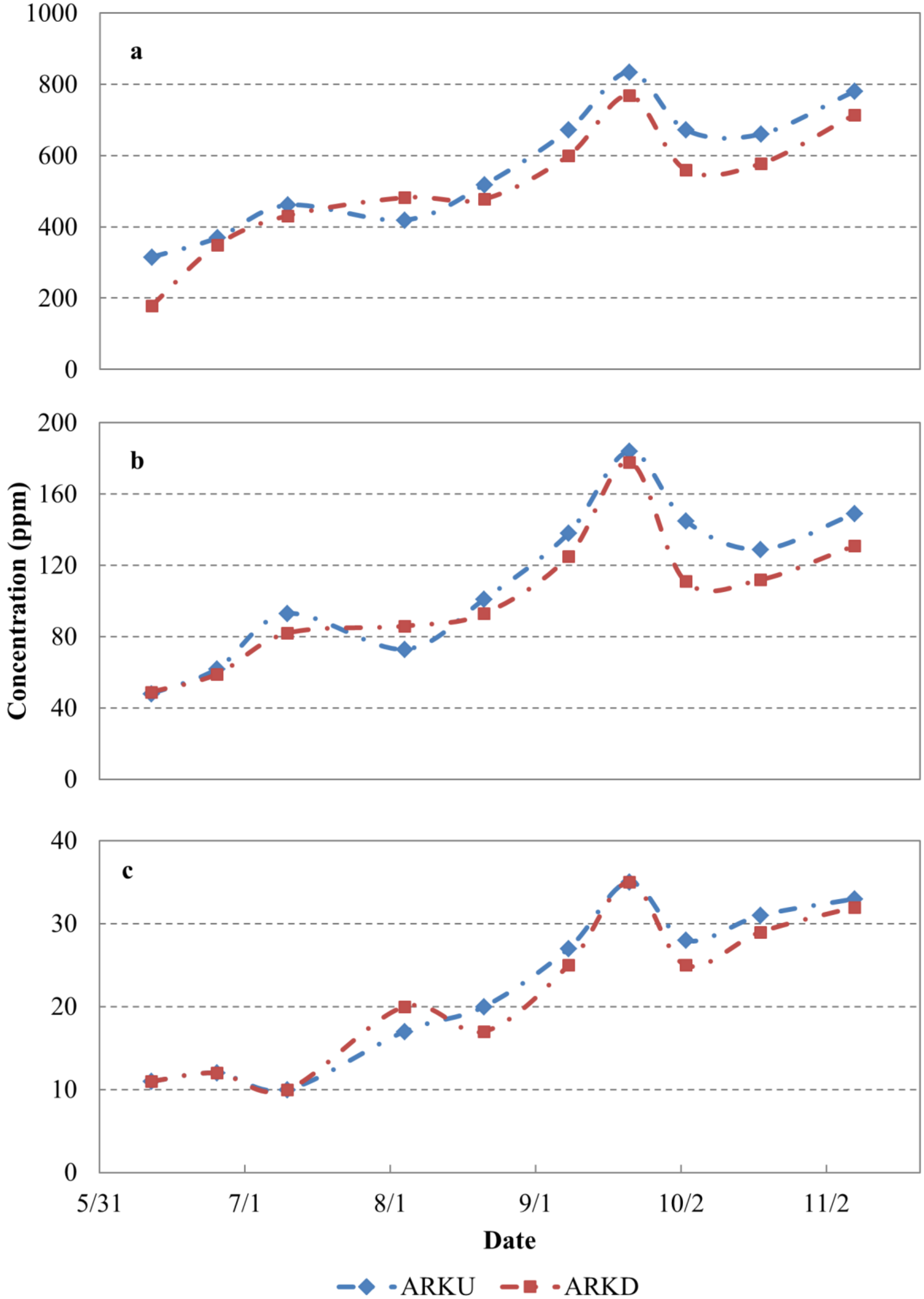

Figure D- 1. Growing season concentration plots of a) Total dissolved solids b) Sulfate-S c) Chloride-Cl.

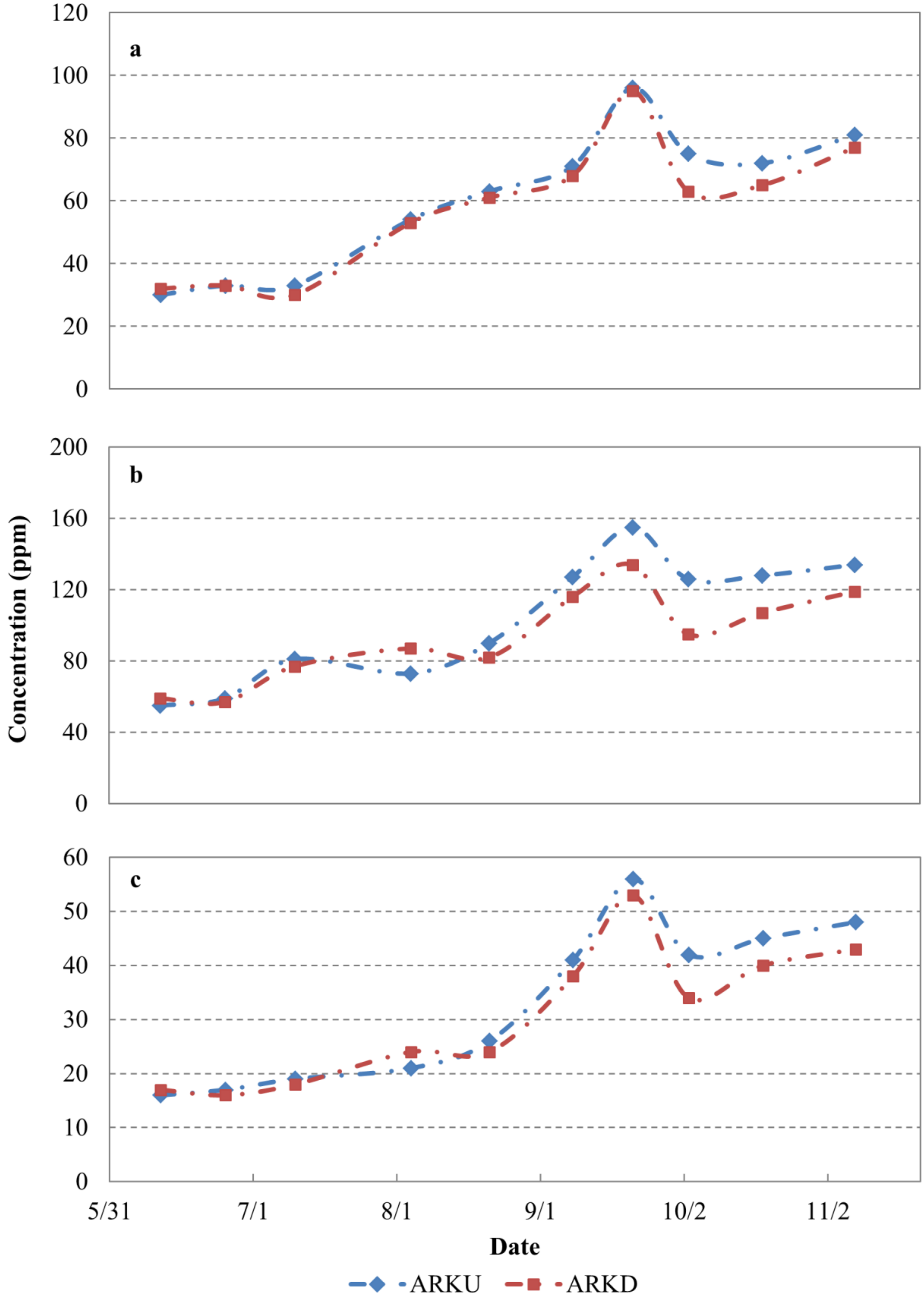

Figure D- 2. Growing season concentration plots of a) Sodium ion b) Calcium ion c) Magnesium ion.

APPENDIX E: BED AND BANK SEDIMENT SAMPLE RESULTS FROM THE ARKANSAS RIVER AND TIMPAS CREEK

Samples for bed sediments and bank soils were collected one time during the study for each reach. Left bank soils, right bank soils, and bed sediments were collected as composite samples from three to five sample points near each well cross section. Bank soils were collected from the top one foot of soil using a one inch diameter hand auger and bed sediments were collected from the top six inches using a long handled plastic scoop. Samples were combined in a clean plastic bucket and mixed thoroughly before a representative sample was taken in a quart plastic bag.

Table E- 1. Sediment sampling results from the Arkansas River and Timpas Creek.

Study Reach	Cross Section	Sample Location	2N KCl NO3-N (ppm)	KCl NH4-N (ppm)	Total N (ppm)	Total P (ppm)	P-Olsen (ppm)	TOC %	Sum of Cations (CEC) me/100g
Arkansas River	A	Left Bank	1.3	3	318	558	13.4	0.43	11.9
		Channel	1.4	2.2	70	268	4	0.07	3.3
		Right Bank	1.2	3.7	532	499	16.3	0.74	33.5
	B	Left Bank	1.2	3.2	412	547	11	0.59	18.6
		Channel	0.8	1.9	44	247	3	0.07	3.2
		Right Bank	1	3.3	740	719	13.2	1.07	25.2
	C	Left Bank	1.9	4	751	649	16.4	0.95	25.3
		Channel	1.4	1.9	91	219	3.3	0.04	2.9
		Right Bank	1.5	3	142	229	7.1	0.04	13.9
Timpas Creek	A	Left Bank	0.6	8.2	1195	726	16.7	1.44	26.7
		Channel	0.9	3	397	459	16.2	0.97	20.9
		Right Bank	0.5	3.2	664	518	4.9	1.89	62.1
	B	Left Bank	0.7	3.6	1148	710	17.4	1.71	31.1
		Channel	1.4	1.5	156	282	11.5	1.53	18.9
		Right Bank	0.6	5.8	1189	813	31.2	1.3	27.3

APPENDIX F: 24-HOUR MONITORING LONGITUDINAL SAMPLING LOCATIONS

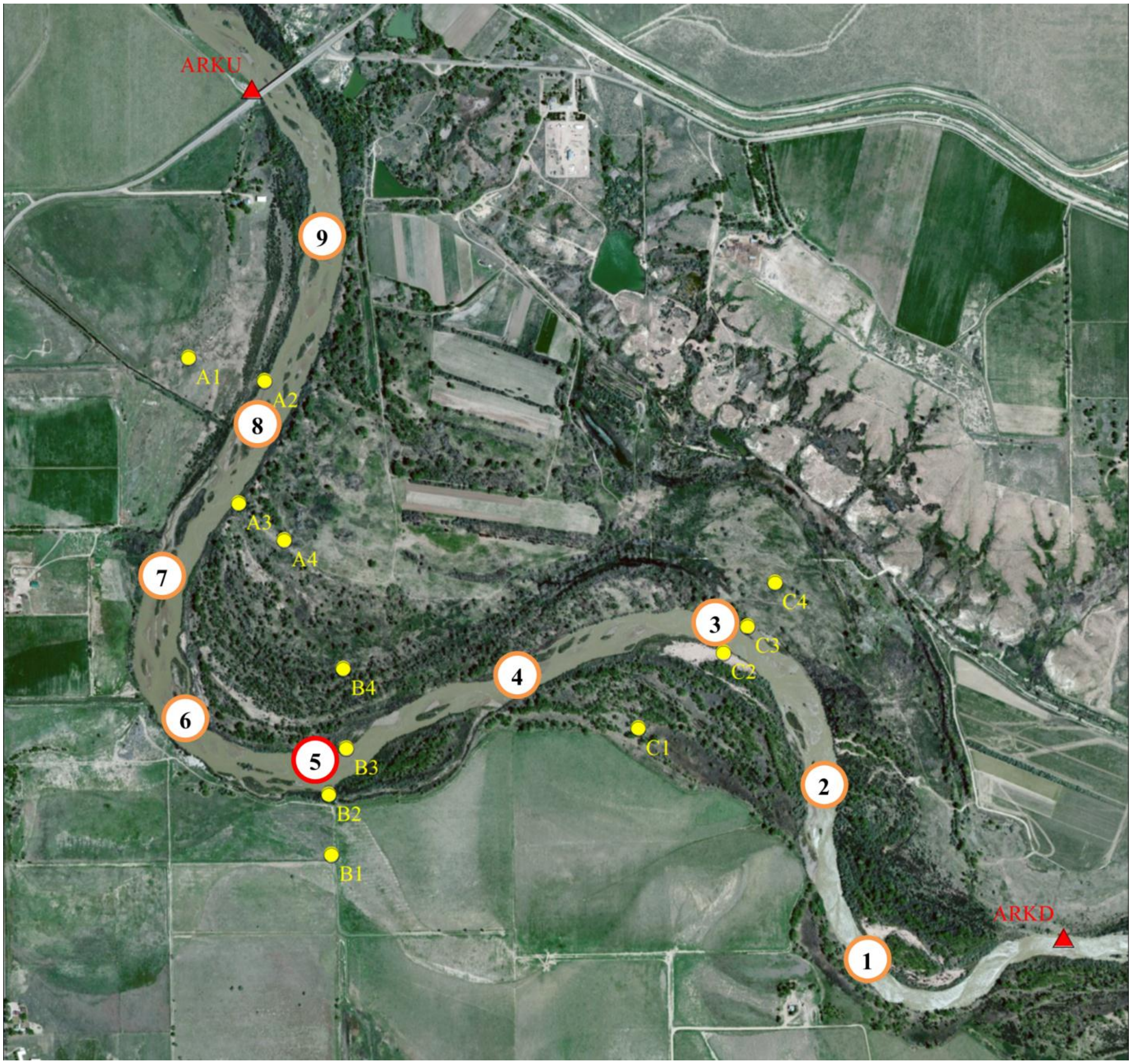

Figure F- 1. Longitudinal sampling locations for the Arkansas River.

Figure F- 2. Longitudinal sampling locations for the Arkansas River.

APPENDIX G: MULTILEVEL SAMPLING AT WELLS ARKA3 AND ARKA4

Multilevel samplers were installed adjacent to wells ARKA3 and A4 and samples collected within 24 hours of sample collection at wells A3 and A4. The samplers are constructed of 2.5 cm PVC pipe, 3 mm polytetrafluoroethylene (PTFE) tubing, 153 µm nytex screen, and zip ties. Sample ports, shown in Figure G-1, are spaced at approximately 0.3 meter intervals and consist of one end of the PTFE tubing covered in nytex screen. A separate tube for each sample port is then run up the PVC pipe and exposed above ground surface for sampling using a peristaltic pump. The exposed 2.5 cm PVC and PTFE tubing were then covered by a piece of 6.35 cm PVC tubing and cap for protection.

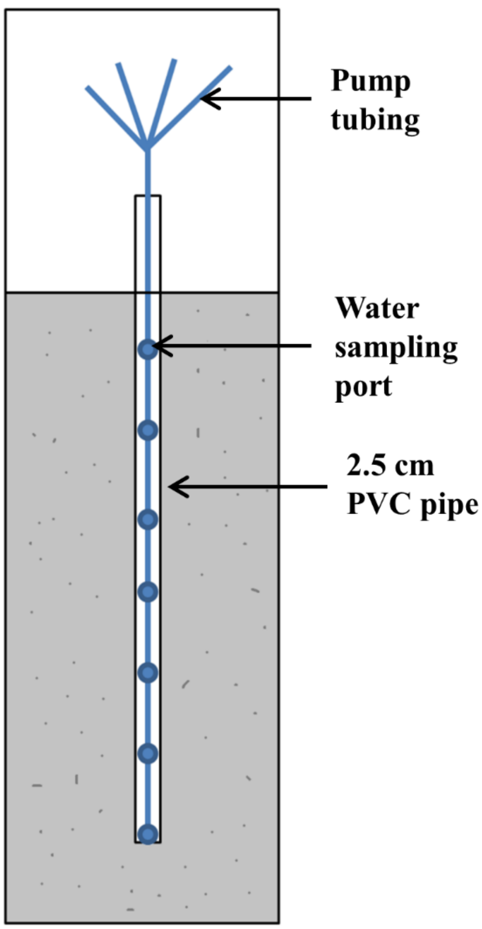

Figure G- 1. Schematic of multilevel sampler

Installation in the field involved using an auger truck drilling or hand auger to the desired depth and pushing the multilevel sampler so that the highest sampling port was approximately 0.3 m below ground surface, allowing the loose sand near the Arkansas River to fill in around it. The sampling ports were primed after installation by pushing distilled water down through the tubing to clear any debris from the nytex screen covering. Unfortunately this did not clear every port and some were unusable after installation.

Sampling from these devices involved attaching a peristaltic pump to the exposed pump tubing and pumping approximately 125 mL into a plastic sample bottle through a 0.45 μm filter. Samples were kept on ice and sent to Ward Laboratories with the rest of the sample. Samples were collected during the June and October sampling events.

Figure G- 2 below shows the results from these sample events. MLS1 is adjacent to well A3 and MLS2 adjacent to A4. Concentrations taken from the adjacent wells are also presented with the data at the approximate depth of collection to provide a check on the multilevel sampler. The June sampling plot shows that the multilevel samples were accurate when compared to the well data and that there is a slight variation as you move deeper into the soil column. The October sampling plot is more difficult to assess due to lack of samples and low concentrations.

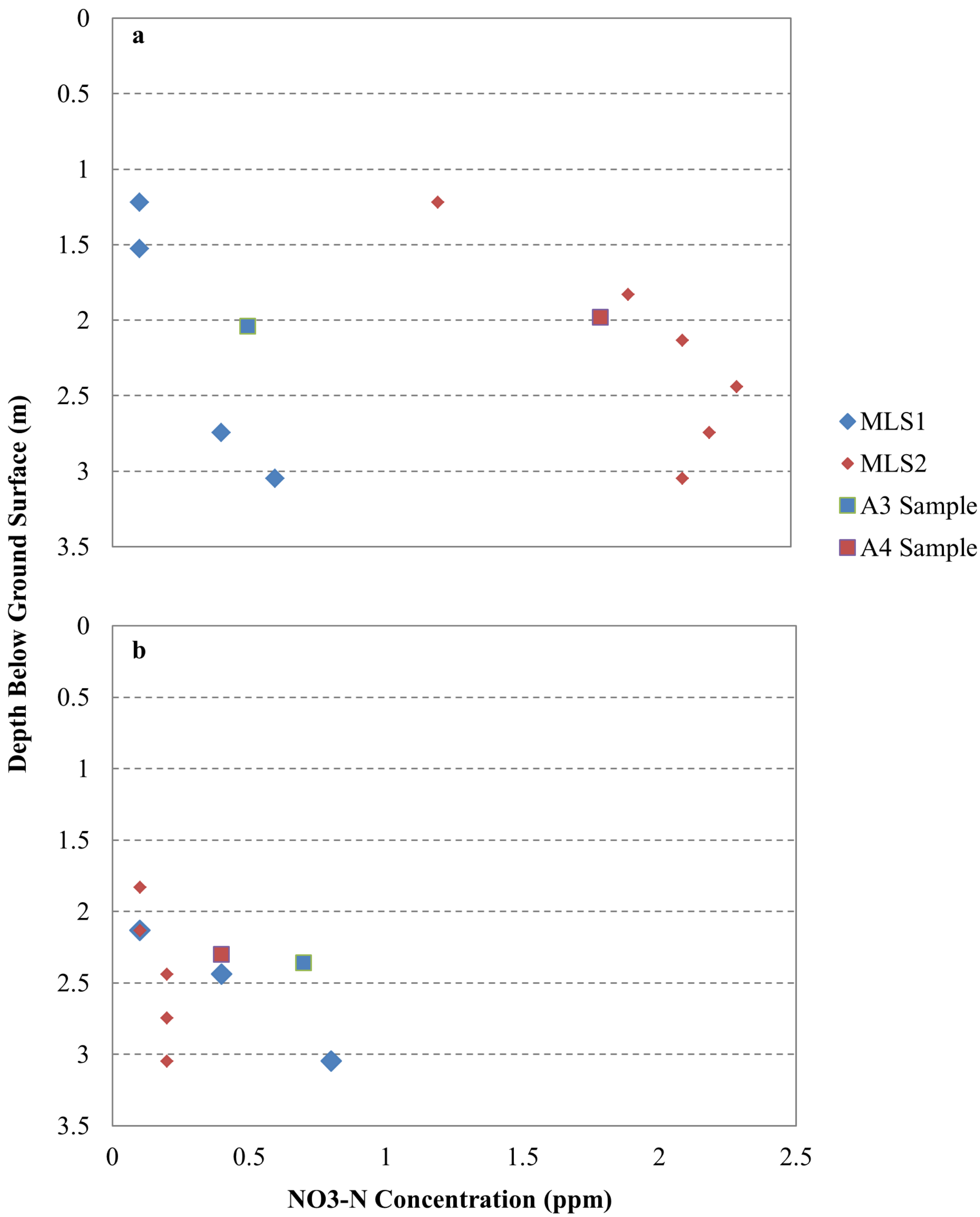

Figure G- 2. NO_3^- concentrations at multiple depths from multilevel samplers in a) June and b) October.

APPENDIX H: AERIAL AND GROUND LEVEL IMAGES OF RIPARIAN ZONE VEGETATION AND VEGETATION NEARBY SELECTED WELLS

Arkansas River

Cross section ARKA: Well A1 is in a pasture with sparse tamarisks and tall grasses. Well A2 is located on the riverbank and is surrounded by a dense stand of tamarisk and riparian willow species. The wells are approximately 195 m apart with 60 m of dense riparian vegetation between them. Well A3 is located on the riverbank and is surrounded by tall grasses and a large plains cottonwoods. Well A4 is located in a dense growth of Russian thistle (tumbleweed) and a few large cottonwoods. The wells are approximately 150 m apart with a mixture of grasses and large trees between them. The wells are located in a wildlife refuge where very little impact from irrigation or agriculture is present.

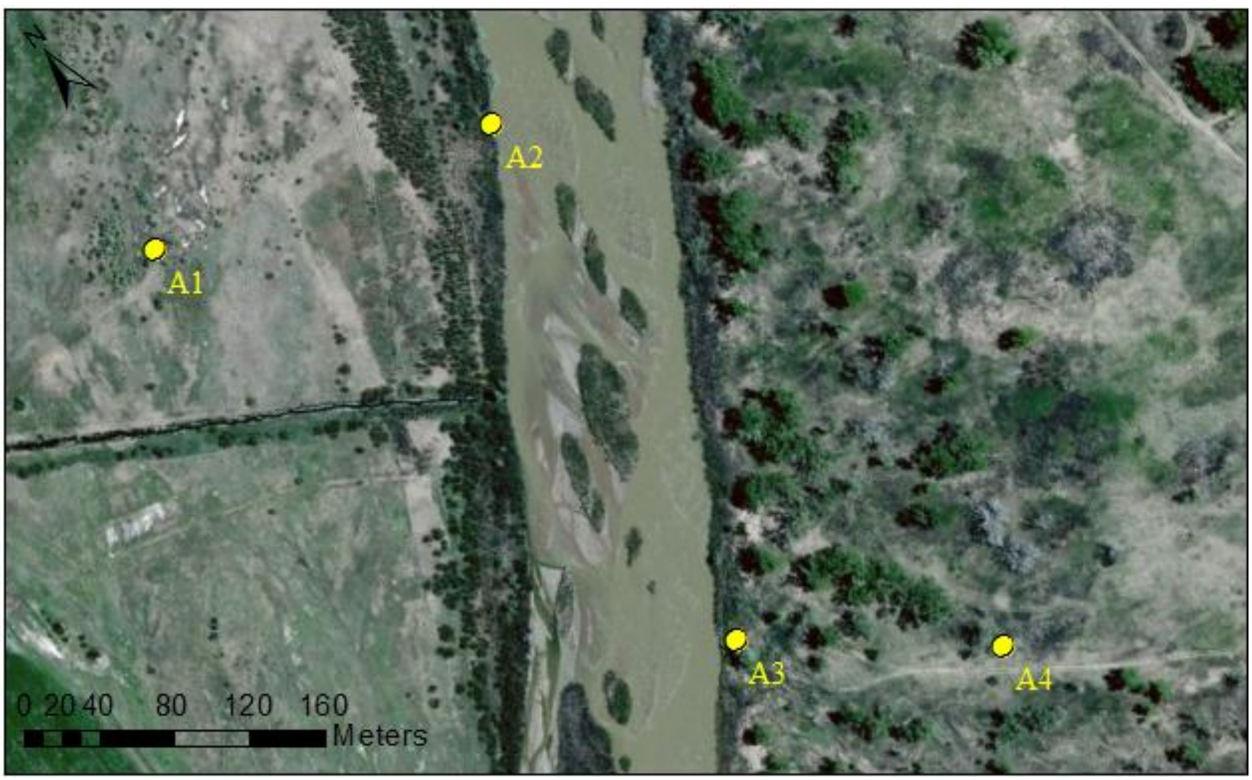

Figure H- 1. Close up aerial view of cross section ARKA.

Figure H- 2. a) View facing northwest across the river, b) view facing southeast from well A4 location, c) well A1 location.

Cross section ARKB: Well B1 is located in an unirrigated pasture next to an abandoned drainage ditch. The primary vegetation type is Russian thistle. Well B2 is located in a densely vegetated riparian zone near the bank of the river surrounded by tamarisk, riparian willow species, and tall grasses. The wells are approximately 160 m apart with 25 m of riparian vegetation between them. Well B3 is located on the riverbank surrounded entirely by riparian willow species and tall wetland grasses. This area was almost entirely submerged by overflow water during the June sampling. B4 is located in the wildlife refuge zone and is surrounded by large tamarisk, cottonwoods, and grasses. The wells are approximately 175 m apart with 135 m of large trees and 30 m of dense riparian vegetation and wetland grasses between them.

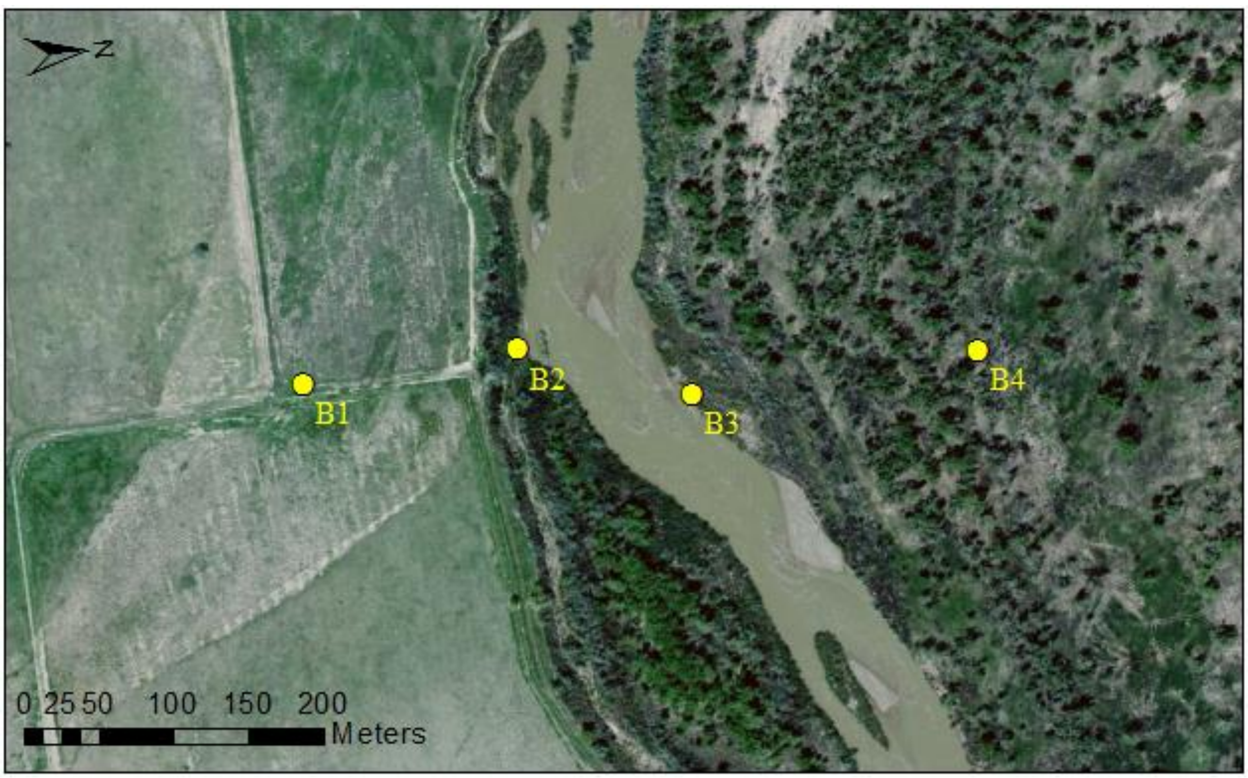

Figure H- 3. Close up aerial view of cross section ARKB.

Figure H- 4. a) View facing south across the river, b) well B3 location, c) well B2 location.

Cross section ARKC: Well C1 is located at the outer edge of a riparian zone approximately 70 m from the edge of a field in pasture. It is surrounded by large cottonwoods and dense bushes and grasses. C2 is located on a sand bar, reinforced by a thin strip of riparian vegetation composed of riparian willow species. The wells are approximately 260 m apart and the space is almost entirely composed of dense vegetation and trees. Well C3 is located on the riverbank with no riparian vegetation other than grasses. C4 is located in an open field down gradient from an irrigation canal with no vegetation other than grasses and a few tamarisks. The wells are approximately 140 m apart and separated by a grassy field.

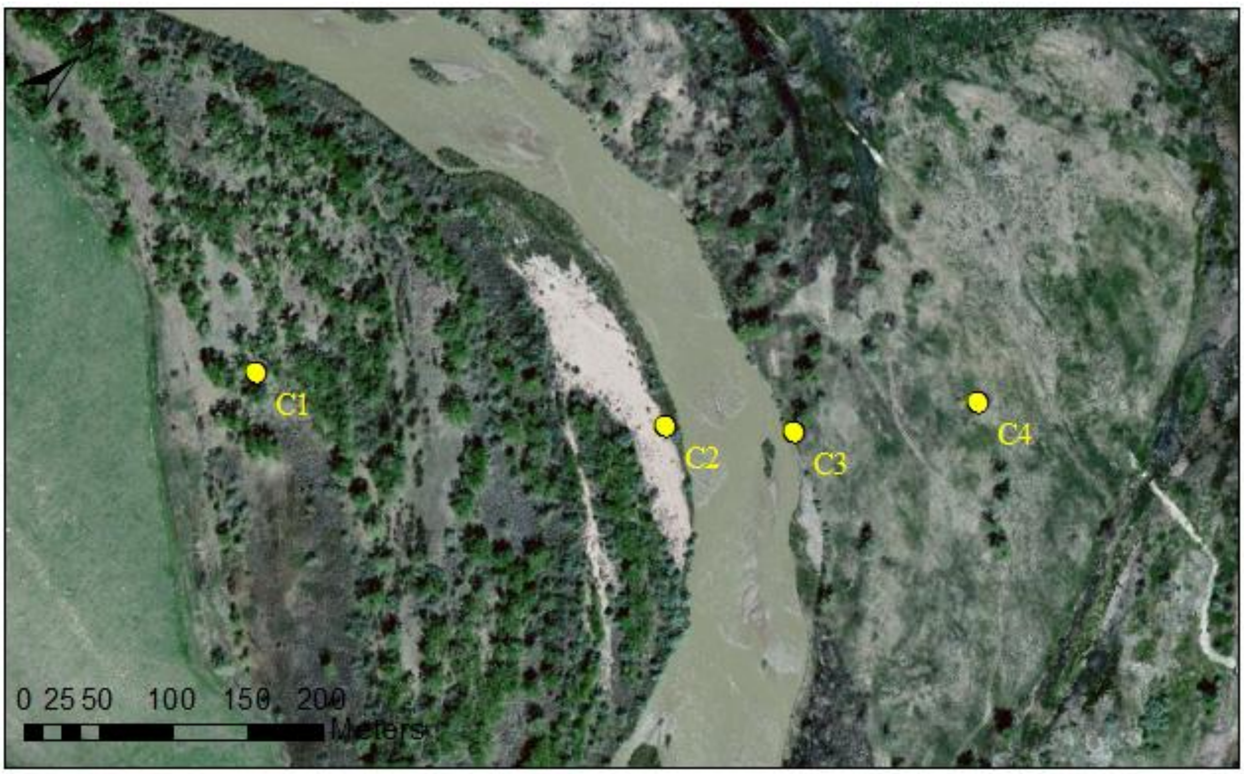

Figure H- 5. Close up aerial view of cross section ARKC.

Figure H- 6. View facing a) northeast and b) facing southwest across the river from C3 location.

Timpas Creek

Cross section TIMA: Well A1 is located just within the vegetated riparian zone, approximately 50 m from a pasture. It is surrounded by large cottonwood trees and tall grasses. A2 is located 15 m from the creek edge and is surrounded by dense riparian vegetation composed of riparian willow species and grasses. The wells are approximately 100 m apart with dense vegetation separating them including the vegetation mentioned above and tamarisk. Well A3 is located 10 m from the creek and is on a steep bank surrounded by small trees and tall grasses. A4 is located in an area with large cottonwoods just up-gradient of a dense community of wetland trees and grasses. The well is 60-70 m from a heavily irrigated field. Wells A3 and A4 are 65 m apart with dense riparian vegetation them.

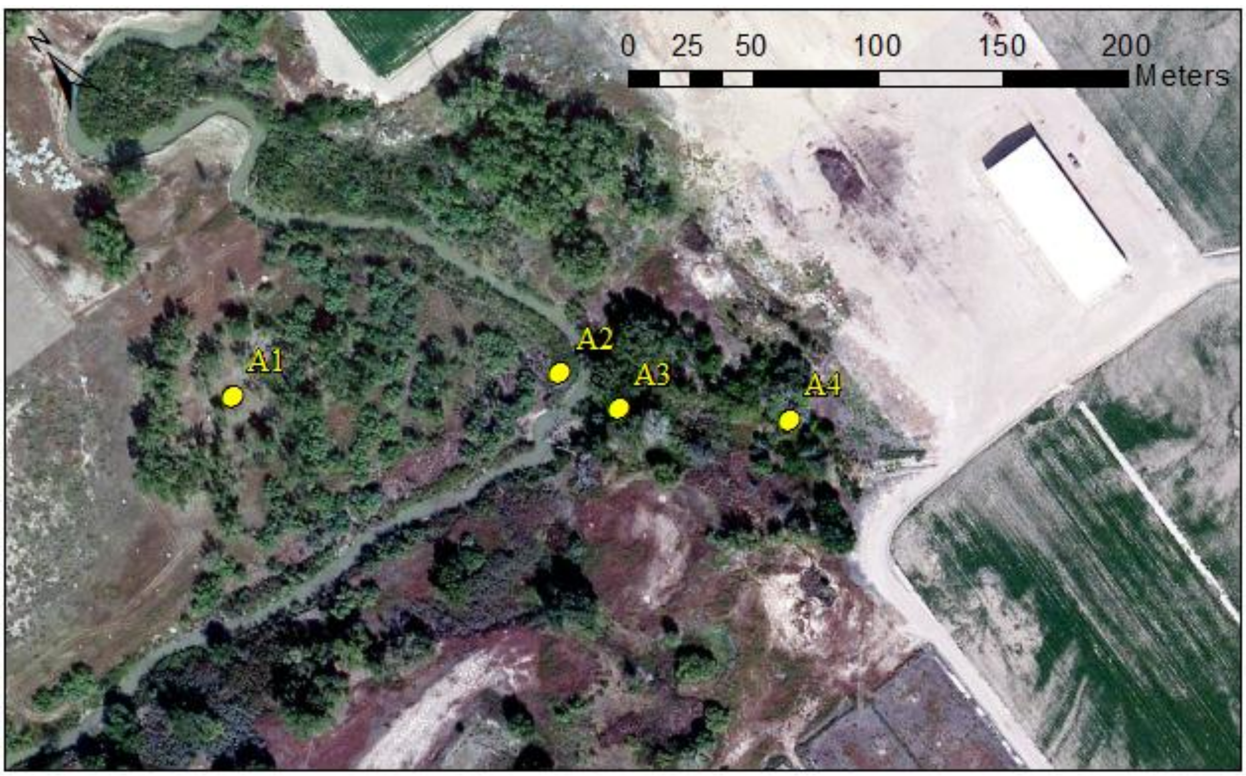

Figure H- 7. Close up aerial view of cross section TIMA.

Figure H- 8. View facing a) northwest and b) west from the well A3 location. c) Well A3 and d) well A2 locations.

Cross section TIMB: Well B1 is located in a pasture surrounded by Russian thistle and bare earth. A2 is located on the west creek bank surrounded by tamarisk shrubs. The wells are 100 m apart with 35 m of riparian vegetation including tamarisk and large cottonwoods between them. Well A3 is located on the east bank of the creek. It is surrounded by a few shrubs but with effectively no riparian vegetation. The farm road and irrigated field are directly adjacent to the creek at this location. A4 is located in an irrigated agricultural field which grew hay during the study period. The wells are 90 m apart with no riparian vegetation between them.

Figure H- 9. Close up aerial view of cross section TIMB.

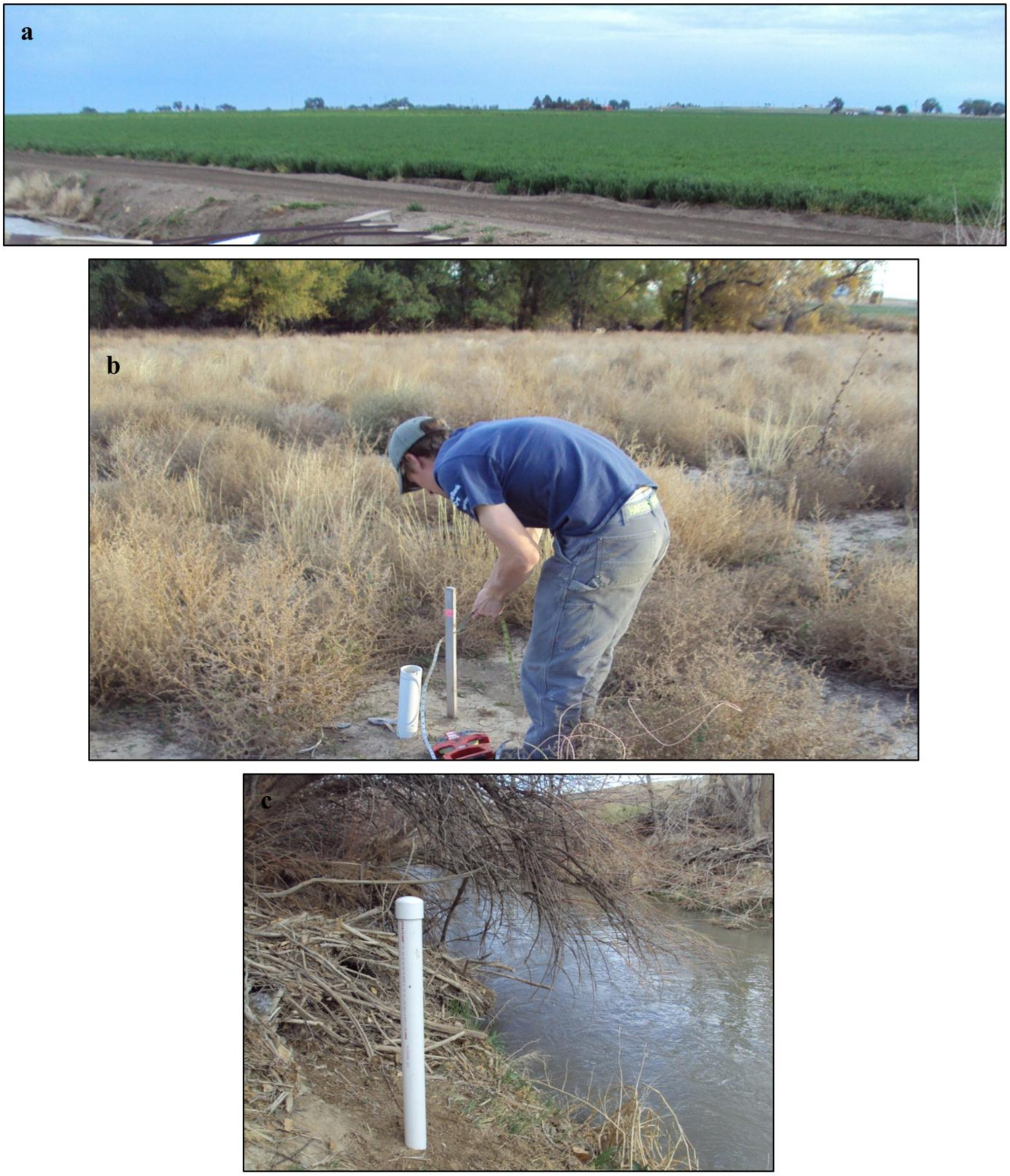

Figure H- 10. a) View of irrigated field containing well B4, b) well B1 location, and c) well B2 location.

APPENDIX I: W-1 IRRIGATION WATER QUALITY SAMPLE PACKAGE

Ward Laboratories in Kearney, Nebraska perform an analysis for dissolved salts and other parameters with their W-1 sample package. The full list of analysis results for this sample package are listed below:

- Sodium
- Calcium
- Magnesium
- Potassium
- Chloride
- pH
- NO_3^-
- Carbonate
- Bicarbonate
- Sulfate
- Electrical Conductivity
- Estimated Total Dissolved Solids
- Total Hardness (Lime)
- Total Alkalinity
- Boron
- Sodium Adsorption Ratio (SAR)
- Adjusted SAR

APPENDIX J: 24-HOUR WATER QUALITY SAMPLE CONCENTRATIONS

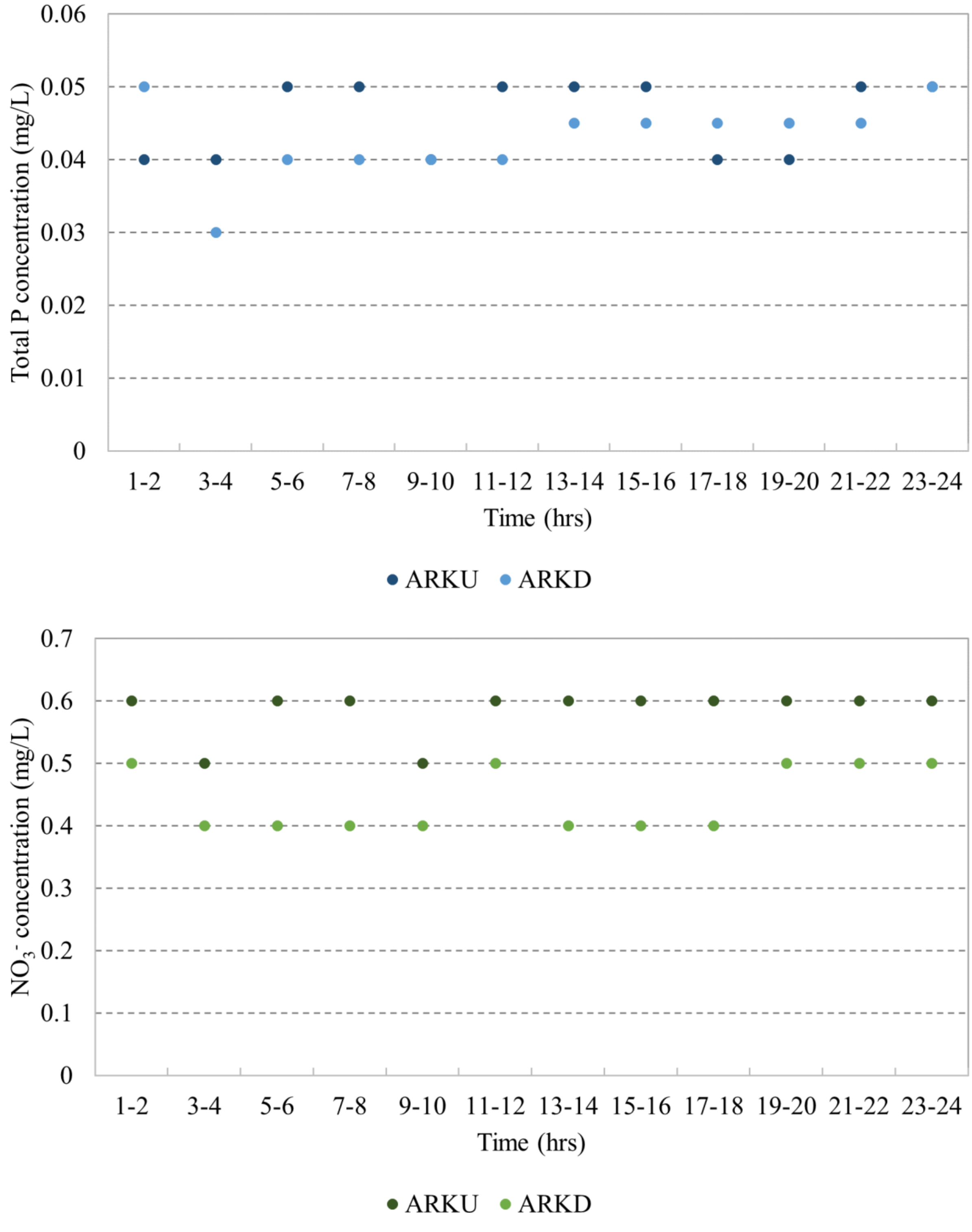

Figure J- 1. Water quality concentrations of Total P and NO_3^- for the Arkansas River, June, 24-hour sample event.

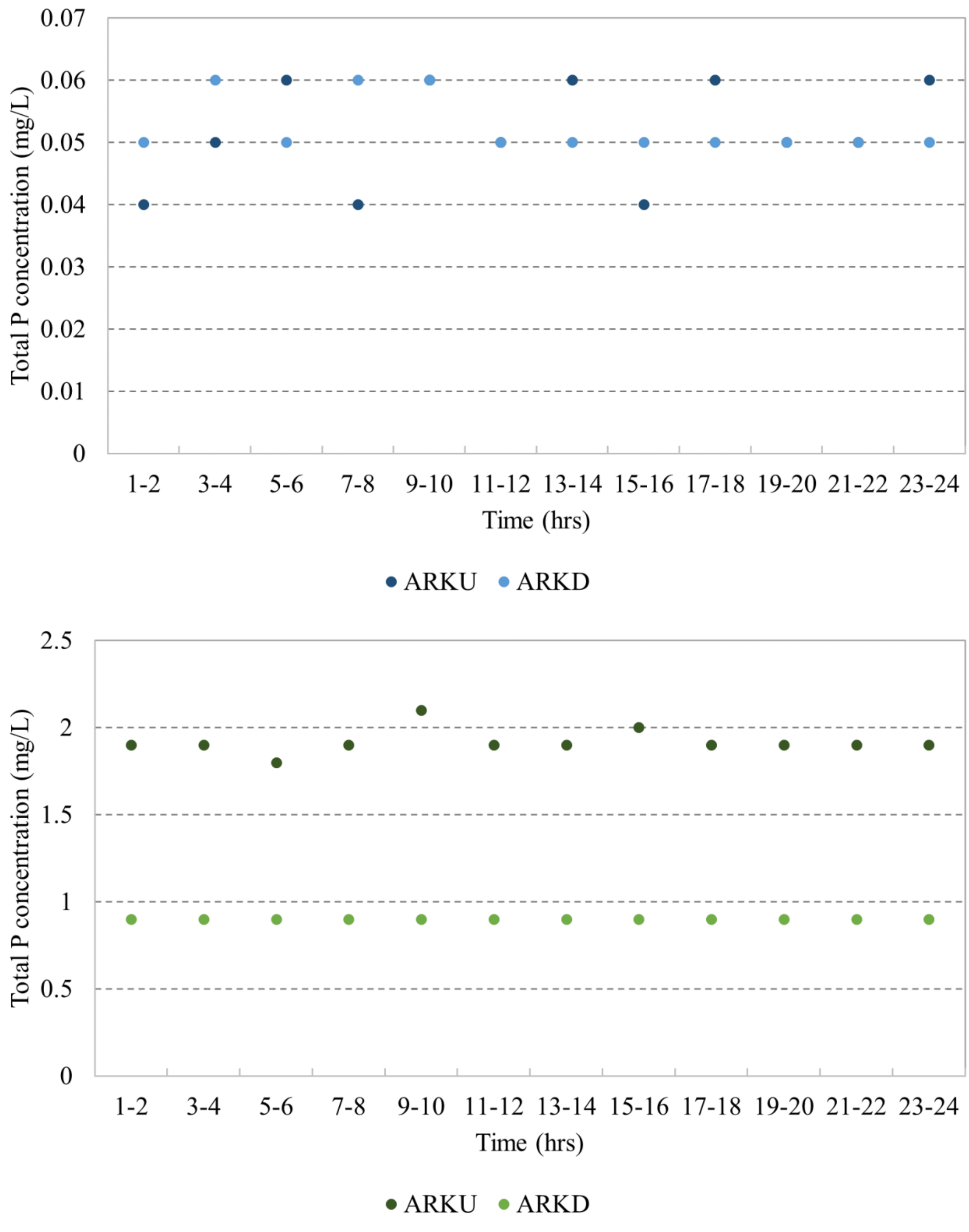

Figure J- 2. Water quality concentrations of Total P and NO_3^- for the Arkansas River, October, 24-hour sample event.

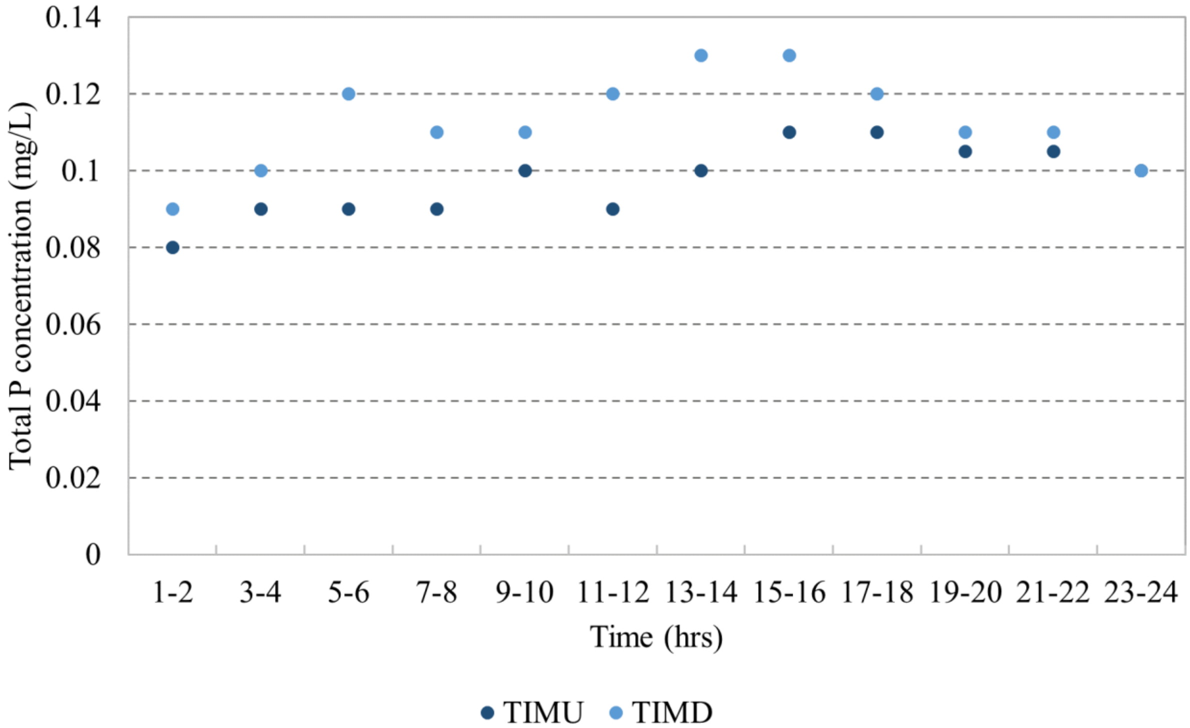

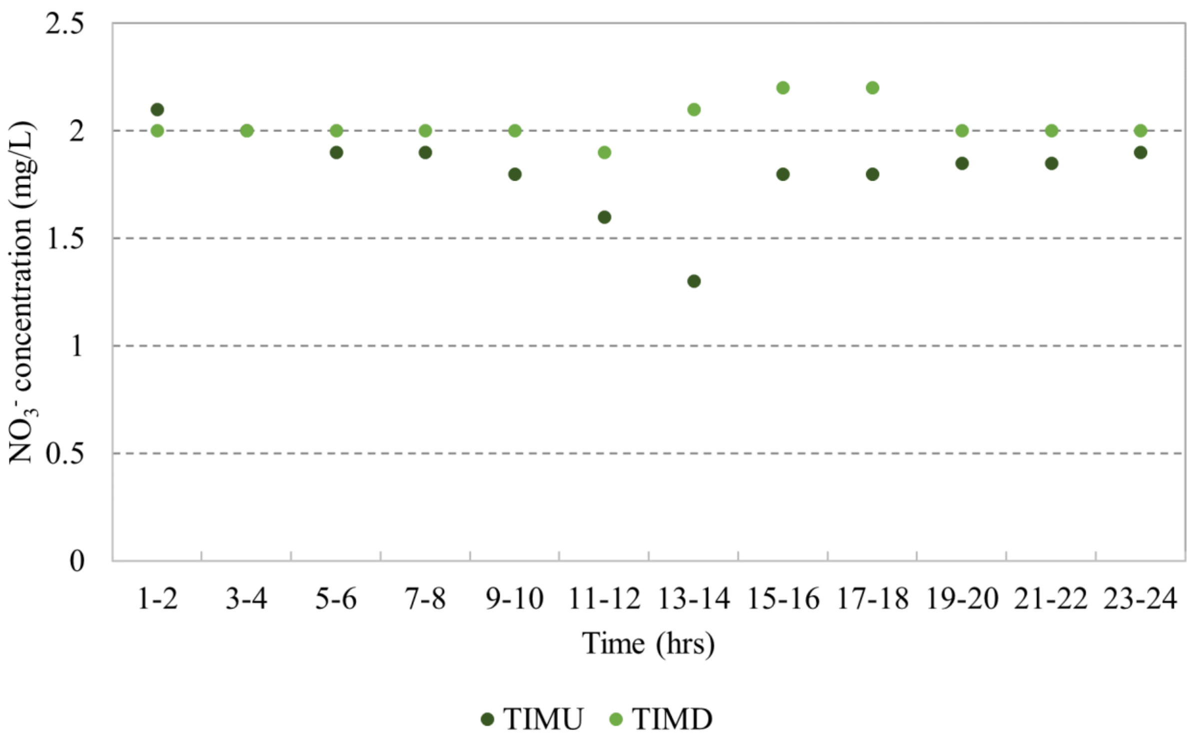

Figure J- 3. Water quality concentrations of Total P and NO_3^- for the Timpas Creek, June, 24-hour sample event.

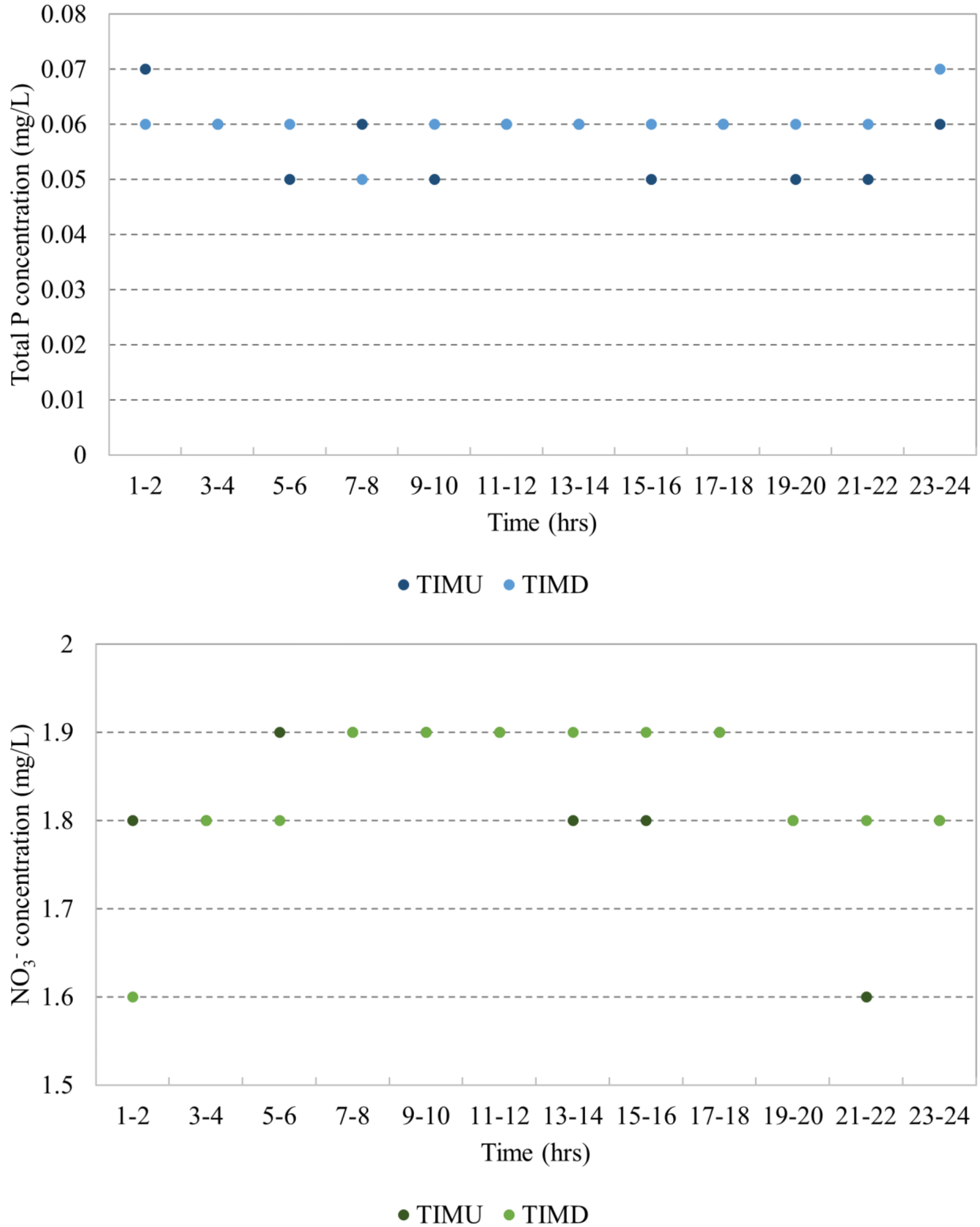

Figure J- 4. Water quality concentrations of Total P and NO_3^- for the Timpas Creek, October, 24-hour sample event.